POLITÉCNICO DE LEIRIA | ESCOLA SUPERIOR DE TECNOLOGIA E GESTÃO

DEVELOPMENT OF A PRE-IMPACT DYNAMICS SIMULATOR FOR A VEHICLE INVOLVED IN A ROAD ACCIDENT

Polytechnic University of Leiria

Higher School of Technology and Management

Master's in Automotive Engineering

Luís Miguel Marques Gomes

Leiria, September of 2024

POLITÉCNICO DE LEIRIA | ESCOLA SUPERIOR DE TECNOLOGIA E GESTÃO

DEVELOPMENT OF A PRE-IMPACT DYNAMICS SIMULATOR FOR A VEHICLE INVOLVED IN A ROAD ACCIDENT

Polytechnic University of Leiria

Higher School of Technology and Management

Master's in Automotive Engineering

Luís Miguel Marques Gomes

Automotive Project Report under the supervision of Professor Sérgio Pereira dos Santos and co-orientation of Professor Carlos Daniel Henriques Ferreira.

Leiria, September of 2024

Originality and Copyright

This project report is original, made only for this purpose, and all authors whose studies and publications were used to complete it are duly acknowledged.

Dedication

This thesis is dedicated to the memory of my beloved grandmother, Glória, who passed away while preparing this work. She was an independent and distinctive person whose presence and wisdom shaped me profoundly. I will forever miss the days spent at her house and cherish the memories of seeing her drive until she was 87.

I also extend this work's dedication to my other grandparents: Melinha, Zeferino and João.

This work is for all of you!

Acknowledgements

I would like to express my deepest gratitude to everyone who has supported me throughout my academic journey and the completion of this Master's thesis.

First and foremost, I would like to thank my supervisor Professor Sérgio Pereira dos Santos for his invaluable guidance, insight, and encouragement, which have been instrumental in shaping my work. A word of recognition is due to Professor Carlos Daniel Henriques Ferreira for co-orientating this work.

I would also like to extend my heartfelt thanks to my family, whose unwavering support and motivation have been a constant source of strength.

To my closest friends, thank you for your encouragement, understanding, and for always being there during both challenging and rewarding moments.

Special thanks to my colleagues and teachers from the University of Minho, as well as my colleagues and teachers from the Polytechnic University of Leiria. Each one of you has greatly enriched my academic experience.

I am also thankful to Carclasse and Mercedes-Benz Portugal, two companies where I had the opportunity to work during my five years of superior studies. The experiences and knowledge gained there have significantly contributed to my professional and personal development.

Thank you all for your encouragement and belief in me.

Abstract

This Master's thesis in Automotive Engineering focuses on the development of a Pre-Impact Dynamics Simulator (PIDS) for vehicles involved in road accidents. In response to the latest European Union (EU) regulation mandating Event Data Recorders (EDR) in all passenger cars and goods vehicles up to 3.5 tonnes circulating in EU since 2022, this report explores how EDR data can enhance the understanding of vehicle trajectories before collisions, i.e., the pre-impact trajectories of vehicles involved in road accidents, thereby contributing to increased rigour and accelerating road accident investigations.

The PIDS integrates pre-impact data extracted from EDRs with vehicle dynamics models, providing reliable reconstructions of pre-impact trajectories. To complement the interpretation of the simulator's results, this Master's thesis also includes a comprehensive scientific review of vehicle dynamics, drivers' behaviours in pre-impact situations, and advanced driver assistance technologies (ADAS). Furthermore, it examines methodologies for reconstructing vehicle collisions at accident sites, with a particular focus on existing kinematic methods and data collection tools.

The validation of the PIDS results was conducted using AVL VSM™ software and it was also applied to real-world case studies, highlighting its effectiveness in accurately reconstructing pre-impact trajectories across various scenarios. The findings underscore the simulator's potential to significantly improve the efficiency and rigour of road accident reconstructions, providing valuable insights for legal, engineering, and road safety applications.

This Master's thesis ends with recommendations for future enhancements to the PIDS, focusing on the use of more complex vehicle dynamics models and the implementation of alternative methods for measuring vehicle speed under rollover conditions.

Keywords: Event Data Recorder, Vehicles Dynamics, Road Accident Reconstruction, Pre-Impact Simulation

Resumo

Esta tese de Mestrado em Engenharia Automóvel tem como objetivo o desenvolvimento de um simulador da dinâmica de pré-impacto (PIDS) para veículos envolvidos em acidentes rodoviários. Em prol da recente legislação da União Europeia (UE), em que desde 2022 todos os veículos ligeiros de passageiros e mercadorias até 3,5 toneladas, circulando na UE, são obrigados a possuir um Gravador de Dados de Evento (EDR), este projeto de dissertação explora como os dados do EDR podem melhorar a compreensão das trajetórias dos veículos antes de uma colisão, isto é, as trajetórias de pré-impacto de veículos envolvidos em acidentes rodoviários e, desta forma, contribuir para o aumento do rigor e acelerar as investigações de acidentes rodoviários.

O PIDS integra dados de pré-impacto extraídos dos EDRs com modelos de dinâmica de veículos, proporcionando reconstituições fiáveis das trajetórias de pré-impacto. Para complementar a interpretação dos resultados do simulador, esta tese de Mestrado inclui, também, uma revisão científica abrangente da dinâmica de veículos, dos comportamentos dos condutores em situações de pré-impacto e das tecnologias avançadas de assistência ao condutor (ADAS). Também se debruça sobre algumas metodologias para a reconstituição da colisão de um veículo no local do acidente, com destaque para os métodos cinemáticas existentes e ferramentas para recolha de informação.

A validação de resultados do PIDS foi realizada utilizando o software AVL VSM™ e, também, aplicou-se o mesmo ao estudo de caso reais, realçando a sua eficácia na reconstituição factual das trajetórias de pré-impacto em diversos cenários. Os resultados destacam o potencial do simulador para melhorar significativamente a eficiência e o rigor das reconstituições de acidentes rodoviários, contribuindo com informações valiosas para aplicações litigiosas, de engenharia e de segurança rodoviária.

Esta tese de Mestrado termina com sugestões para aperfeiçoamentos futuros do PIDS, centradas, nomeadamente, na utilização de modelos de dinâmica de veículos mais complexos e implementação de métodos alternativos para a medição da velocidade do veículo em condições de capotamento.

Palavras-chaves: Gravador de Dados de Evento, Dinâmica de Veículos, Reconstituição de Acidentes Rodoviários, Simulação de Pré-Impacto

Contents

List of Figures

List of Tables

List of Abbreviations and Acronyms

ABS	Antilock Braking System
ACM	Airbag Control Module
ADAS	Advanced Driver Assistance Systems
AEB	Automatic or Autonomous Emergency Braking
AI	Artificial Intelligence
ASR	*Antriebsschlupfregelung* (Traction Control System)
ATS	Advances in Transportation Studies
CDR	Crash Data Retrieval
COG	Centre of Gravity
D2M	Direct to Module
DLC	Direct to Link Connector
DOF	Degrees Of Freedom
EBA	Emergency Brake Assist
EBS	Equivalent Barrier Speed
EDR	Event Data Recorder
EEPROM	Electrically Erasable Programmable Read-Only Memory
EES	Equivalent Energy Speed
ESA	Evasive Steering Assist
EU	European Union
FEA	Finite Elements Analysis
FWD	Front Wheel Drive
GIDAS	German In-Depth Accident Study
ISO	International Standard Organisation
LiDAR	Light Detection and Ranging
NHTSA	National Highway Traffic Safety Administration
OBD	On-Board Diagnostics
OTA	Over The Air
PDOF	Principal Direction of Force
PIDS	Pre-Impact Dynamics Simulator
SAE	Society of Automotive Engineers
SRS	Supplemental Restraint System
UN	United Nations
V2I	Vehicle-to-Infrastructure
V2V	Vehicle-to-Vehicle
VIN	Vehicle Identification Number

1. Introduction

Road accidents are a well-known concern for Car Traffic Authorities around the world and, most of the times, investigators are subject to the information that can be obtained at the road accident site. Sometimes, the information that can be collected is limited and it is on that basis that a forensic investigation is made to draw conclusions about the accident and with the final goal, besides assigning litigious responsibilities, to enhance road safety. Therefore, understanding a vehicle pre-impact trajectory, i.e., understating its trajectory and behaviour instants before collision can enhance the rigour and the acceleration of a road accident investigation.

Following what has been already said, the motivation of this Master's thesis is to use Event Data Recorders (EDR) pre-crash data, a mandatory technology that has been implemented in European Union (EU)'s countries since 2022, to allow Investigators to analyse the behaviour of vehicles involved in road accidents moments before collision.

The EDR is a technology deployed in modern vehicles that records vehicle instrumentation data before, during, and after a collision. It is considered the official recorder of data concerning a vehicle's pre-impact trajectory, ensuring that its data is factually connected to the vehicle's instrumentation data, which assures Investigators of its reliability.

Thus, the goal of this Master's thesis in Automotive Engineering is to develop a Pre-Impact Dynamics Simulator (PIDS) that uses EDR pre-crash data to reconstruct a vehicle pre-impact trajectory. With this, it is intended to introduce a new technical procedure to enhance the rigour and the acceleration of road accidents' investigations.

This approach not only enables forensic investigators to gain a more comprehensive understanding of pre-impact scenarios but also facilitates quicker and more precise analyses. Additionally, this Master's thesis complements the simulator development with a thorough scientific review of vehicle dynamics, including planar motion and longitudinal, lateral, and vertical dynamics, as well as the study of drivers' behaviour during pre-impact events, such as reaction times and emergency manoeuvres. The role of Advanced Driver Assistance Systems (ADAS) in mitigating accidents is also explored to understand their influence on pre-impact dynamics.

To ensure the robustness and applicability of the simulator, the PIDS will be validated using AVL VSM™ software, a widely recognised tool in vehicle dynamics simulation. Moreover, the simulator is going to be applied to two real-world case studies to demonstrate its effectiveness in replicating factual pre-impact trajectories under various conditions. These case studies underscore the practical value of the PIDS in providing reliable insights that are essential for accident investigations, legal proceedings, and engineering applications.

The results of this dissertation project highlight the potential of the PIDS to significantly enhance the rigour of road accident reconstructions. The findings also suggest future improvements, including the incorporation of more advanced vehicle dynamics models and alternative methodologies for analysing rollover scenarios.

In summary, this Master's thesis contributes to the field of road accident reconstruction by developing a tool that utilises EDR data and simulation techniques. It provides a foundation for improving forensic investigations and supports the broader goal of enhancing road safety.

1.1. Thesis Organisation

In this subchapter, it is presented a brief overview of each chapter's content:

- Chapter 1: Introduction – An overview of this Master's thesis is made by introducing the context, motivation, and objectives of this work;

- Chapter 2: State of the Art – Presentation of some current techniques to reconstruct the pre-impact dynamics of vehicles (e.g., EDR data, Artificial Intelligence (AI), Biomechanical analysis);

- Chapter 3: Science Review of Vehicle Dynamics – It presents a review of the scientific literature concerning Vehicle Dynamics, namely, vehicle coordinate system, vehicle planar dynamics models, vehicle longitudinal, lateral and vertical dynamics, and vehicle planar motion;

- Chapter 4: Drivers' Behaviour in Pre-Impact Events and On-Board Assistance Technologies – It is included some topics concerning drivers' behaviours in pre-impact situations (e.g., their reaction times, what defines emergency braking), as

well as some advanced on-board assistance technologies (ADAS) to help the driver mitigate or avoid a road accident;

- Chapter 5: Event Data Recorder (EDR) – It introduces the EDR technology itself, explaining its origins, its regulations, what data elements are recorded, how that data can be extracted and what it looks like;

- Chapter 6: Road Accident Reconstruction Methodologies – It presents some topics regarding road accident reconstruction methodologies, more specifically, kinematic methods and how to collect information at a road accident site;

- Chapter 7: Pre-impact Dynamics Simulator Development – The structure of the simulator that was developed (PIDS), its validation in AVL VSM™ software and its application in two real-world cases are presented;

- Chapter 8: Conclusions and Future Work – The global conclusions and areas of future improvements concerning the simulator are presented.

2. State of the Art

Over the past few years, reconstructing the pre-impact dynamics of vehicles involved in road accidents became a critical aspect of understanding the reasons for a road accident and determining the liability of those involved. Nowadays, advancements in data collection tools, sensor technology, computational modelling, and Artificial Intelligence (AI) have significantly enhanced the accuracy and detail of pre-impact vehicle dynamics reconstruction. These advancements are crucial for a more precise understanding of the vehicle behaviour in the instants leading up to a collision, as well as improving road safety, enhancing vehicle design, and aiding legal investigations.

The use of Event Data Recorders (EDR) has become an indispensable tool for capturing vehicles' pre-crash dynamics data. EDRs provide detailed, time-stamped data for some seconds before vehicles crash, offering critical insights into how vehicles were manoeuvred in the instants leading up to the impact.

Using Advanced Driver Assistance Systems (ADAS) generates rich streams of data on vehicle dynamics. Integrating ADAS data with EDR output helps reconstruct the pre-impact scenario with unprecedented accuracy, by capturing automatic corrective actions taken by the vehicle's control systems, as well as driver's responses. In addition, data from those systems help Investigators understand whether vehicle automation was functioning properly during the pre-impact phase.

Data from Vehicle-to-Vehicle (V2V) and Vehicle-to-Infrastructure (V2I) Over the Air (OTA) communication represent a major advancement in reconstructing pre-impact dynamics, by the fact that connected vehicles share real-time data with other vehicles and surrounding infrastructure. Upon a crash, this type of data provides critical insights into the speed, trajectory and actions of nearby vehicles that may have influenced the crash. This data can be used also to validate, for example, EDR output data.

Light Detection and Ranging (LiDAR)-based Pre-Impact Trajectory Mapping enables Investigators to analyse vehicles' trajectories and deceleration paths based on physical evidence from their accident scenes. These high-precision 3D models help in visualizing the movements of vehicles before a crash, ensuring accurate speed and direction estimations.

Simulation software and modelling techniques, such as PC-Crash, Virtual CRASH, and HVE simulate the pre-impact behaviour of vehicles based on physical laws and the data collected from their accident scenes. Combining Finite Elements Analysis (FEA) and Vehicle Kinematic Models, these simulations can assess the impact of different vehicle variables on the trajectory leading up to a collision and accurately simulate how each vehicle behaved seconds before impact.

Recent techniques of AI and Machine Learning Algorithms started increasingly being used to enhance accident reconstruction, especially in analysing large datasets from vehicles' sensors, telematics, and surveillance footage. These techniques can identify patterns in vehicle behaviour, helping reconstruct scenarios more quickly and accurately. For this matter, predictive models shall be used to simulate hypothetical scenarios, contributing to the determination of the most likely pre-impact conditions.

Video and Camera data integration from vehicle internal sources (e.g., dash cameras) and other external sources (e.g., traffic cameras) provides additional perspectives on pre-impact dynamics. Combining multiple sources of video data with, for example, EDR and telematics records enables Investigators to verify the accuracy of the sensors' data and assess other external factors like vehicle positioning, driver behaviour, and external conditions (e.g., meteorological conditions) during the pre-impact period.

Biomechanical analysis is becoming increasingly incorporated into the reconstruction of pre-impact dynamics, allowing the understanding of how drivers react during the seconds before a crash. Modern vehicles equipped with internal cameras and driver monitoring systems (e.g., eye tracking, head position sensors, hands position sensors) provide data on drivers' attention and response times.

In summary, these technologies allow Investigators to accurately simulate the actions of vehicles and drivers in the instants leading up to a crash, providing a comprehensive understanding concerning the reason for a road accident. The increasing reliance on AI and Machine Learning further enhances the ability to simulate complex pre-impact scenarios, ensuring that reconstructions are both timely and precise. These advancements are crucial for legal proceedings, insurance claims, and the development of safer vehicle technologies.

3. Science Review of Vehicle Dynamics

3.1. Vehicle Coordinate System

When studying vehicle dynamics, it is important to obey a standardized vehicle coordinate system. This document will obey to International Standard Organisation (ISO) 8855 (2011) which defines the principal terms used for road vehicle dynamics.

The vehicle's body (Figure 3.1) is characterised by three translational and three rotational Degrees of Freedom (DOF). Its coordinate system, a rectangular right-handed system, has its origin at the vehicle's Centre of Gravity (COG) (Robert Bosch GmbH, 2018).

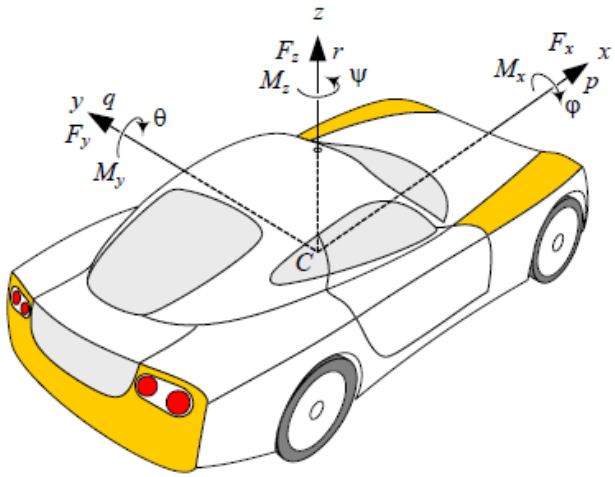

Figure 3.1 – Vehicle coordinate system following ISO 8855 (Adapted from Jazar (2008)).

Concerning the translational motions, they can be summarised as follows (Robert Bosch GmbH, 2018):

- The *x*-axis points forward (in the direction of travel, located at the vehicle's centre plane). In *x* direction is called *linear* or *longitudinal motion*;
- The *y*-axis points left when viewed in the direction of travel (perpendicular to the vehicle's centre plane). In *y* direction is called *lateral motion*;
- The *z*-axis points upwards. In the *z* direction is called *lift motion*.

On the other hand, the rotational motions can be defined as (AVL LIST GMBH, 2023; Robert Bosch GmbH, 2018):

- Pure rotation about the *x*-axis is called *roll* (positive on a left turn);
- Pure rotation about the *y*-axis is called *pitch* (positive when the vehicle is decelerating);
- Pure rotation about the *z*-axis is called *yaw* (positive on a left turn).

3.2. Vehicle Planar Dynamics Models

The study of vehicle planar dynamics is characterized when the forward velocity, lateral velocity and yaw values of the vehicle are important and sufficient to examine the vehicle's behaviour. When these conditions are met, the planar model is applicable (Jazar, 2008).

3.2.1. Two-wheel Model

When the roll motion of the vehicle is ignored and the vehicle's *xy* plane remains parallel to the road's *XY* plane, the *Two-wheel model* (or *Bicycle model*) can be used (Figure 3.2). Using this model, the vehicle's movement shall be considered similar to a flat box moving on a horizontal surface, which means that only translation in the *x* and *y* directions, and rotation about the *z*-axis (three DOF) are considered. Furthermore, the vehicle is reduced to a two-wheeled model (Jazar, 2008).

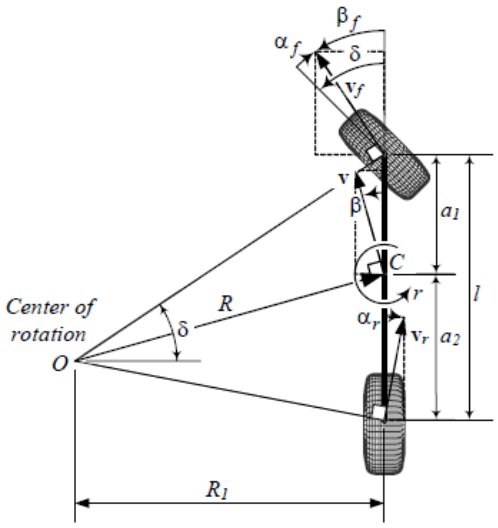

Figure 3.2 – Two-wheel model schematic (Adapted from Jazar (2008)).

The force system applied on a Two-wheel model (the front wheel is steerable) is expressed in equations 3.1, 3.2 and 3.3.

$$F_x = F_{x_F} \cos\delta + F_{x_R} - F_{y_F} \sin\delta \quad (3.1)$$

$$F_y = F_{y_F} \cos\delta + F_{y_R} + F_{x_F} \sin\delta \quad (3.2)$$

$$M_z = a_1 F_{y_F} - a_2 F_{y_R} \quad (3.3)$$

Where F_{x_F}, F_{x_R}, F_{y_F} and F_{y_R} are the planar forces on the tire print of the front and rear wheels, δ is the cot-average of the outer and inner steer angles, and a_1 and a_2 are the distances from the front wheel and rear wheel to the vehicle's COG, respectively (Jazar, 2008).

The Two-wheel model is considered an easily understandable and simple vehicle planar dynamics model, therefore being usually the first approach to vehicle dynamics studies. However, in some applications, its capabilities and range of application are not advanced enough (Fernández, 2012).

3.2.2. Two-track Vehicle Dynamics Model

When a 3 DOF vehicle dynamics model (e.g., Two-wheel model, 3.2.1) is not the most suitable solution for a given application, i.e., the necessary level of detail concerning the vehicle's dynamics cannot be obtained, a more complex vehicle dynamics model needs to be used (Fernández, 2012).

Taking into consideration the existing theory concerning vehicle dynamics, a *Two-track vehicle model* (Figure 3.3) may be used. This model has up to six DOF, which means, beyond the DOF of the Two-wheel model, the roll and pitch motions plus the vehicle's vertical dynamics can also be considered.

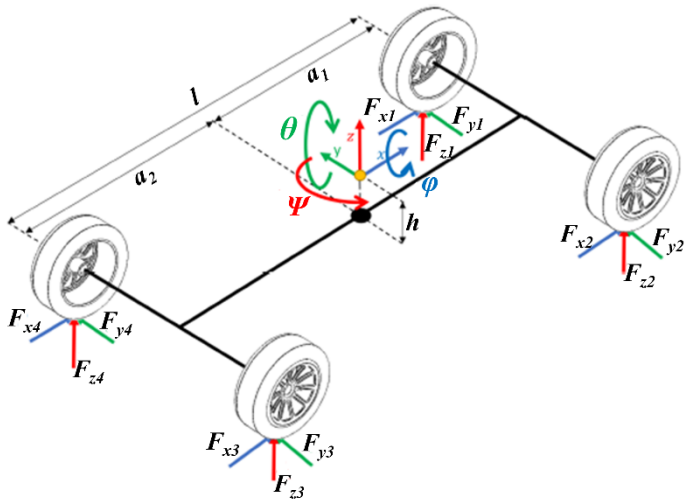

Figure 3.3 – Two-track vehicle dynamics model schematic (Adapted from Francisco (2022)).

Considering a vehicle planar motion, the vehicle's velocities and accelerations can be calculated by applying Newton's equations for the equilibrium of forces and momentum. The main external forces on the vehicle are generated by the tire-road contact and must be balanced with the vehicle's inertial forces (Equations 3.4, 3.5, and 3.6).

$$\sum_{wheel,i=1}^{j} F_{x_i} + \left[F_{ext_{x1}} + F_{ext_{x2}} + \cdots + F_{ext_{xk}} \right] = m \cdot a_x \tag{3.4}$$

$$\sum_{wheel,i=1}^{j} F_{y_i} + \left[F_{ext_{y1}} + F_{ext_{y2}} + \cdots + F_{ext_{yk}} \right] = m \cdot a_y \tag{3.5}$$

$$\sum_{wheel,i=1}^{j} T_{z_i} = I_z \cdot \dot{r}_z \tag{3.6}$$

Equations 3.4, 3.5 and 3.6, are suitable to calculate the vehicle's longitudinal and lateral motion plus the yaw motion like the Two-wheel model, however, it is an upgraded version since some extra external forces may be added (F_{ext}) (e.g., rolling resistance, drag resistance and road slope) and each tyre has its contribution to the overall vehicle's resultant force and momentum system.

3.3. Vehicle Vertical Dynamics

According to Wallentowitz (2004), real-world roads are actually somewhat uneven, which causes vertical movements of the vehicle and the passengers during driving. Small road unevenness in comparison to the tyre contact patch size can be compensated by the tyre's elasticity, whereas larger unevenness needs to be compensated with an element between the wheel and the vehicle structure, so that vertical accelerations do not transfer into the vehicle's structure. The suspension's job in vehicles is to reduce these vertical movements.

A suspension system is characterised by a length compensation element, whose force is a function of the length variation (Hooke's Law), which can be attributed to the spring (the different parts connected with springs generate the oscillating system) and an Energy absorbing element, the shock absorber (or damper).

The main essential criteria specifying the quality of a suspension system are:

- Suspension comfort for the passengers (effective acceleration affecting the passengers);
- Forces affecting the load (effective value of structure acceleration);
- Wheel load variation (effective value of the dynamic wheel load) which influences, for example, the grip between tyres and the road.

3.3.1. Longitudinal Mass Transfer During Acceleration and Braking

When a vehicle is accelerating or braking, the load (m_V) is transferred longitudinally between axles. When accelerating, the load is transferred longitudinally from the front axle to the rear axle in proportion to the longitudinal acceleration (a_x) and the ratio of the COG's height (h) to the wheelbase (l) (Gillespie, 1992). When braking, the opposite occurs.

Equations 3.7 and 3.8, define the vertical forces under the front and rear wheels when accelerating or braking, F_{z_F} and F_{z_R} respectively. Concerning the second member of equations 3.7 and 3.8, the first part represents the *static part* and the second part the *dynamics part* (Jazar, 2008).

$$F_{z_F} = m_V\ g\ \frac{a_2}{l} \pm m_V\ a_x \frac{h}{l} \tag{3.7}$$

$$F_{z_R} = m_V\ g \frac{a_1}{l} \pm m_V\ a_x \frac{h}{l} \tag{3.8}$$

When accelerating, the dynamics part gain of equation 3.7 is negative and in equation 3.8 is positive.

Picking up the first member and the first part of the second member for each equation 3.7 and 3.8, the longitudinal distances between the vehicle's COG for the front and rear axles, a_1 and a_2 respectively, can be obtained (equations 3.9 and 3.10).

$$a_1 = \frac{m_{Ra} \cdot l}{m_V} \tag{3.9}$$

$$a_2 = \frac{m_{Fa} \cdot l}{m_V} \tag{3.10}$$

Where m_{Ra} and m_{Fa} are the masses of the rear and front axles, respectively.

The vehicle's COG height, if not provided, must be experimentally determined.

Complementing what has been already stated so far, if the road's slope with an angle ϕ is considered, equations 3.9 and 3.10 can be transformed into equations 3.11 and 3.12. The dynamic parts are not influenced by the road's inclination (Jazar, 2008).

$$F_{z_F} = m_V\ g\ \left(\frac{a_2}{l}\cos\phi - \frac{h}{l}\sin\phi\right) \pm m_V\ a_x \frac{h}{l} \tag{3.11}$$

$$F_{z_R} = m_V\ g \left(\frac{a_1}{l}\cos\phi + \frac{h}{l}\sin\phi\right) \pm m_V\ a_x \frac{h}{l} \tag{3.12}$$

3.4. Vehicle Lateral Dynamics

When a vehicle is cornering, lateral acceleration will be present and, therefore, the tyres must develop lateral forces and slip angles will be present at each wheel. The slip angle, α, is the angle between the tyre's direction of heading and its direction of travel (Figure 3.4) (Gillespie, 1992).

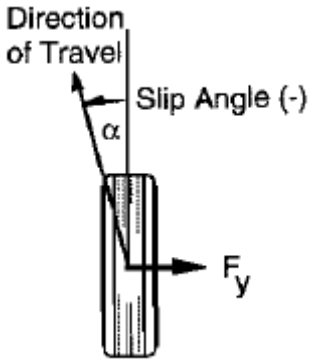

Figure 3.4 – Schematic of a tyre's slip angle, α (Adapted from Gillespie (1992)).

At low slip angles (≤ 5 degrees) the cornering force (F_y) at each tyre (i) grows linearly with the slip angle and can be represented by equation 3.13. The relationship between the cornering force and the slip angle is designated as *cornering stiffness*, C_α.

$$F_{y_i} = C_{\alpha_i}\, \alpha_i \tag{3.13}$$

The cornering stiffness is dependent on many variables (e.g., tyre size and type, number of plies, cord angles, wheel width) but load and inflation pressure are the main variables. The value should be consulted within the tyre manufacturer.

The sum of all tyres' cornering forces gives the vehicle's total lateral force.

3.4.1. Cornering Equations

For analysing the cornering equations of a vehicle, it is simpler to represent it by the Two-wheel model (Gillespie, 1992).

Taking into consideration equation 3.2, for a vehicle travelling forward with a speed of *"V"*, the sum of the forces in the lateral direction from the tyres must equal the mass times the centripetal acceleration, as represented by equation 3.14.

$$\sum F_y = F_{y_F} \cos\delta + F_{y_R} + F_{x_F} \sin\delta = \frac{m_v V^2}{R} \tag{3.14}$$

In addition, the vehicle needs to be in a moment equilibrium about the COG, therefore, the sum of the moments from the front and rear lateral forces must be zero (equation 3.15).

$$F_{y_F} \cos\delta \, a_1 + F_{x_F} \sin\delta \, a_1 - F_{y_R} a_2 = 0 \tag{3.15}$$

3.5. Longitudinal Dynamics

When accelerating or braking a vehicle, longitudinal forces must develop between the tyre and the ground. Considering equation 3.16, when a moment is applied to the spin axis of the tire, slip ratio occurs and a longitudinal force is generated, F_{x_i}, at the tire print and, that longitudinal force, is proportional to the normal force, F_{z_i} (Jazar, 2008).

$$F_{x_i} = \mu_{x_i} F_{z_i} \tag{3.16}$$

When accelerating, the relationship between the vehicle's longitudinal forces and its normal forces can be represented by equation 3.17:

$$F_{x_F} + F_{x_R} = -\left(\frac{F_{z_F} a_1 - F_{z_R} a_2}{h}\right) \tag{3.17}$$

As noted by Jazar (2008), the following point shall be considered. For example, when a vehicle is Front Wheel Drive (FWD), $F_{x_R} = 0$. The vertical tire print forces, F_{z_F} and F_{z_R}, will be the same, however, the required horizontal force to achieve the same longitudinal acceleration must be provided by solely the front wheels.

On the other hand, when braking, the relationship between the vehicle's longitudinal forces and its normal forces, can be represented by equations 3.18 and 3.19:

$$F_{x_F} = \frac{F_{z_F}\, a_1 - F_{z_R}\, a_2}{h} \cdot \frac{\beta_p}{(\beta_p + 1)} \tag{3.18}$$

$$F_{x_R} = \frac{F_{z_F}\, a_1 - F_{z_R}\, a_2}{h} \cdot \frac{1}{(\beta_p + 1)} \tag{3.19}$$

In the previous equations, β_p represents the "brake balance" which designates the brake force distribution between the front and rear axles. Some typical values for β_p are $\cong 2$ (front/rear = 66/33 [%]) on dry asphalt and $\cong 1{,}5$ (front/rear = 60/40 [%]) on wet asphalt (Guiggiani, 2014).

3.6. Vehicle Planar Motion

To define the motion of a vehicle characterised by a planar dynamics model, the *Newton-Euler equations of motion* can be used (equations 3.20, 3.21 and 3.22) (Jazar, 2008).

$$F_x = m\dot{v}_x - m\omega_z v_y \tag{3.20}$$

$$F_y = m\dot{v}_y - m\omega_z v_x \tag{3.21}$$

$$M_z = \dot{\omega}_z I_z \tag{3.22}$$

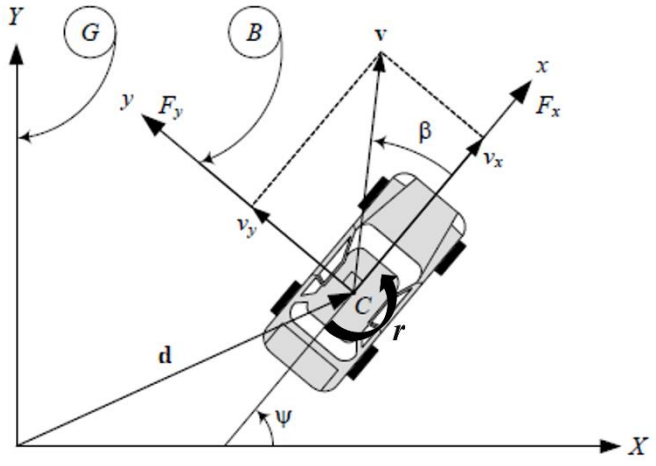

Figure 3.5 – Planar motion of a rigid vehicle (Adapted from Jazar (2008)).

When the translational and rotational velocities of a rigid vehicle are known, its path of motion (Figure 3.5) as a function of time can be obtained by integration using equations 3.23, 3.24 and 3.25 (Guiggiani, 2014; Jazar, 2008).

$$x = x_0 + \int \left(v_x \cos\psi - v_y \sin\psi\right) dt \tag{3.23}$$

$$y = y_0 + \int \left(v_x \sin\psi + v_y \cos\psi\right) dt \tag{3.24}$$

$$\psi = \psi_0 + \int r\, dt \tag{3.25}$$

4. Drivers' Behaviour in Pre-Impact Events and On-Board Assistance Technologies

This chapter aims to discuss drivers' behaviour when facing a pre-impact event (e.g., reaction time and reaction manoeuvres) and modern technologies developed to help drivers mitigate or attenuate the impact.

4.1. Reaction Time

The reaction time when driving can be defined as the time between the perception (identification) of a situation (cognitive stimulation) and the moment in which the driver initiates a response (action) to that situation by assuming the vehicle's control (Autoridade Nacional Segurança Rodoviária [ANSR], n.d.).

The drivers may have the perception that the reaction is instantaneous but, in reality, between the *perception* and the *action* there is a time gap. Different studies show different mean reaction time values. However, it can be considered that a reasonable reaction time is typically between 1 and 2 seconds (J. Martins, 2020).

Many times, people say that a good driver is someone who has good reflexes, something that is a false statement. There is a clear difference between *reaction time* and *reflex act*. In situations in which the drivers react without having previously precepted, that behaviour is called the *reflex response*. The overwhelming majority of response actions to a given traffic situation are not reflex responses, but responses following a precepted situation (ANSR, n.d.). Therefore, it is more correct to say that a good driver is someone who has good reaction times.

According to Green (2000), the reaction time can be divided into five main categories:

1. Sensation: The time it takes to detect an object in the roadway (e.g., an object moving in the roadway). Usually, auditory signals promote better reaction times than visual ones;
2. Perception: The time needed to recognise the meaning of the sensation (e.g., the moving object is a bicycle, a vehicle, …). Multiple signals may promote a slower reaction (increasing reaction time);

3. Awareness: The time necessary to decide if a reaction needs to be made and to mentally program the reaction (e.g., brake or steer?);
4. Response: The time it takes to initiate the programmed action. Normally, the more complex the movement, the longer the movement time;
5. Actuation: The time it takes to actuate (e.g., braking). For example, a braking actuation is usually 0,2 seconds slower than a steer intervention.

It shall be noted that the reaction time may be negatively affected by other factors, such as the physical and psychological state of the driver, the presence of alcohol in the blood (the higher the amount of alcohol present in blood, the higher the reaction time), fatigue, drowsiness, age, intake of medications that act on the nervous system (e.g., antidepressants, anxiolytics, …) and other external factors (use of telephone, for example) (ANSR, n.d.).

A curious fact is that the reaction time tends to decrease with the increase of speed by the fact that, usually, the drivers' state of alert increases with speed (increase in adrenaline), as well as with the danger of the road or driving. At higher speeds, the value tends to stabilize, with no significant changes (Green, 2000; J. Martins, 2020).

4.2. Emergency Braking

Emergency braking is one common behaviour of a driver when faced with an imminent collision. Emergency braking is characterised by the driver's request for the full braking system's power.

In the past, when braking assistance technologies did not exist, to perform an emergency braking, theoretically the driver would have to press violently the brake pedal to get full braking power. However, that hardly happened because a very high force in the brake pedal was necessary, and that force was difficult to achieve (physical effort); quite often the most likely outcome was for the wheels to lock due to friction losses. This would create unnecessarily long braking distances and a lack of vehicle stability.

Nowadays, all vehicles sold in European Union (EU) are equipped with a system specially developed for emergency braking assistance, which is designated by EBA (Emergency Brake Assist) (not to be confused with AEB (Automatic or Autonomous Emergency Braking), which is an Advanced Driver Assistance System (ADAS)).

The EBA system, launched in 1995, is defined by the following operating characteristics (Robert Bosch GmbH, 2018):

1. It interprets a rapid application of the brakes that fails to apply maximum braking force as an intention by the driver to carry out full braking. The system generates the braking pressure required to achieve a full braking effect;
2. The driver can "cancel" the full braking request at any time;
3. The pedal feedback is not altered under normal braking conditions;
4. The basic braking-system function is not diminished if the EBA fails;
5. It is designed to prevent accidental activation.

It is an absolute requirement that EBA (as well as all other brake-assistant system variants) shall be used in conjunction with an Antilock Braking System (ABS), due to the actively generated rapid brake-pressure rise beyond the wheel-lock limit.

Drivers usually think that ABS is the emergency braking assistance system, which is not correct. Engineering speaking, ABS is nothing more, nothing less than a *Wheel-Slip Control System* under braking (under acceleration, the same wheel-slip control principle will be managed by the ASR (*Antriebsschlupfregelung* or Traction Control System). The main goal of this system (ABS) is to ensure the optimum transmission of forces between tyres and road to keep the vehicle directionally stable and more easily controllable for the driver when braking (Robert Bosch GmbH, 2018). ABS is activated in conjunction with EBA as well as, for example, in a scenario when a vehicle has one half on a section of paved road and the other half on a section of muddy road, even with a very low speed and a light press on the brake pedal, the ABS will activate, since the wheels on the muddy section will tend to lock/decelerate faster than the ones in the paved road's section (an emergency braking is not being requested).

J. Martins (2020) states that in emergency braking, when ABS is already being activated, it does not really prevent accidents. This is usually related to the fact that drivers think that ABS reduces braking distance and promotes more powerful braking, which is not necessarily true. Faced with this false sense of security, some drivers tend to drive faster, and more aggressively, leaving the braking point for later.Clique ou toque aqui para introduzir texto.

4.3. Reaction Manoeuvres

The article from Mahmoudzadeh et al. (2019), identifies braking, lane changing and reducing speed as key manoeuvres that drivers use to avoid a collision. The performing of these manoeuvres is influenced by driver characteristics (e.g., age and gender), vehicle type, road conditions, and distractions (e.g., cell phone use and cognitive distractions).

In addition, cell phone use and cognitive distractions notably reduce the probability of performing effective manoeuvres, with cell phone use decreasing effectiveness by 66,4%. This article also concludes that environmental conditions also have an impact when performing manoeuvres; driving during weekends, on roads with curves, and multi-lane paths increases the likelihood of drivers performing manoeuvres.

Other articles published in the Advances in Transportation Studies (ATS) International Journal show that drivers could exhibit different types of behaviour to avoid collisions. These studies conclude that drivers often react by braking hard or swerving to avoid impact and they tend to focus intensely on the threat, which can affect their response's effectiveness.

Behaviour models, such as the Benefit/Cost/Deficit (BCD), suggest that drivers weigh the perceived benefits of certain actions against potential costs and deficits. An example can be a driver choosing to swerve instead of brake if he believes he has a higher chance of avoiding a collision with less risk of injury.

In addition, ADAS (subchapter 4.4) can significantly influence drivers' behaviour, often prompting quicker and more decisive actions to mitigate road accidents.

4.4. Advanced Driver Assistance Systems (ADAS)

ADAS have a wide range of applications. They can be divided into active systems (intervention in the driving dynamics) and passive systems (no intervention in the driving dynamics). These systems can also be divided into two categories: Comfort/Convenience and Safety. The first category is for the systems that support the driver with the long-term goal of fully automated driving and the second category belongs to the systems with the aim of accident avoidance or mitigation of accident consequences (Robert Bosch GmbH, 2018).

The main objective of these systems is to make the vehicle capable of perceiving its surroundings, interpreting them, identifying critical situations, and assisting the driver in performing manoeuvres.

A study performed in 2015 by the German In-depth Accident Study (GIDAS) analysed vehicle accidents involving personal injury, to assess the effectiveness of passenger-car functions of driver assistance (Robert Bosch GmbH, 2018). From that study, the following information can be retrieved:

- 26% of accidents occurred when turning or when crossing intersections;
- 18% of accidents did not involve other car (e.g., collision in a tree).
- 17% of occurrences were rear-ending accidents;
- 15% of occurrences were due to other car accidents;
- 10% of accidents were caused by drivers' errors;
- 6% of collision accidents took place during overtaking;
- 4% of accidents occurred when driving in the same direction, when changing lanes;
- 4% of accidents involved pedestrians.

These accidents could have been avoided with ADAS systems (e.g., Intersection Assistant, Lane Departure Warning, Overtaking Assistant, Emergency Braking systems, …).

A research made by BOSCH, at the time of publication of (Robert Bosch GmbH, 2018), concluded that up to 40% of accidents involving personal injury and passenger cars, still did not involve the operation of a vehicle-safety system.

A study made by the University of North Carolina at Charlotte (Gouribhatla & Pulugurtha, 2022) concluded that vehicles with ADAS like Lane Departure Warning, Blind Spot Assistant and Over Speed Warning, significantly influence driving behaviour, reducing lane departures and speeding. Furthermore, its impact varies with driving scenarios (e.g., rural, urban, freeway), meteorological conditions (e.g., lighting, weather) and drivers' characteristics.

Also, Utriainen et al. (2023) concluded that despite the presence of active safety systems (up to Society of Automotive Engineers (SAE) Level 2, i.e., partial driving automation), most fatal not-at-fault crashes involving modern passenger cars remain unavoidable. Should not be forgotten that these systems have limitations, therefore, they might not be able to prevent certain types of accidents. Since the results of this article indicate that current active safety systems may be able to prevent not-at-fault party fatal crashes only in a few cases, it

concludes that drivers' role in road safety still remains quite important, despite the deployment of active safety systems.

The article also highlights the importance of passive safety features (e.g., airbags, seatbelt pre-tensioners), which play a crucial role in protecting drivers during collisions; the combination of both active and passive safety measures is necessary for the best possible protection.

Another conclusion is that the development of Evasive Steering Assist (ESA) systems is essential to prevent not-at-fault crashes (enhancing vehicle control and responsiveness).

5. Event Data Recorder (EDR)

5.1. Introduction

When investigating a road accident, single pieces of information cannot provide a complete picture of what occurred and who was at fault. For example, eyewitness accounts of the accident are notoriously unreliable and environmental factors or road debris can change between the occurrence of the event and the on-scene investigation. Even a video may not capture key in-vehicle actions that influenced a crash (or event) (Robert Bosch GmbH, n.d.).

Road accident specialised Investigators know this too well and, for them, any comprehensive investigation requires a detailed analysis of the various human, vehicular, and environmental factors that may have influenced or caused the event. Because of these requirements and the advancement of technology in vehicles, a reliable source of information has emerged: The *Event Data Recorder* (EDR).

The EDR is a complementary safety function of the Airbag Control Module (ACM) and the overall vehicle safety system. It is usually called the "black box" for motor vehicles, as there are functional similarities between this device and the flight recorders found in aircraft, although they are systems with important differences, therefore, they should not be compared. For example, the EDR only records vehicle data in certain circumstances, i.e., only records data for a few seconds and does not record audio, video, or images from inside the vehicle, which means that it only records raw data from the vehicle's instruments and sensors. On the other hand, an aircraft flight recorder records the whole flight and records voice communications inside the aircraft's cockpit.

The EDR records vehicle data in two scenarios:

1. When there is a deployment event (e.g.: airbag, seat belt pre-tensioner);
2. When there is a non-deployment event that meets certain criteria (e.g.: an abrupt change in speed or direction that can indicate an external impact).

When these scenarios are met, the EDR records data from the vehicle's sensors and instruments for a few seconds (usually 5 seconds), recording important variables such as the vehicle speed, throttle pedal position, and other factors before, during and after a vehicle crash.

5.2. An Overview of EDR History

The development of the EDR for motor vehicles began in 1998, in the United States of America (USA), when the National Highway Traffic Safety Administration (NHTSA) started its development. At that time, American car manufacturers voluntarily supported that initiative. After that, in 2006, 64% of cars produced in the USA were equipped with an EDR for evaluation and in 2013 the regulation 49 CFR Part 563 (Code of Federal Regulations, 2013) was implemented and from there, every vehicle (American, European, or Asian) that is sold in the USA or Canada must be equipped with an EDR.

In Europe, more concrete in 2021, it was announced by the European Union (EU) Commission that EDR will soon become mandatory in EU following the United Nations (UN) Regulation No. 160 (EU Darts Group, n.d.; United Nations Economic Commission for Europe, 2021a) with 41 data elements for recording (mandatory and non-mandatory recording data).

The latest regulation EU 2022/545 (European Commission, 2022), which supplements the regulation EU 2019/2144 (European Parliament & Council of the European Union, 2019), added a further 24 data elements (a total of 65 data elements encompassing mandatory and non-mandatory recording data), concerning the specific test procedures and technical requirements for the type-approval of motor vehicles categories M1 and N1 concerning their EDR, states the following:

- From July 6th, 2022, new EU homologations or national homologations must comply with the regulation EU 2022/545 and with the technical requirements of 01 Series of Amendments to UN Regulation No 160 (United Nations Economic Commission for Europe, 2021b).

- Until July 1st, 2024, national authorities must accept non-EU homologations that comply with UN Regulation No 160 to obtain an EU homologation in conformity with the regulation EU 2022/545.

- From July 6th, 2024, new registrations concerning EU homologations or national homologations must comply with the regulation EU 2022/545 and with the technical requirements of 01 Series of Amendments to UN Regulation No 160.

- Until July 1st, 2026, national authorities must accept new registrations concerning non-EU homologations that comply with UN Regulation No 160 to obtain an EU homologation in conformity with the regulation EU 2022/545.

For notice, a M_1 motor vehicle category stands for: "Vehicles that were designed and built for the transport of passengers with, at least, four wheels and with no more than 8 seated seats, not including the driver's seat"; a N_1 motor vehicle category stands for: "Vehicles used for the transport of goods and having a maximum mass not exceeding 3,5 tonnes".

5.3. Vehicle Data Recorded by EDR

This subchapter will present which mandatory vehicle data elements are recorded by EDRs following the respective American or EU regulations (subchapter 5.2). In this report, it will be only presented the mandatory recorded vehicle data elements that are the most important from the point of view of studying vehicle dynamics behaviour before impact. For other vehicle data elements, the concerned regulation must be consulted.

Starting with American Regulation 49 CFR Part 563 (Code of Federal Regulations, 2013), Table 5.1 shows the mandatory data that is relevant for studying a vehicle's pre-impact dynamics.

Table 5.1 – Mandatory EDR data elements from American regulation 49 CFR Part 563 for studying a vehicle pre-impact dynamics.

DATA ELEMENT	*RECORDING INTERVAL/TIME (RELATIVE TO TIME ZERO)*	*DATA SAMPLE RATE (Hz)*
Delta-V, longitudinal	0-250 ms or 0 to End of Event Time plus 30 ms (whichever is shorter)	100
Maximum delta-V, longitudinal	0-300 ms or 0 to End of Event Time plus 30 ms (whichever is shorter)	N/A
Time, maximum delta-v	0-300 ms or 0 to End of Event Time plus 30 ms (whichever is shorter)	N/A
Speed, vehicle indicated	**-5.0 to 0 sec**	**2**
Engine throttle, % full (or accelerator pedal, % full)	**-5.0 to 0 sec**	**2**
Service brake, ON/OFF	**-5.0 to 0 sec**	**2**
Ignition cycle, crash	-1.0 sec	N/A
Ignition cycle, download	At the time of download	N/A
Multi-event, number of events	Event	N/A
Time from event 1 to 2	As needed	N/A

Complete file recorded (yes, no)	Following other data	N/A

An amendment to regulation 49 CFR Part 563 was published in January 2022 (National Highway Traffic Safety Administration, 2022), extending the recording period for certain data elements from the currently 5 seconds to 20 seconds, as well as increasing their sampling frequency from 2 Hz to 10 Hz (i.e., from 2 samples per second to 10 samples per second). The mandatory data elements affected by this amendment are highlighted in bold in Table 5.1. At the time of elaboration of this report, reliable information sources were not found regarding when this amendment would enter into force.

Concerning the European regulation EU 2022/545 (European Commission, 2022), its mandatory data relevant for studying a vehicle's pre-impact dynamics is shown in Table 5.2.

Table 5.2 - Mandatory EDR data elements from European regulation EU 2022/545 for studying a vehicle's pre-impact dynamics.

DATA ELEMENT	*RECORDING INTERVAL/TIME (RELATIVE TO TIME ZERO)*	*DATA SAMPLE RATE (Hz)*
Delta-V, longitudinal	0-250 ms or 0 to End of Event Time plus 30 ms (whichever is shorter)	100
Maximum delta-V, longitudinal	0-300 ms or 0 to End of Event Time plus 30 ms (whichever is shorter)	N/A
Time, maximum delta-v, longitudinal	0-300 ms or 0 to End of Event Time plus 30 ms (whichever is shorter)	N/A
Speed, vehicle indicated	-5.0 to 0 sec	2
Engine throttle, % full (or accelerator pedal, % full)	-5.0 to 0 sec	2
Service brake, ON/OFF	-5.0 to 0 sec	2
Ignition cycle, crash	-1.0 sec	N/A
Ignition cycle, download	At time of download	N/A
Time from event 1 to 2	As needed	N/A
Complete file recorded (yes, no)	Following other data	N/A
Delta-V, lateral	0-250 ms or 0 to End of Event Time plus 30 ms (whichever is shorter)	100

Maximum delta-V, lateral	0-300 ms or 0 to End of Event Time plus 30 ms (whichever is shorter)	N/A
Time, maximum delta-v, lateral	0-300 ms or 0 to End of Event Time plus 30 ms (whichever is shorter)	N/A
Time, maximum delta-v, resultant	0-300 ms or 0 to End of Event Time plus 30 ms (whichever is shorter)	N/A
Engine RPM	-5.0 to 0 sec	2
ABS activity	-5.0 to 0 sec	2
ESP activity	-5.0 to 0 sec	2
Steering wheel angle	-5.0 to 0 sec	2
Longitudinal acceleration (pre-crash)	-5.0 to 0 sec	2
Lateral acceleration (pre-crash)	-5.0 to 0 sec	2
Yaw rate	-5.0 to 0 sec	2
ASR Activity	-5.0 to 0 sec	2

Looking at Tables 5.1 and 5.2, it can be observed that the minimum requirements of the European regulation, in terms of mandatory data elements to be recorded, exceed those of the American regulation.

5.4. Retrieving Vehicle Pre-Crash Data from an EDR

To extract a vehicle's pre-crash data from an EDR, specialised tools are needed, which means, tools that contain hardware and software specific to this procedure. In addition to that, only a trained specialist shall perform this procedure, in order to protect the integrity of the EDR data, as well as allowing the data to remain unchanged for future access and road accident investigations.

The specialised tools can be manufacturer-specific or aftermarket-compatible ones. If none of these tools can be used, the electronic control unit which contains the EDR data (usually the ACM) needs to be sent to its manufacturer to extract the data.

Usually, the tool which is the most frequently used, is the aftermarket-compatible BOSCH Crash Data Retrieval tool (BOSCH CDR tool). This tool has "read-only" permissions for EDR data and, therefore, does not modify, erase or reset data on the EDR (the integrity of the EDR data is protected). The BOSCH CDR tool contains both hardware (interface modules and associated cables and adapters to connect to the vehicle) and software (Windows-based software that translates EDR data into a CDR report in PDF or CSV file formats) to retrieve data (Robert Bosch GmbH, n.d.). The following car manufacturers are not compatible with this tool, and they use their proprietary data-retrieval tools to extract data from their EDRs: Genesis, Hyundai, Jaguar Land Rover, KIA, and Tesla.

The pre-crash data from an EDR can be extracted in two ways. The most frequent and easy one is via the On-Board Diagnostics (OBD) port, in other words, retrieval using the Direct Link Connector (DLC) mode. To use this mode, the electronic structure of the vehicle must be operational. When this does not happen, for example, in a severely damaged vehicle with power loss, the Direct-to-Module (D2M) mode needs to be used. For using this last mode, the specialised tool is connected directly to the Electronic Control Unit (ECU) containing the EDR pre-crash data where vehicle-specific instructions, cables, and adapters are needed (e.g., ACM connectors are not standardised). The D2M mode is more time-consuming and complex because it requires the disassembly of the ECU from the vehicle, and it requires extra caution by the fact that the ECU is powered outside the vehicle and a major hit can start an event and overwrite new data over the desired one (Francisco, 2022).

5.5. EDR Data Output

Taking as an example the BOSCH CDR Tool, the EDR data can be exported in both PDF and CSV format files, as already mentioned in the last subchapter. In the CSV format file, the CDR file information and the raw data of every data point are obtained. On the other hand, in the PDF format file, a more complete report is obtained, which contains the CDR file information, the explanation of the data limitations regarding the concerned EDR and the data organised into graphics and tables (Francisco, 2022).

In the CDR file information (Figure 5.1), it can be retrieved, for example, the following information: The Vehicle Identification Number (VIN) corresponding to the EDR data (user input), EDR data imaging date, crash date, CDR tool version and license information, EDR

device type and the number of events recorded. In addition to this, there exists a text box for comments inputted by the user.

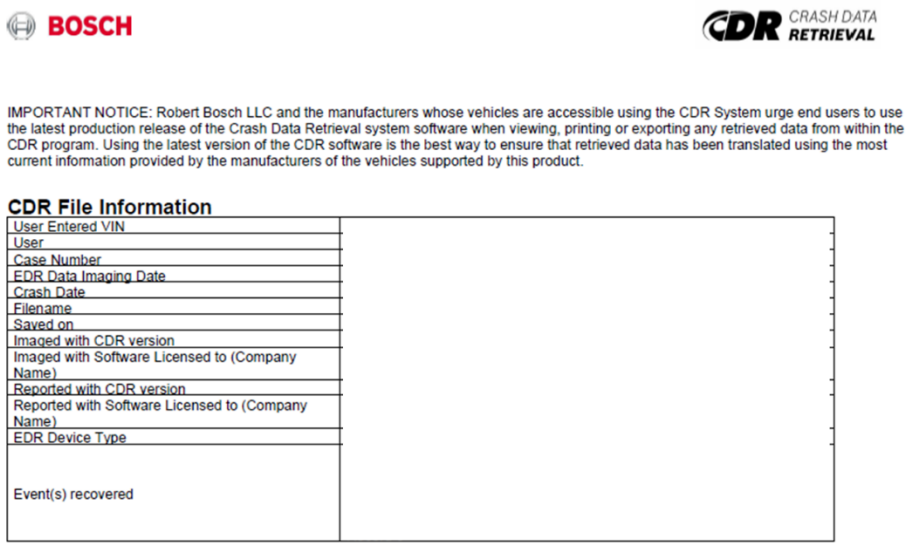

BOSCH

CDR CRASH DATA RETRIEVAL

IMPORTANT NOTICE: Robert Bosch LLC and the manufacturers whose vehicles are accessible using the CDR System urge end users to use the latest production release of the Crash Data Retrieval system software when viewing, printing or exporting any retrieved data from within the CDR program. Using the latest version of the CDR software is the best way to ensure that retrieved data has been translated using the most current information provided by the manufacturers of the vehicles supported by this product.

CDR File Information

User Entered VIN	
User	
Case Number	
EDR Data Imaging Date	
Crash Date	
Filename	
Saved on	
Imaged with CDR version	
Imaged with Software Licensed to (Company Name)	
Reported with CDR version	
Reported with Software Licensed to (Company Name)	
EDR Device Type	
Event(s) recovered	

Figure 5.1 – Example of BOSCH CDR file information.

Next, the data limitations concerning the EDR are addressed, such as those related to recorded crash events, data elements, and data element sign conventions (Figure 5.2).

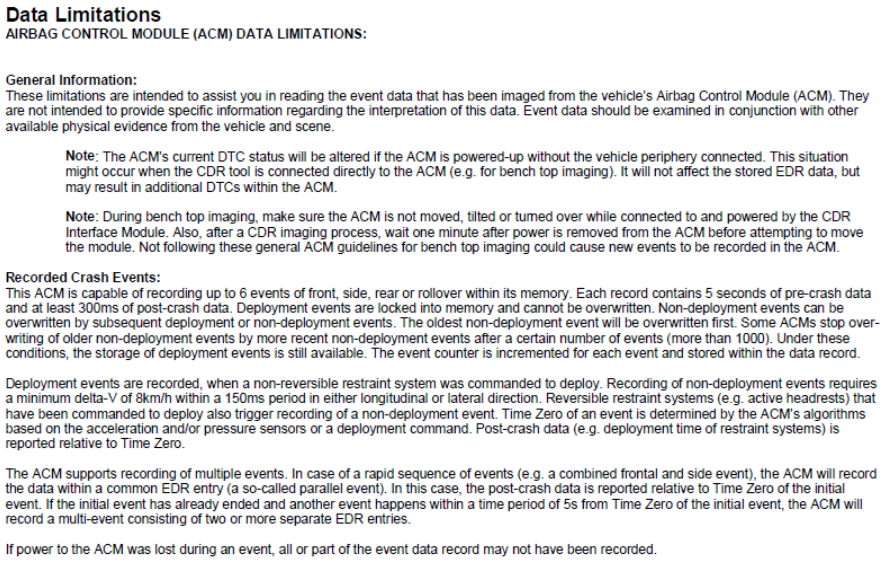

Data Limitations

AIRBAG CONTROL MODULE (ACM) DATA LIMITATIONS:

General Information:
These limitations are intended to assist you in reading the event data that has been imaged from the vehicle's Airbag Control Module (ACM). They are not intended to provide specific information regarding the interpretation of this data. Event data should be examined in conjunction with other available physical evidence from the vehicle and scene.

Note: The ACM's current DTC status will be altered if the ACM is powered-up without the vehicle periphery connected. This situation might occur when the CDR tool is connected directly to the ACM (e.g. for bench top imaging). It will not affect the stored EDR data, but may result in additional DTCs within the ACM.

Note: During bench top imaging, make sure the ACM is not moved, tilted or turned over while connected to and powered by the CDR Interface Module. Also, after a CDR imaging process, wait one minute after power is removed from the ACM before attempting to move the module. Not following these general ACM guidelines for bench top imaging could cause new events to be recorded in the ACM.

Recorded Crash Events:
This ACM is capable of recording up to 6 events of front, side, rear or rollover within its memory. Each record contains 5 seconds of pre-crash data and at least 300ms of post-crash data. Deployment events are locked into memory and cannot be overwritten. Non-deployment events can be overwritten by subsequent deployment or non-deployment events. The oldest non-deployment event will be overwritten first. Some ACMs stop over-writing of older non-deployment events by more recent non-deployment events after a certain number of events (more than 1000). Under these conditions, the storage of deployment events is still available. The event counter is incremented for each event and stored within the data record.

Deployment events are recorded, when a non-reversible restraint system was commanded to deploy. Recording of non-deployment events requires a minimum delta-V of 8km/h within a 150ms period in either longitudinal or lateral direction. Reversible restraint systems (e.g. active headrests) that have been commanded to deploy also trigger recording of a non-deployment event. Time Zero of an event is determined by the ACM's algorithms based on the acceleration and/or pressure sensors or a deployment command. Post-crash data (e.g. deployment time of restraint systems) is reported relative to Time Zero.

The ACM supports recording of multiple events. In case of a rapid sequence of events (e.g. a combined frontal and side event), the ACM will record the data within a common EDR entry (a so-called parallel event). In this case, the post-crash data is reported relative to Time Zero of the initial event. If the initial event has already ended and another event happens within a time period of 5s from Time Zero of the initial event, the ACM will record a multi-event consisting of two or more separate EDR entries.

If power to the ACM was lost during an event, all or part of the event data record may not have been recorded.

Figure 5.2 – Example of BOSCH CDR file containing EDR data limitations.

The “System Status at Event” (Figure 5.3) outputs some data concerning internal information of the EDR and some characteristics of the event. Since in some road accidents, the EDR records more than one event (multiple events), some of the information might be repeated for each one of them, depending on the system. Data examples:

- Event type: Frontal crash, rear crash, lateral crash, …

- Ignition cycle at crash and download: Indicates the number of ignition cycles (how many times the ignition was switched on) when the crash took place and when the data was exported (download). These numbers must be close to each other.

- Number of Events and the time between them or the time between the initial event: In the case of multiple events, the “initial event” usually refers to the first event to be registered in the timeline. Example: In a multiple events scenario where three events were recorded, the third event is the most recent one and the first event is the oldest one in the timeline.

- Vehicle information: mileage, VIN, …

- EDR internal information: Serial number, hardware and software part number, complete file recorded (if the EDR data recorded was completed or interrupted during the Event) and other specific information.

- Post-crash information: Information regarding the maximum lateral, longitudinal and resultant speed variation (Δv) after impact and for how much time.

BOSCH CDR CRASH DATA RETRIEVAL

System Status at Event (Record 1, Most Recent)

Event Counter at Event (Counts)	
Event Type	
Multi-Event, Number of Events	
Time from Initial Event to Current Event (msec)	
Time from Previous Event to Current Event (msec)	
Vehicle Mileage (km)	
Operating Time (min)	
Ignition Cycle at Event (Cycles)	
Ignition Cycle at Download (Cycles)	
Maximum Delta-V, Longitudinal (MPH [km/h])	
Time, Maximum Delta-V, Longitudinal (msec)	
Clipping Time, Longitudinal Acceleration Sensor (msec)	
Maximum Delta-V, Lateral (MPH [km/h])	
Time, Maximum Delta-V, Lateral (msec)	
Clipping Time, Lateral Acceleration Sensor (msec)	
Time, Maximum Delta-V, Resultant (msec)	
Time from Last Speed Data Sample (Precrash) to Time Zero (msec)	
Vehicle Identification Number (VIN)	
Part Number, ACM	
Complete File Recorded	

Figure 5.3 – Example of BOSCH CDR file containing System Status at Event outputs.

"Deployment Command Data" (Figure 5.4) consists of information concerning the vehicle's Supplemental Restraint Systems (SRS), for example: the time to deploy a seat belt pre-tensioner or an airbag.

Deployment Command Data (Record 1, Most Recent)

Pretensioner, Time to 1st Stage Deployment, Driver (msec)	18
Belt-Load Limiter, Time to Deployment, Driver (msec)	Not Deployed
Sill-End Pretensioner, Time to Deployment, Driver (msec)	Not Deployed
Frontal Airbag, Time to 1st Stage Deployment, Driver (msec)	18
Frontal Airbag, Time to 3rd Stage (Vent) Deployment, Driver (msec)	Not Deployed
Frontal Airbag, 3rd Stage (Vent) Disposal, Driver	Not Deployed
Knee Airbag, Time to Deployment, Driver (msec)	18
Side Airbag, Time to Deployment 1st Stage, Driver (msec)	Not Deployed
Side Curtain/Tube Airbag, Time to Deployment, Driver Side (msec)	Not Deployed
Pretensioner, Time to 1st Stage Deployment, Front Passenger (msec)	18
Belt-Load Limiter, Time to Deployment, Front Passenger (msec)	Not Deployed
Sill-End Pretensioner, Time to Deployment, Front Passenger (msec)	Not Deployed
Frontal Airbag, Time to 1st Stage Deployment, Front Passenger (msec)	18
Frontal Airbag, Time to 2nd Stage Deployment, Front Passenger (msec)	Not Deployed
Frontal Airbag, 2nd Stage Disposal, Front Passenger	Not Deployed
Frontal Airbag, Time to 3rd Stage (Vent) Deployment, Front Passenger (msec)	Not Deployed
Frontal Airbag, 3rd Stage (Vent) Disposal, Front Passenger	Not Deployed
Knee Airbag, Time to Deployment, Front Passenger (msec)	Not Deployed
Side Airbag, Time to Deployment 1st Stage, Front Passenger (msec)	Not Deployed
Side Curtain/Tube Airbag, Time to Deployment, Passenger Side (msec)	Not Deployed
Pretensioner, Time to 1st Stage Deployment, 2nd Row, Passenger Side (msec)	Not Deployed
Side Airbag, Time to Deployment 1st Stage, 2nd Row, Driver Side (msec)	Not Deployed
Side Airbag, Time to Deployment 1st Stage, 2nd Row, Passenger Side (msec)	Not Deployed
Rollover Protection System, Time to Deployment, Driver (msec)	Not Deployed
Rollover Protection System, Time to Deployment, Passenger (msec)	Not Deployed
Battery Disconnect, Time to Deployment (msec)	Not Deployed
High-Voltage Battery Deactivation, Time to Deployment (msec)	Not Deployed

Figure 5.4 – Example of BOSCH CDR file containing Deployment Command Data outputs.

"Pre-Crash Data -1 Sec" (Figure 5.5) contains information recorded one second before the Event, mainly, the status of the seat belts (if they were belted or not) and some other information concerning the airbags (if the airbag warning lamp was ON, for example).

Pre-Crash Data -1 Sec (Record 1, Most Recent)

Safety Belt Status, Driver	Belted
Seat Track Position Switch Status, Driver	Data Not Available
Safety Belt Status, Front Passenger	Not Belted
Seat Track Position Switch Status, Front Passenger	Data Not Available
Occupant Size Classification, Front Passenger	Data Not Available
Frontal Airbag Disable Indicator Status, Passenger	Off
Airbag Warning Lamp, Status	Off
Frontal Airbag Suppression Switch Status, Front Passenger	Not Suppressed

Figure 5.5 - Example of BOSCH CDR file containing Pre-Crash Data -1 Sec outputs.

"Pre-Crash Data -5 to 0 Sec" (Figure 5.6) shows all the mandatory data plus the optional ones (when applicable) from -5 to t_0.

Pre-Crash Data -5 to 0 sec (Record 2)

Time (sec)	Engine RPM (Combustion Engine) (RPM)	ABS Activity	Stability Control	Steering Input (deg)	Speed, Vehicle Indicated (MPH [km/h])	Accelerator Pedal (%)	Service Brake Activation
-5.0	5,760	No ABS Activity	No ESC Activity	0	57 [91]	50	Off
-4.5	4,736	No ABS Activity	No ESC Activity	0	61 [98]	100	Off
-4.0	4,864	No ABS Activity	No ESC Activity	0	65 [104]	0	Off
-3.5	4,800	No ABS Activity	No ESC Activity	0	63 [102]	0	On
-3.0	4,416	No ABS Activity	No ESC Activity	0	58 [94]	0	On
-2.5	4,096	No ABS Activity	No ESC Activity	0	54 [87]	0	On
-2.0	3,712	No ABS Activity	No ESC Activity	0	50 [80]	0	On
-1.5	3,392	No ABS Activity	No ESC Activity	0	45 [73]	0	On
-1.0	2,752	No ABS Activity	No ESC Activity	2	38 [61]	0	On
-0.5	2,176	No ABS Activity	No ESC Activity	0	30 [48]	0	On
0.0	1,984	No ABS Activity	No ESC Activity	4	24 [38]	0	On

Figure 5.6 - Example of BOSCH CDR file containing Pre-Crash Data -5 to 0 Sec outputs.

"Crash Pulse" (Figure 5.7) compiles both longitudinal and lateral acceleration pulses after t_0 during the time interval specified in the data limitations (usually 300 milliseconds).

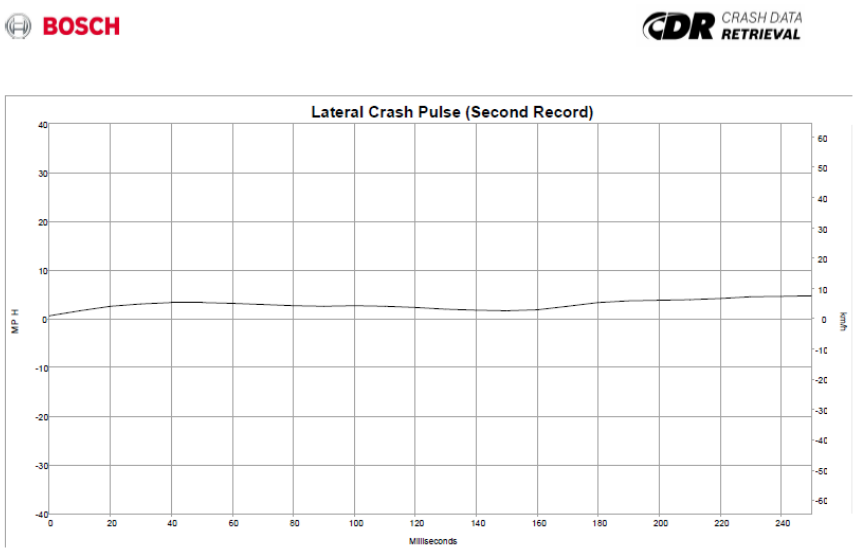

Figure 5.7 - Example of BOSCH CDR file containing Crash Pulse outputs.

"Normal acceleration" shows the normal acceleration (*z*-axis) after t_0 during the time interval specified in the data limitations (same appearance as Figure 5.7 but measurement in *g*).

"Vehicle Roll Angle" presents the vehicle's rotation and velocity around the *x*-axis after t_0 during the time interval specified in the data limitations (same appearance as Figure 5.7 but measurement in degrees). When this data is available, it can be evaluated, for example, rollover behaviours.

At the end, the EDR's internal Electrically Erasable Programmable Read-Only Memory (EEPROM) data is presented in hexadecimal format (Figure 5.8).

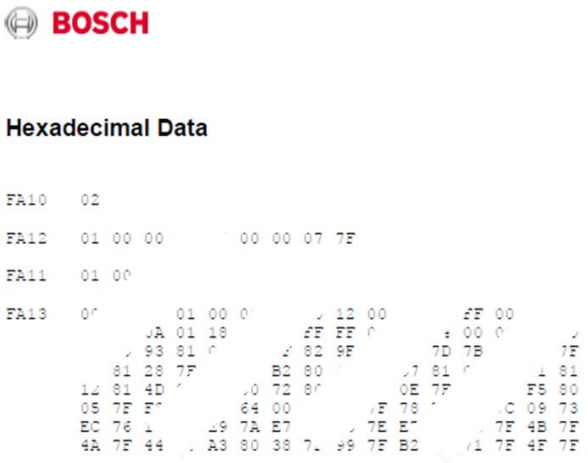

Figure 5.8 - Example of BOSCH CDR file containing hexadecimal data.

6. Road Accident Reconstruction Methodologies

In this chapter, it will be presented some methodologies to perform a reconstruction of a road accident. The following subjects will be discussed:

- Existing kinematic methods;
- Methods to collect information at the scene of a road accident;
- 2D and 3D sketches of a road accident scene.

6.1. Kinematic Methods

Kinematic methods are essential in the reconstruction of a road accident because they provide some clues to understand vehicle dynamics during an impact (collision).

Some kinematic methods will be described in the next subchapters.

6.1.1. Deformability/Rigidity of vehicles

Kinematic methods are essential in road accident reconstruction because they provide clues for understanding vehicle dynamics during a collision.

J. Martins (2020) states that a more rigid vehicle, colliding at the same speed, will dissipate the same energy (all its kinetic energy) with less deformation. Consequently, the collision will have a shorter distance and duration. Still, the collision's accelerations felt by the occupants will be greater (although nowadays, these accelerations can be mitigated with a vehicle's Supplemental Restraint System (SRS)).

When a vehicle suffers a collision there is a linear relationship between the deformation and the force needed to produce that deformation.

The force (F) needed for the impact that deformed the vehicle is given by equation 6.1:

$$F = A + B\,C \tag{6.1}$$

Where:

- A – Maximum force that does not result in permanent deformation [N/m];
- B – Relationship between force and deformation [N/m^2];

- C – Depth of deformation per width unit [m];
- F – Force per width unit [N/m].

To understand the calculations to obtain A, B and C components, please refer to J. Martins (2020).

The energy (E) dissipated during impact is given by equation 6.2:

$$E = \left[AC + \left(\frac{B}{2}\right)C^2 + \frac{A^2}{2B}\right]L = \frac{1}{2}m(\Delta v)^2 \tag{6.2}$$

Where:

- E – Energy dissipated during impact [J];
- m – Vehicle's mass [kg];
- L – Total deformation width [m].

Taking the last equation into account, it is also possible to define the collision's relative speed (equation 6.3):

$$\Delta v = \sqrt{\frac{BL}{m}\left(C + \frac{A}{B}\right)} \tag{6.3}$$

6.1.2. Equivalent Energy Speed (EES)

The Equivalent Energy Speed (EES) is a parameter used in crash analysis to determine the amount of energy required for permanent deformation during a collision, in other words, this model represents the kinetic energy (of speed) that was converted into deformation during an impact. The EES is obtained from the energy dissipated during impact ($E_{deformation}$) and the vehicle's mass (m) (equation 6.4) (J. Martins, 2020).

$$EES = \sqrt{\frac{2E_{deformation}}{m}} \tag{6.4}$$

In parallel, when a vehicle crashes into a rigid barrier it stores energy to recover (elastic energy, $E_{elastic}$). A new parameter can be used: the Equivalent Barrier Speed (EBS), which is the speed at which a vehicle collides into a rigid barrier (equation 6.5).

$$EBS = \sqrt{\frac{2(E_{deformation} + E_{elastic})}{m}} \tag{6.5}$$

The coefficient of recovery (k), equation 6.6, can be defined as the quotient between the vehicle's velocity after the collision (recovery speed) and the vehicle's speed before collision into a rigid barrier (EBS).

$$k = \frac{v_{recovery}}{EBS} \tag{6.6}$$

The previous equation (6.6) can be applied to a collision between two vehicles. It can be written as the quotient between the speed difference of the two vehicles after collision and before collision (equation 6.7).

$$k = \frac{v_{rec,2} - v_{rec,1}}{EBS_2 - EBS_1} \tag{6.7}$$

The relationship between EES and EBS is the following (equation 6.8):

$$EES = EBS\sqrt{1 - k^2} \tag{6.8}$$

6.1.3. Delta-V

Considering the literature (Francisco, 2022; Ruth, 2019; Shelby, 2011) the Delta-V (Δv) method is commonly used in road accident reconstruction to estimate the change in velocity sustained by a vehicle during a collision (change in velocity between pre-collision (v) and post-collision ($\tilde{v}$) trajectories of a vehicle, equation 6.9), therefore, it quantifies the severity of the collision. This method began to be used in the 1970s and it is considered by some researchers to be the best single predictor of crash severity.

$$\Delta v = \tilde{v} - v \tag{6.9}$$

It can be defined a simplistic equation for Δv by considering a planar crash between two vehicles. Vehicle 1 with mass m_1 is travelling at a pre-collision velocity v_1 and is encroaching on Vehicle 2, which moves at a lower velocity, with mass m_2 and pre-collision velocity v_2. The Δv for each vehicle is presented by the equations 6.10 and 6.11:

$$\Delta v_1 = \tilde{v}_1 - v_1 \tag{6.10}$$

$$\Delta v_2 = \tilde{v}_2 - v_2 \tag{6.11}$$

Vehicle 1, which is travelling at higher velocity, collides with vehicle 2. Assuming that the collision can be considered inelastic, which means that the kinetic energy of the system is not conserved, and applying the law of conservation of momentum, since a closed system between the two vehicles is being considered, the quantity of movement after the collision is given by $(m_1 + m_2) \cdot \tilde{v}$. The equation which conserves momentum during the collision is presented in equation 6.12 (considering that the vehicles stay together).

$$\begin{aligned} m_1 v_1 + m_2 v_2 = (m_1 + m_2)\tilde{v} \ \leftrightarrow \\ \leftrightarrow \tilde{v} = \frac{m_1 v_1 + m_2 v_2}{(m_1 + m_2)} \end{aligned} \tag{6.12}$$

Considering equations 6.12, the previous equations 6.10 and 6.11 can be rewritten (equations 6.13 and 6.14).

$$\Delta v_1 = \frac{m_2}{m_1 + m_2}(v_2 - v_1) \tag{6.13}$$

$$\Delta v_2 = \frac{m_1}{m_1 + m_2}(v_1 - v_2) \tag{6.14}$$

This is a simplistic overview, since a one-dimensional scenario is being considered (the two vehicles are travelling in the same linear dimension), whereas typically two-dimensional trajectories should be considered. Another point is that an inelastic scenario is also being considered, and collisions always have some elastic effects (a coefficient of restitution). Based on this, Shelby (2011) states that calculations with these simplifications may result in an error factor of 10% to 30% between the calculated and the real values.

To complement what has been written in this subchapter, another type of approach is to use velocity vectors to describe the collision. Using this, the pre- and post-collision velocities and direction of both vehicles can be known by retrieving some information from the accident's local scene.

Three vectors can be used:

- **Approach Velocity Vector**: It indicates the pre-collision speed and direction of the first vehicle;
- **Change in Velocity Vector**: It indicates the pre-collision speed and direction of the second vehicle (which can be converted to the force impaired on the first vehicle from the second vehicle during impact);
- **Departure Velocity Vector**: It indicates the post-collision speed and direction of the first vehicle.

In Figure 6.1, it can be observed that the first vehicle (blue arrow) is hit by the second vehicle (green arrow) by a specified Principal Direction of Force (PDOF) angle (the PDOF angle represents the difference in direction between the Approach Velocity Vector and the Change in Velocity Vector), changing the trajectory's direction of the first vehicle (red arrow) by a departure angle, θ (the departure angle represents the difference in direction between the Approach Velocity Vector and the Departure Velocity Vector). This approach facilitates the study of impact angles between the two vehicles.

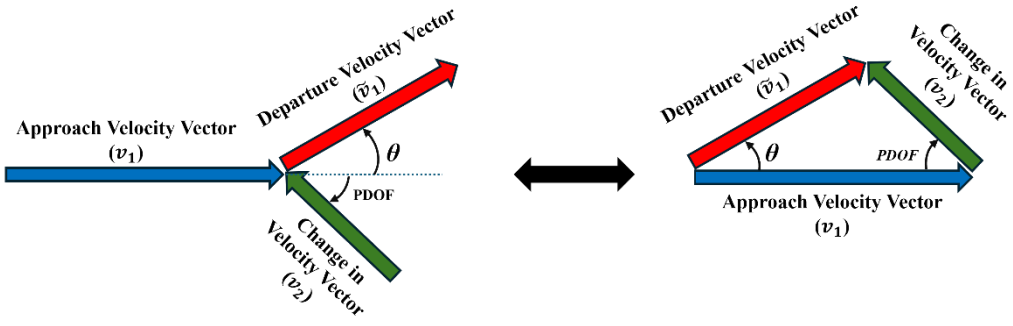

Figure 6.1 – Principal Direction of Force (PDOF) triangle schematic.

6.1.4. Impulse-Momentum Method

According to Brach & Brach (2011), the Impulse-Momentum method in road accident reconstruction is used to analyse the forces involved in a collision and determine various parameters such as the velocity of the vehicles at the time of impact. It is based on the principle of conservation of linear momentum, which states that the total linear momentum of a closed system remains constant if no external forces act on it.

The Planar Impact Mechanics states that the rotational effects can be treated rigorously. This also can be treated as the *Rigid-Body Impact Theory* which means that, during a collision, the rotational inertia is considered, as well as each vehicle's pre-impact dimensions.

Figure 6.2 shows the free-body diagram of the planar impact of two vehicles.

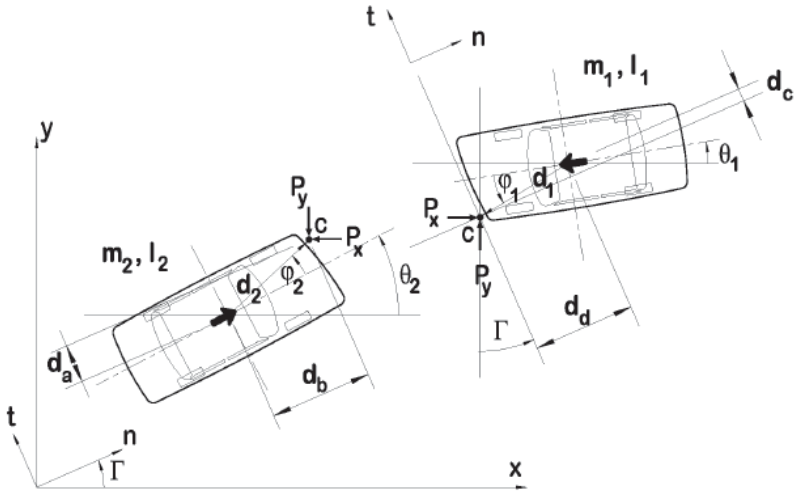

Figure 6.2 – Free-body diagram of the planar impact of two vehicles (Adapted from Brach & Brach (2011)).

From Figure 6.2 it can be observed that vehicles 1 and 2 with mass m_1 and m_2 and with inertia I_1 and I_2, respectively, collide at point "C". An impact plane (*nt*) is formed which has an offset of Γ relative to the plane *xy*. The point "C" is located relative to the centres of gravity by distances, d_1 and d_2, and angles φ_1 and φ_2, respectively. The angles θ_1 and θ_2 indicate the vehicle's orientation at the time of impact.

The distances d_a, d_b, d_c and d_d are the moment arms of the normal and tangential impulse components P_n and P_t. These distances can be obtained using equations 6.15, 6.16, 6.17 and 6.18.

$$d_a = d_2 \sin(\theta_2 + \varphi_2 - \Gamma) \quad (6.15)$$

$$d_b = d_2 \cos(\theta_2 + \varphi_2 - \Gamma) \quad (6.16)$$

$$d_c = d_1 \sin(\theta_1 + \varphi_1 - \Gamma) \quad (6.17)$$

$$d_d = d_1 \cos(\theta_1 + \varphi_1 - \Gamma) \quad (6.18)$$

In some situations, the *Point-Mass Collision Theory* can be used instead of the previous (general) method which is complex and time-consuming. The Point-Mass Collision Theory can be used, mainly, when the post-impact rotational velocities of vehicles are relatively small. This method consists of reducing the whole vehicle to a single point.

Some considerations should be made when using this method:

1. The initial directions of travel of the vehicles are known;
2. After the collision, it is assumed that each vehicle travels to rest over a known, approximately straight-line path;
3. The postimpact motion is over a relatively flat surface with uniform drag coefficients (*f*);
4. The effect of forces other than the intravehicular contact forces can be neglected (e.g., friction between the wheels and the ground).

Considering the previous factors, it shall be assumed that the collision should be at a relatively high speed and involve considerable damage.

Using equations 6.19 and 6.20, a good approximation concerning the vehicles' velocities just before the impact can be obtained. Equation 6.19 represents the conservation of momentum in the *x* direction and equation 6.20 in the *y* direction.

$$m_1 v_1 cos\theta_1 + m_2 v_2 cos\theta_2 = m_1 \tilde{v}_1 cos\varphi_1 + m_2 \tilde{v}_2 cos\varphi_2 \quad (6.19)$$

$$m_1 v_1 sin\theta_1 + m_2 v_2 sin\theta_2 = m_1 \tilde{v}_1 sin\varphi_1 + m_2 \tilde{v}_2 sin\varphi_2 \quad (6.20)$$

Following the consideration "3.", the post-impact velocities ($\tilde{v}_1$ and $\tilde{v}_2$) can be calculated using the stopping distance formula, equation 6.21. *f* represents the drag coefficient, *g* the acceleration of gravity and *d* the distance travelled in a straight line.

$$\tilde{v} = \sqrt{2fgd} \quad (6.21)$$

Looking closely at equations 6.19 and 6.20, it can be seen that they assume that no energy is dissipated during a collision by deformation of the vehicles' bodies; therefore, they assume a purely elastic collision.

Since a purely elastic collision does not happen, these equations can be improved using the *Monte Carlo Method*. It consists of adding a *T* vector to equations 6.19 and 6.20 that represents an equivalent quantity of motion to the dissipated strain energy.

Using this method, equations 6.19 and 6.20 can be rewritten, and equations 6.22 and 6.23 can be obtained.

$$m_1 v_1 cos\theta_1 + m_2 v_2 cos\theta_2 = m_1 \tilde{v}_1 cos\varphi_1 + m_2 \tilde{v}_2 cos\varphi_2 + T cos\alpha \quad (6.22)$$

$$m_1 v_1 sin\theta_1 + m_2 v_2 sin\theta_2 = m_1 \tilde{v}_1 sin\varphi_1 + m_2 \tilde{v}_2 sin\varphi_2 + T cos\alpha \quad (6.23)$$

6.2. Methods for Collecting Information at the Scene of a Road Accident

Collecting information at the scene of a road accident is fundamental for a road accident investigation. The information is usually collected using measurement and photography tools and it shall be taken with impartiality and rigor. During the information-collecting phase, all hypotheses are open and all possible crash scenarios shall be considered.

At the scene of a road accident, Investigators usually try to collect information that may provide clues as to how the accident occurred; below is a list of some relevant pieces of information:

- Braking marks;
- Skid marks;
- Vehicle(s) position(s);
- Debris;
- Remains;
- Scratch marks;
- Shape of damages.

The following subchapters will present some of the most used road accident data collection tools.

6.2.1. Measuring Tape and Measuring Wheel

Using a measuring tape and/or a measuring wheel is the easiest way to acquire information in a road accident. These measurement tools are mainly used to build sketches, and their accuracy depends on the operator's skills.

They usually give good results in straight and plane sections, although, the result's quality may decrease with the road's complexity (e.g., turns, bumps), plus human error.

6.2.2. Photogrammetry

Photogrammetry is the process of obtaining quantitative dimensional information about physical objects through the process of recording, interpreting, and measuring photographic images (Brach & Brach, 2011).

There are two types of photogrammetry: "aerial" photogrammetry (two cameras with parallel view lines, at a fixed, known distance apart) and "close-range" photogrammetry (two or more camera positions with large differences in view angles and variable separation distance from the objects being measured). The last one is the one which is applicable in the field of automotive accident reconstruction (distance from camera to object is short when compared to aerial photogrammetry).

"Reverse projection" photogrammetric method is used to extract information about the location or size of an object that is no longer visible at the accident scene (when the object is contained in a single scene photograph). Usually, this information pertains to the position of a vehicle, vehicle component, or mark made by a vehicle.

The "Planar" photogrammetric method is another way of determining the location of a mark (or other similar physical evidence) that has been captured on a photograph taken at an accident scene. This method can be used when the mark lies on a surface that can be reasonably approximated by a geometric plane (e.g., road's surface). Using a mathematical transformation between the planar coordinate system affixed to the film plane and the planar coordinate system on the road's surface, certain information about the road surface is available.

"Three-Dimensional" photogrammetric method is used when reverse projection and planar photogrammetric methods cannot be applied which means that this method offers the only means for the extraction of useful dimensional information from an accident scene (e.g.,

an unmeasured rest position of a vehicle shown in photographs is required for reconstruction purposes). This method is considered to be complicated, therefore, it has traditionally been beyond the reach of most road accident reconstructions.

6.2.3. Light Detection and Ranging (LiDAR)

The operation principle of a Light Detection and Ranging (LiDAR) tool consists of projecting a laser beam onto a surface and taking into account the time between the emission and reflection of the laser beam, the distance to the object can be obtained. This tool gathers the evidence quickly and efficiently by creating 3D point clouds of on-scene information (FARO, n.d.).

These days, it exists various applications of LiDAR tools, e.g., terrestrial, mobile and drones.

"Terrestrial laser scanning" consists of LiDARs mounted on tripods where they capture high-resolution, three-dimensional data of the crash site (this method is mostly used for detailed, localized surveys, providing precise measurements of distances, angles, and surfaces).

"Mobile LiDAR Technology" offers a versatile and efficient means of quickly capturing data over larger areas (quickly scanning extensive stretches of roadways, capturing detailed information while in motion). This method is necessary for reconstructing accidents that involve long skid marks, debris fields, or multiple collision points spread over a distance.

"LiDAR Drones" provide high-resolution, aerial views of the crash site, capturing data from angles that ground-based scanners cannot achieve. The aerial perspective is particularly useful for understanding the overall layout of the accident scene (e.g., the relationship between different elements of the accident). It shall be noticed that the data's accuracy is not as detailed as the one provided by a terrestrial laser scanner.

6.2.4. Drones

With Drones (Unmanned Aerial Vehicle), accident reconstruction is simpler and more efficient by the fact the significant reduction in time required to map out the scene of an accident site.

From research made by Purdue University, USA (The Drone Centre, 2023), Investigators can map an accident site in just five to eight minutes using drones.

Drones provide visual data, from different angles and heights, which can be used to generate actionable insights using mapping software, e.g., 2D orthomosaic maps or 3D models.

6.3. 2D and 3D Sketches of a Road Accident Scene

A sketch of an accident scene (commonly known by the French word *"croquis"*) is a draft where it is possible to show the accident location and all the information concerning the accident itself (e.g., where the vehicles are located, point of impact, braking distances). As already mentioned, the sketch is a draft, therefore, it does not have to be to scale (R. F. G. Martins, 2018).

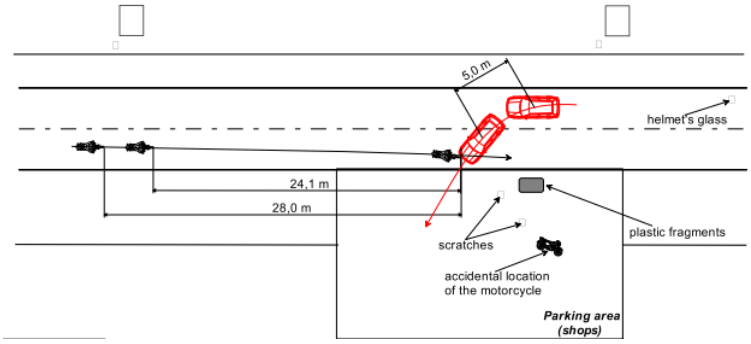

Figure 6.3 – Example of a sketch (*croquis*) of a road accident (Adapted from Wrona & Rybicka (2021)).

Concerning a bidimensional (2D) *croquis*, the most frequently used because of its simplicity, the first step consists of drawing the place where the accident took place. Usually, there are three ways of making a *croquis*: a draft by hand, a draft with a computer or a computer-scaled one (e.g., using a satellite image of the accident site using Google Maps)

The second step consists of drawing the important information about the accident (examples already mentioned). There are mainly three possibilities for presenting the information:

- Measurements by Cartesian coordinates: The measurements are presented orthogonally based on a Cartesian referential. For this, a fixed point of the accident site is the origin of this referential (e.g., tree, lamp post). The measurements are taken from that defined origin;
- Measurements by triangles: The measurements are taken from two reference points;

- Measurements by linear distance: The measurements are taken using a linear measurement between what is being measured and a reference/fixed point.

On the other hand, nowadays, the use of three-dimensional (3D) *croquis* is a reality (Figure 6.4). R. F. G. Martins (2018) states that a 3D *croquis* allows the reconstruction of a road accident in sloped locations and with precision (a thing that a 2D *croquis* cannot deliver since the third dimension does not exist). In addition to this, the author also states that it allows Investigators to reinforce statements like "Driver from Vehicle A could not see Vehicle B by the fact that a tree was present". The quality of a 3D *croquis* can be impacted by meteorological conditions (e.g., rain, sunlight, shades), the presence of trees near the road, tunnels and stopped vehicles.

Figure 6.4 – Example of a 3D *croquis* (Adapted from R.F.G. Martins (2018)).

7. Pre-impact Dynamics Simulator Development

As stated in Chapter 1, this project aims to recreate vehicles' trajectories before collisions using data retrieved from Event Data Recorders (EDR), integrate this data through a vehicle dynamics model, and thereby accelerate the accident reconstruction process.

The steps for construction, validation and application of a Pre-Impact Dynamics Simulator (PIDS) to achieve this project's goal are described in this chapter.

In subchapter 7.1, the simulator's structure will be presented. In chapter 7.2, the simulator's dynamics results will be validated using AVL VSM™ software and, finally, in subchapter 7.3, the simulator will be applied to two different real-world cases.

7.1. Simulator Structure

This subchapter pretends to present the structure of the PIDS developed, i.e., the dynamics models applied, how data is organised and imported for the simulator, which inputs it needs, its calculations and its outputs.

The simulator was developed and programmed in Python language and its main requirements consist of three fundamental components:

1. Receive, as an input, previously collected and organised EDR data in a CSV file. For this, a universal file template had to be made, so that it is able to work with different EDRs, i.e., it had to be the most universal possible. The simulator's operation is based on the structure of that universal template file.
2. It must read the input data file, treat it and make calculations using a vehicle dynamics model.
3. It must generate a vehicle's 2D pre-impact trajectory and other outputs previously defined by the user, which will be studied and evaluated afterwards.

7.1.1. Organisation and EDR Data Import

To run the simulator, it needs to be provided with EDR data. It cannot simply be provided an EDR PDF or CSV report format files because their structure will change from EDR to EDR and, for the simulator to read and interpret those files, it would require much deeper programming knowledge, which is not the intended objective of this project.

Taking this into consideration, the solution was to create a universal Excel template file (Appendix A, Figure A.1) that would fit most EDR reports. Once filled with the required EDR data, it can be converted to a CSV format file and, with basic programming knowledge, the Python code of the simulator can read and interpret the data (the programming structure will be presented with more detail in subchapter 7.1.4).

Now, it will be described the Excel template file itself, which will be the basis for importing data for the simulator (PIDS inputs). This phase requires the user to perform some manual tasks in order to transfer the required EDR data from the proprietary EDR report into the universal template Excel file. The template gathers the following information:

1. "GENERAL INFORMATIONS" section: "Number of Events" and "Norm" of the data to be imported (European or American). The "Number of Events" will be an input for the simulator to run the Python code while the "Norm" is just a label for information.

2. "SYSTEM STATUS AT EVENT (SSAE)" section: Inputs from data concerning internal information of EDR and some characteristics of the Event. The mandatory input data from this section to run the Python code are: "In. Event to Curr. Event. (sec)" (Time between the initial event to current event), "Last Data Sample (sec)" (time elapsed since the last reading of data in the vehicle's communication networks) and "Prev. Event to Curr. Event. (sec)" (Time between the last and current events). For further details, please refer to subchapter 5.5.

3. "PRE-CRASH DATA (PCD)" section: Inputs from EDR pre-crash data (-5 to t_0):
    - Time (Instant of time of data line) (*s*);
    - Vehicle Speed (*km/h*);
    - TPS (Throttle Position Sensor) (*%*);
    - Engine rpm (number of engine revolutions) (*rpm*);
    - Steering input (Steering wheel angle) (º);
    - Service Brake Actuation (Actuation of brake pedal) (Boolean);
    - ABS Activity (Actuation of Antilock Braking System (ABS)) (Boolean);
    - ESP Activity (Actuation of Electronic Stability Program (ESP)) (Boolean);

- Longitudinal Acceleration (longitudinal acceleration sustained by the vehicle, *x*-axis) (*g*);
- Lateral Acceleration (lateral acceleration sustained by the vehicle, *y*-axis) (*g*);
- Angular velocity (rotational velocity of the vehicle along the normal *z*-axis) ($^{o}/_{s}$).
- Event (Comparison control variable for programming purposes, not retrieved from EDR report. Must correspond to the event number in question);
- Algorithm triggering (Comparison control variable for programming purposes, not retrieved from EDR report. It should be "1" at t_0 of each event) (Boolean).

The last two variables are required to calculate the Principal Direction of Force (PDOF) and the departure angles at the time of impact.

4. "SIGN CONVENTION INPUTS (SCI)" section: Boolean inputs from sign convention for lateral movement (0 - positive from left to right, 1 – positive from right to left), steering and yaw rate (or angular velocity) (for the last two variables: 0 – positive clockwise, 1 – positive counter-clockwise). These inputs are needed to express some variables according to the norm ISO 8855 (for further details please refer to subchapter 3.1).

5. "BICYCLE MODEL INPUTS (BMI)" section: Inputs for vehicle dynamics models calculations:
   - Vehicle mass (*kg*);
   - Tyre Cornering Stiffness Front (*N/rad*);
   - Tyre Cornering Stiffness Rear (*N/rad*);
   - FRONT axle weight (*kg*);
   - REAR axle weight (*kg*);
   - Steering ratio (relationship between steering wheel angle and wheel angle);
   - COG height (Centre of Gravity's (COG) height) (*m*);
   - Wheelbase (*m*).

6. "POST-CRASH DATA (POCD)" section: Inputs concerning the event sum of both post-crash ΔV longitudinal and ΔV lateral parcels. The user must make the sum of each variable in advance for all available instants of time and introduce them accordingly to the norm ISO 8855 (for a rear impact, ΔV longitudinal is positive and, for a right-side impact, ΔV lateral is positive) (refer to subchapter 7.1.3).

For the sections SSAE, PCD and POCD, the first line (or the first 5-second block in the case of the PCD section) refers to the most recent event, i.e., data should be introduced from the most recent event to the oldest. A direct attribution to the event number in the EDR report must not be made as it may not match the desired order. This evaluation must be carried out carefully and rigorously by the user.

7.1.2. Pre-Impact Dynamic Models

To calculate a vehicle pre-impact trajectory, it will be needed to implement a mathematical vehicle dynamics model. For this project, the model to be implemented will be based on the Two-wheel model previously described in subchapter 3.2.1.

First, let's consider Figure 3.2 to begin the approach. From Figure 3.2, the angles δ, α_f, α_r can be extracted and be consolidated in Figure 7.1.

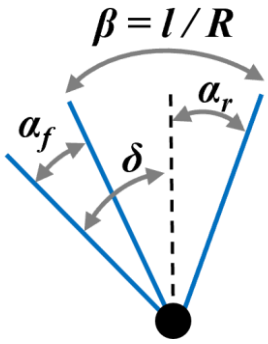

Figure 7.1 – Two-wheel model angles relationship.

By analysing both Figure 3.2 and 7.1, it can be observed that β, which is the global sideslip angle (Jazar, 2008), can be obtained using equation 7.1 and its relationship equals the vehicle wheelbase (l) divided by the radius of turn (R), that relationship is shown in equation 7.2 (Gillespie, 1992).

$$\beta = \delta - \alpha_f + \alpha_r \tag{7.1}$$

$$\beta = \frac{l}{R} \tag{7.2}$$

Equation 7.1 will be the reference equation to construct the vehicle dynamics model. From Gillespie (1992), the difference between α_f and α_r is given by equation 7.3.

$$\alpha_f - \alpha_r = \frac{K}{g} a_y \tag{7.3}$$

That difference equals the "Understeer Gradient" (K) divided by the acceleration of gravity (g) multiplied by the vehicle lateral acceleration (a_y). "K" (equation 7.4) determines the magnitude and direction of the steering inputs required and equals the difference between the ratio of the load of both front and rear axles to the cornering stiffness of the tyres on the axle (Gillespie, 1992).

$$K = \frac{F_{z_F}}{C_{\alpha_F}} - \frac{F_{z_R}}{C_{\alpha_R}} \tag{7.4}$$

The loads of front and rear axles (F_{z_F} and F_{z_R}) can be calculated using equations from 3.7 to 3.10.

Having done all the necessary calculations and introducing the necessary inputs from the EDR template, β can be obtained and the vehicle longitudinal and lateral velocities, v_x and v_y respectively, can be calculated (equations 7.5 and 7.6).

$$v_x = V \cos \beta \tag{7.5}$$

$$v_y = V \sin \beta \tag{7.6}$$

Since the vehicle motion is being calculated for discrete instants of time, equations from 3.23 to 3.25 can be adapted, and the vehicle pre-impact trajectory can now be calculated using equations 7.7, 7.8 and 7.9.

$$x_i = x_{i-1} + \int_{t_{i-1}}^{t_i} \left(v_{x_{i-1}} \cos\psi_i - v_{y_{i-1}} \sin\psi_i\right) dt \tag{7.7}$$

$$y_i = y_{i-1} + \int_{t_{i-1}}^{t_i} \left(v_{x_{i-1}} \sin\psi_i - v_{y_{i-1}} \cos\psi_i\right) dt \tag{7.8}$$

$$\psi_i = \psi_{i-1} + \int_{t_{i-1}}^{t_i} r_{i-1}\, dt \tag{7.9}$$

From what has been stated so far, it cannot be considered this set of equations as belonging to a vehicle planar motion because this Two-wheel model takes into consideration the longitudinal mass transfer during acceleration and braking (it is not considered the vehicle *xy* plane to be parallel to the road), so this model can be referred as an upgraded Two-wheel model.

For vehicles with EDRs that comply with the latest regulation (European Union (EU) 2022/545), this upgraded Two-wheel model can be used because it can be retrieved from the EDR report the longitudinal acceleration (a_x), lateral acceleration (a_y) and angular velocity (r) variables. However, this regulation is very recent, which means that most vehicles circulating at the time of elaboration of this report which have EDRs, still comply with older regulations that, in terms of variables for use in dynamics calculations, it can only be considered the vehicle speed and steering wheel angle.

To apply this simulator to EDRs with older regulations, the dynamics model previously presented needs to be simplified so that it may be used in these cases. Equation 7.1 still is the reference equation to construct the second simplified vehicle dynamics model. On the other hand, equation 7.3 needs to be transformed in equation 7.10 so that a_y can be replaced with variables that are known or that can be analytically determined.

$$\alpha_f - \alpha_r = K\frac{V^2}{R} \tag{7.10}$$

If equation 7.10 is replaced in equation 7.1, it cannot be solved analytically by the fact that it has two unknown variables. However, it can be worked around by solving a two-equation system with both equation 7.1 replaced with equation 7.10 and equation 7.2. Solving that system, β and the radius of turn (R) can be obtained.

One very important detail cannot be forgotten, the behaviour of "*K*". As seen for the other model (in equation 7.4), "*K*" was variable because it depended on longitudinal mass transfer during vehicle movement. Since for this simplified model a_x is not considered, in equations 3.7 and 3.8 the parcels of the dynamic component will be considered equal to zero, which means, it will not be considered longitudinal mass transfer during vehicle movement and F_{z_F} and F_{z_R} will be constant throughout the movement of the vehicle, in other words, "*K*" will be constant and can be obtained by using equation 7.11.

$$K = \frac{m_V}{l}\left(\frac{a_2}{C_{\alpha_F}} - \frac{a_1}{C_{\alpha_R}}\right) \tag{7.11}$$

Variables a_1 and a_2 can still be calculated using equations 3.9 and 3.10 and components v_x and v_y can still be calculated using equations 7.5 and 7.6. Last but not least, it must be kept in mind that the yaw rate (or angular velocity), r, needs to be calculated for this model (equation 7.12).

$$r = \frac{V}{R} \tag{7.12}$$

Finally, a vehicle's pre-impact trajectory can be calculated using equations 7.7, 7.8 and 7.9. This second dynamics model can be considered for a vehicle with planar motion (*xy* plane parallel to the road) using the Two-wheel model.

In Table 7.1, a summary of the steps required to find a vehicle's pre-impact trajectory, using both dynamics models, is shown.

Table 7.1 – Steps to calculate a vehicle's pre-impact trajectory for new and old EDR regulations.

STEP	*NEW EDR REGULATION*	*OLD EDR REGULATION*
1	Calculate distances from axles to the centre of gravity (COG), a_1 and a_2 (Equations 3.9 and 3.10).	
2	Calculate Vertical Reactions, F_{z_F} and F_{z_R} (Equations 3.7 and 3.8).	Calculate "Understeer Gradient" (*K*) (Equation 7.11).
3	Calculate "Understeer Gradient" (*K*) (Equation 7.4).	Calculate global sideslip angle, β and radius of turn (*R*) (Equations 7.1, 7.2 and 7.10).
4	Calculate global sideslip angle, β (Equation 7.1).	Calculate angular velocity, r (Equation 7.12).
5	Calculate longitudinal velocity and lateral velocity, v_x and v_y respectively (Equations 7.5 and 7.6).	
6	Calculate the vehicle's pre-impact trajectory (Equations 7.7, 7.8 and 7.9).	

7.1.3. Post-Crash Dynamic Model

After colliding, a vehicle usually follows a decelerated motion until its final resting position. That decelerated motion is normally accompanied by extreme accelerations/decelerations sustained by the vehicle.

As a result, the EDR will also record variables during this post-crash phase, usually at an increased rate of, at least, 100 Hz, normally during 300 ms after t_0. The variables to be recorded depend on the EDR legislation, but usually are available post-crash longitudinal and lateral accelerations and, sometimes, additional longitudinal and lateral Δv. If only the post-crash longitudinal and lateral accelerations are available, it is necessary to integrate them in order over time, to find the longitudinal and lateral Δv for each time step.

This information is very important since it allows to determine the direction and magnitude of both the "Change in Velocity" and "Departure Velocity" vectors (subchapter 6.1.3). The importance of calculating these parameters is due to the fact that, after a collision, a vehicle rotates and, for example, when there are multiple events that are paired together, it is necessary to know when and how much the vehicle rotated (for each t_0), so it can be added or subtracted that post-crash rotation from the rotation previously accumulated by the vehicle, during its trajectory.

It will be now introduced the stepwise procedure to calculate a vehicle's rotation after a collision:

1. Calculate the total longitudinal and lateral Δv from the post-crash information of the EDR report. The totals are calculated by making the sum of each variable in advance for all available instants of time. As already mentioned, if only longitudinal and lateral accelerations are available, each instant of time needs to be integrated as a function over time and the totals, for each component, are obtained by the sum of all integrated parcels.

2. Introduce those values in the simulator's Excel template file in the "POST-CRASH DATA (POCD)" section for each event (when applicable). Those values should be introduced according to subchapter 7.1.1.

3. For each event, the simulator calculates the total Δv (Change in Velocity vector) using equation 7.13.

$$\Delta v = \sqrt{{\Delta v_x}^2 + {\Delta v_y}^2} \tag{7.13}$$

4. The simulator calculates the Principal Direction of Force (PDOF) angle, which is the angle between the Approach and Change in Velocity vectors (equation 7.14).

$$PDOF = \tan^{-1}\left(\frac{\Delta v_y}{\Delta v_x}\right) \tag{7.14}$$

5. Taking into consideration the last speed registered by the EDR for each event at t_0 (Approach vector, V_1), the Departure Velocity vector (V_3) can be obtained using equation 7.15.

$$V_3 = \sqrt{{V_1}^2 + \Delta v^2 - 2\, V_1\, \Delta v \cos(PDOF)} \tag{7.15}$$

6. Finally, the departure angle (θ), which determines the rotation of the vehicle after collision, can be obtained (equation 7.16).

$$\theta = \sin^{-1}\left(\frac{\sin(PDOF)\ \Delta v}{V_3}\right) \tag{7.16}$$

These post-crash model steps were based on Ruth (2019).

For programming purposes and to minimize inputs from the user, the simulator calculates the absolute value of the departure angle (θ), i.e., the absolute value of equation 7.16. Its sign is determined based on Table 7.2 and Figure 7.2. In summary, when Δv_x and Δv_y have the same signal, the vehicle rotation is oriented clockwise, otherwise, the rotation is oriented anticlockwise (rotation towards *z* normal axis).

Table 7.2 – Vehicle rotation orientation around *z* normal axis after collision summary.

QUADRANT	*Δv_x SIGN*	*Δv_y SIGN*	*VEHICLE ROTATION*
1	-	-	
2	+	-	
3	+	+	
4	-	+	

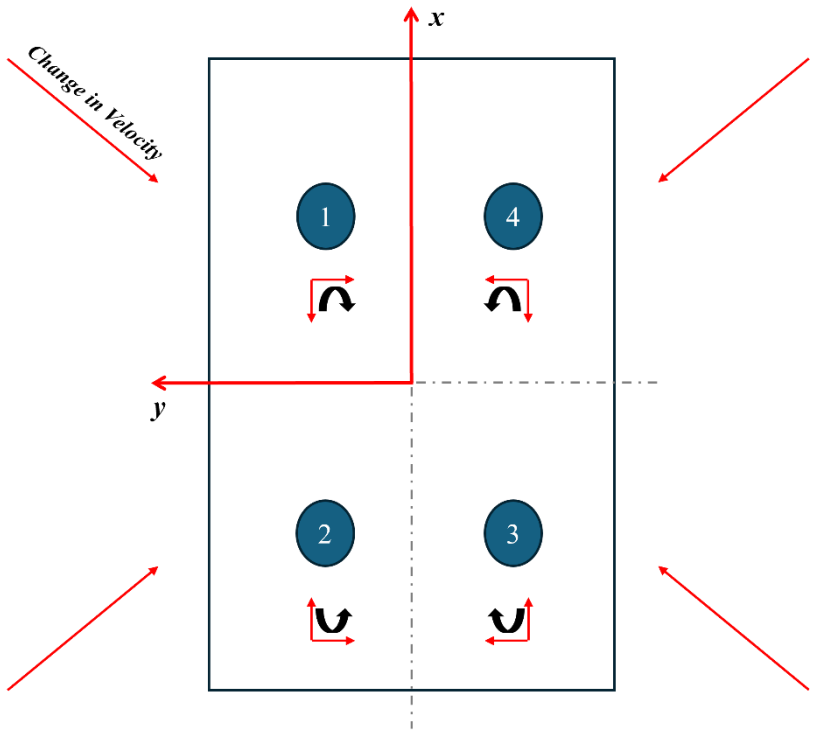

Figure 7.2 – Schematic of vehicle rotation orientation around *z* normal axis after collision.

7.1.4. Inputs, Calculations and Outputs

The simulator's Python programming structure will now be presented; its code is listed in Appendix B. Both dynamics models were programmed to import their input data through a separate Python file (EDR_INPUT.py). That Python file organises chronologically the data from the Excel file, that was previously converted to a CSV format file. The operating schematic of the "EDR_INPUT" Python file is shown in Figure 7.3.

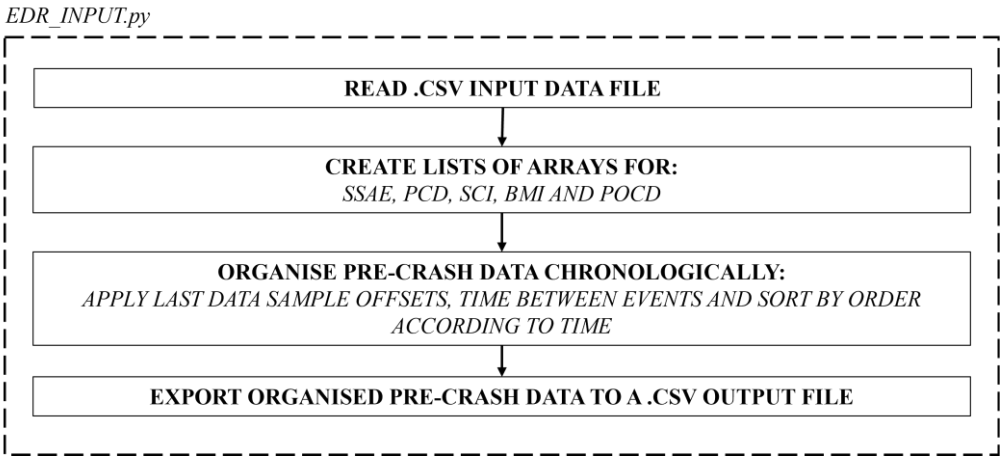

Figure 7.3 – "EDR_INPUT" Python file operation schematic.

With the input template file data organised, both dynamics model Python files will import the data and use it to perform the necessary dynamics calculations to obtain a 2D vehicle pre-impact trajectory.

The Python file operation schematic for old regulation EDRs, designated as "BICYCLE MODEL_EDR.py", is shown in Figure 7.4.

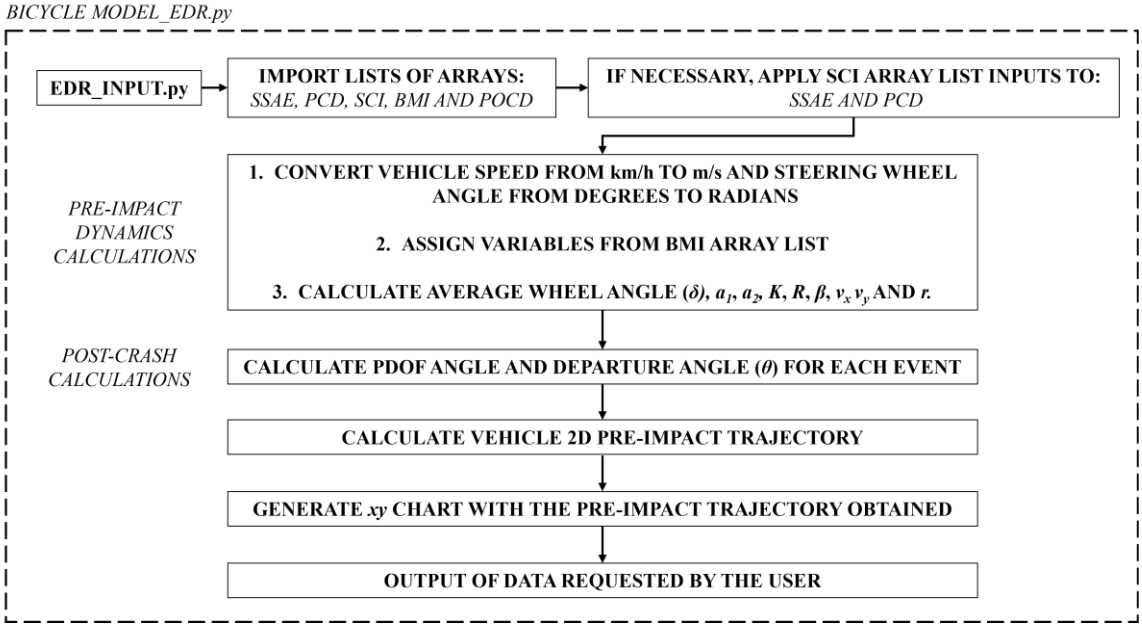

Figure 7.4 - "BICYCLE MODEL_EDR" Python file operation schematic.

Concerning new regulation EDRs, the simulator's Python file for this case ("BICYCLE MODEL_EDR_SERIES01".py) is presented in Figure 7.5.

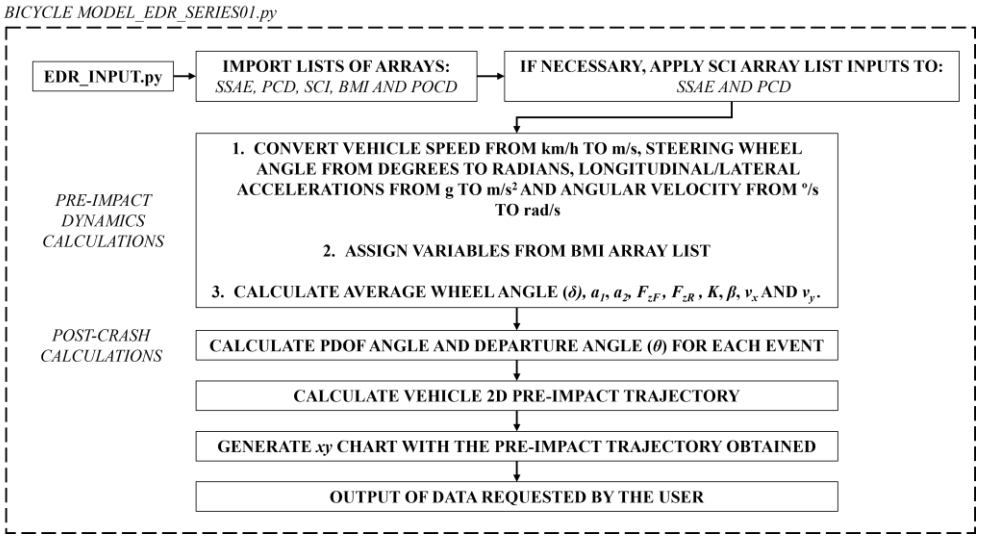

Figure 7.5 - "BICYCLE MODEL_EDR_SERIES01" python file operation schematic.

7.2. Validation of Simulator Dynamics Results with AVL

Once the simulator structure has been defined, the next step will be to validate its results. This involves determining whether pre-defined vehicle dynamics inputs yield a similar and approximate pre-impact trajectory. Additionally, the deviations in the results will be evaluated, along with a study on how errors in the input variables affect the final trajectory.

For this purpose, a vehicle's trajectory will be generated using AVL VSM™ software. This software is a real-time simulation tool for vehicle development, focusing on vehicle characteristics, driving behaviour and energy efficiency. It is also possible for virtual vehicle models to be created and tested with realistic 3D tracks and environment simulations.

The goal is to assume that the vehicle dynamics variables generated from the trajectory simulated using AVL software represent a hypothetical trajectory from a real-world scenario with an EDR. These variables will be entered into the PIDS template file, imported into PIDS Python code, and used to generate its trajectory output for analysis and comparison with AVL software-generated trajectory.

7.2.1. Validation of Vehicle Pre-Impact Trajectory "A"

The first trajectory to validate the simulator's results is based on a standard oval track from AVL VSM™ software and it will be designated as trajectory "A" (Figure 7.6).

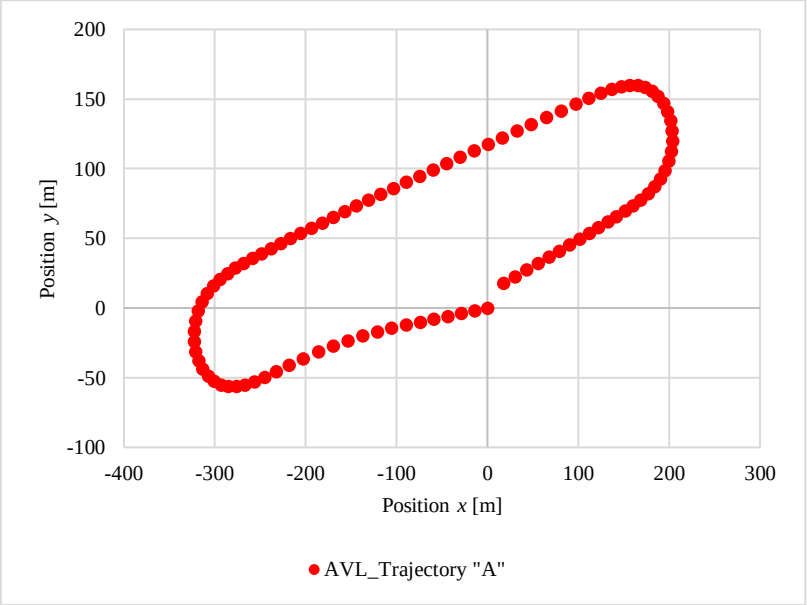

Figure 7.6 – Vehicle trajectory "A" generated in AVL.

This trajectory has a total distance of approximately 1164 meters and was performed in 49.5 seconds. The vehicle dynamics inputs during the trajectory are shown in Appendix C, Table C.1. Concerning the simulator, those inputs correspond to the "Pre-Crash Data" (or PCD) and they are already organised chronologically, i.e., the data is not presented as in the developed template but as if it had been already processed by Python code.

The vehicle characteristics to be applied to PIDS simulator are presented in Table 7.3. This data corresponds to the "Bicycle Model Inputs (BMI)" section of the PIDS template file.

Table 7.3 – Vehicle characteristics used to validate the pre-impact dynamics models (Trajectory "A").

VEHICLE CHARACTERISTIC	*VALUE*
Vehicle's mass [kg]	1400
Tyre Cornering Stiffness Front [N/rad]	58000
Tyre Cornering Stiffness Rear [N/rad]	42310
Front axle weight [kg]	868
Rear axle weight [kg]	532
Steering ratio	16
COG height [m]	0.516
Wheelbase [m]	2.7

Having imported both data from Table C.1 and Table 7.3 to the simulator's Python code, it was possible to obtain two vehicle trajectories (Figure 7.7). The trajectory defined as "EDR_Steering and Velocity" refers to old regulation EDRs, where only steering wheel angle and vehicle speed can be retrieved for dynamics calculations purposes. Trajectory "EDR_01 Series of Amendments" concerns newer EDRs that comply with legislation EU 2022/545, where also longitudinal acceleration, lateral acceleration and angular velocity can be retrieved. The *x* and *y* positions of the trajectories, as a function of time, are shown in Table C.2. Furthermore, their initial *x* and *y* positions are referenced at the origin of the Cartesian coordinate system (0,0) with an initial heading of approximately 188º.

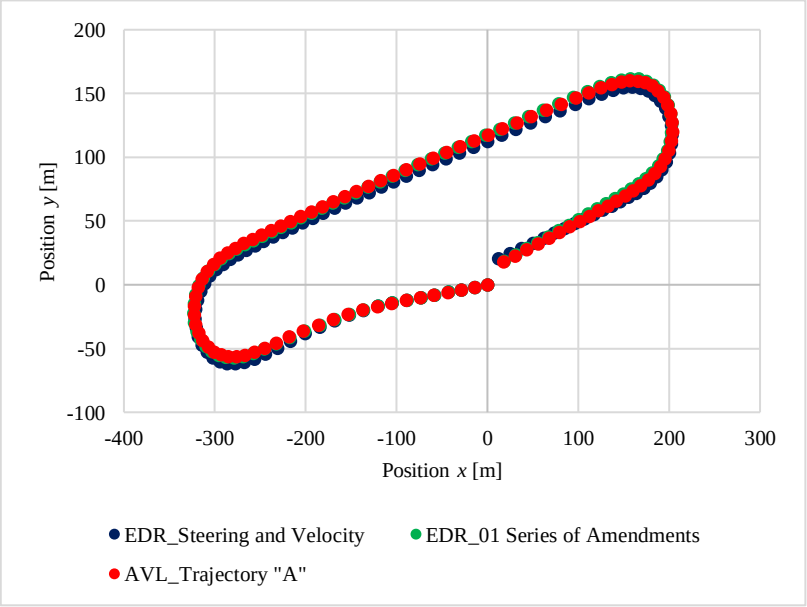

Figure 7.7 – Comparison of trajectories between AVL trajectory "A" and simulator-generated ones.

In a first visual analysis of Figure 7.7, it can be observed that the three trajectories are pretty similar in terms of shape, which means that for some applications that do not need deeper trajectory studies, both models provide a clear understanding concerning the type of trajectory and movements made by the vehicle. However, this report aims to go further by analysing the deviation of the results concerning the simulator-generated trajectories compared to the AVL software, over time, for each *x* and *y* position component.

The deviation of the results analysis will be based on equation 7.17, which represents the relative percentage error. The theoretical value refers to the AVL trajectory and the experimental value to the EDR trajectory. Since AVL software generates a simulated trajectory for a given vehicle dynamics behaviour, that simulation will have an error that is not known. Therefore, it must be assumed that the simulation value obtained in AVL is the most likely compared to a real-world scenario and consider this analysis as a measurement of the deviation between the results of the two dynamics simulators, rather than an error.

$$Error\ (\%) = \frac{|Experimental\ value - Theoretical\ value|}{Theoretical\ value} \cdot 100 \qquad (7.17)$$

First, it will be evaluated the *x*-position component (Figure 7.8).

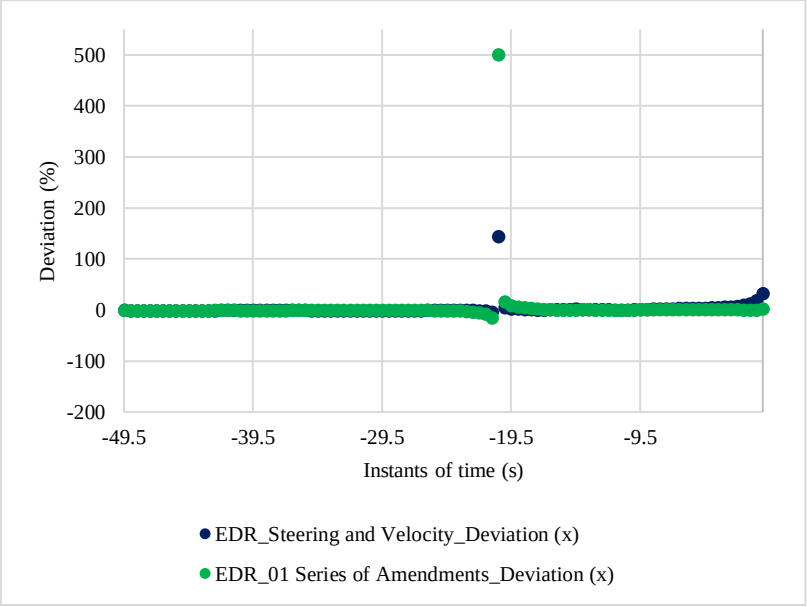

Figure 7.8 – Deviation of results analysis for *x*-component concerning AVL trajectory "A" (100 data points).

It is noticed immediately that for both EDR trajectories, there is an abnormal peak corresponding to the instant of time -20.5 s which corresponds to (*x*;*y*) position (0.488;117.7) [*m*] of AVL trajectory. Since from 100 data points, only at this point there is a gross divergence between the AVL trajectory and the EDR trajectories (it is not a representative data point of the overall behaviour of the deviation results over time), this point should not be considered for analysis and proceed only with the other 99 data points (Figure 7.9).

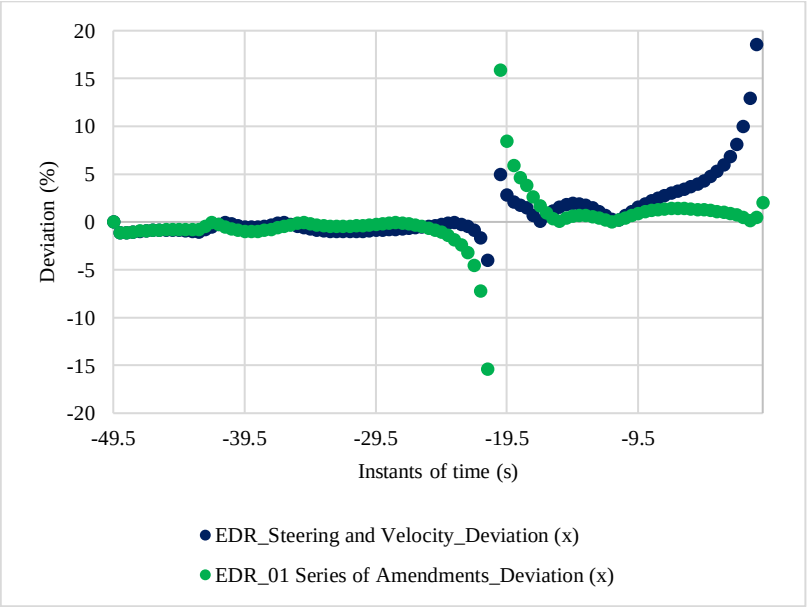

Figure 7.9 - Deviation of results analysis for *x*-component concerning AVL trajectory "A" (99 data points).

Analysing Figure 7.9, it can be observed that at instants -21.0 s and -20.0 s, the deviation of results diverges considerably from the normal behaviour along the trajectory. However, some conclusions can still be drawn at this point. The instants -21.0 s, -20.5 s, and -20.0 s represent the phase where the *x*-position component changes from negative to positive, which also causes the deviation to shift from negative to positive. During this transition phase, the deviation increases for a brief period but then decreases and stabilizes. Additionally, it can also be observed that for the "EDR_Steering and Velocity" trajectory, the deviation starts to increase again from the time instant -10.0 s, whereas, for the "EDR_01 Series of Amendments" trajectory, it is only seen a slight increase in deviation at the instant of time 0 s.

Considering these 99 data points, for trajectory "EDR_Steering and Velocity" the average deviation of results obtained for the *x*-position component was 2.12% and for "EDR_01 Series of Amendments" was 1.37%.

Concerning the deviation of results obtained in terms of total distance travelled by the vehicle in the *x*-position component, for "EDR_Steering and Velocity" was 0.26% and for "EDR_01 Series of Amendments" was 0.0028%.

Now, let's evaluate the *y*-position component (Figure 7.10).

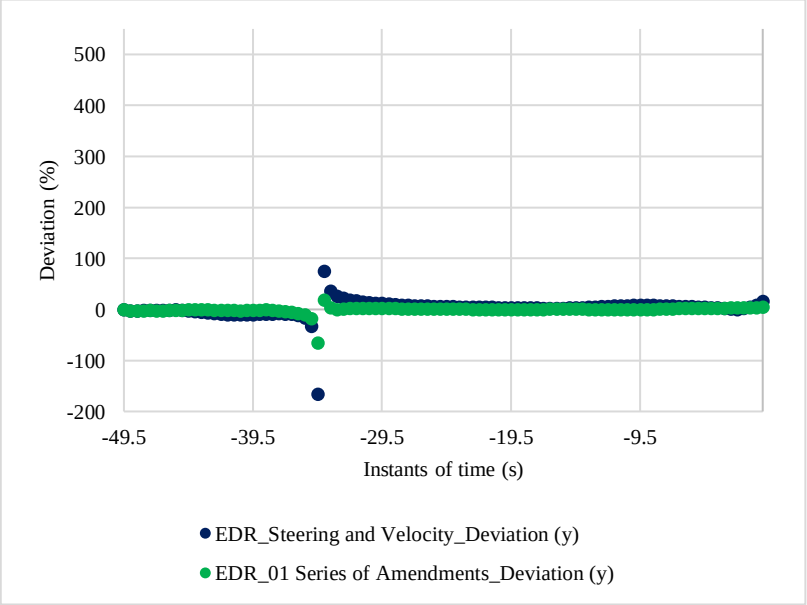

Figure 7.10 – Deviation of results analysis for *y* component concerning AVL trajectory "A" (100 data points).

As observed in Figure 7.8, it is immediately noticed that both EDR trajectories in the *y*-position component exhibit an abnormal peak at the time instant -34.5 s, which corresponds to the (*x*;*y*) position (-318.3; -1.920) [*m*] in the AVL trajectory. In this case, it will be proceeded as it has been done for the *x*-position component and exclude this point from the results' deviation analysis, focusing only on the remaining 99 data points (Figure 7.11).

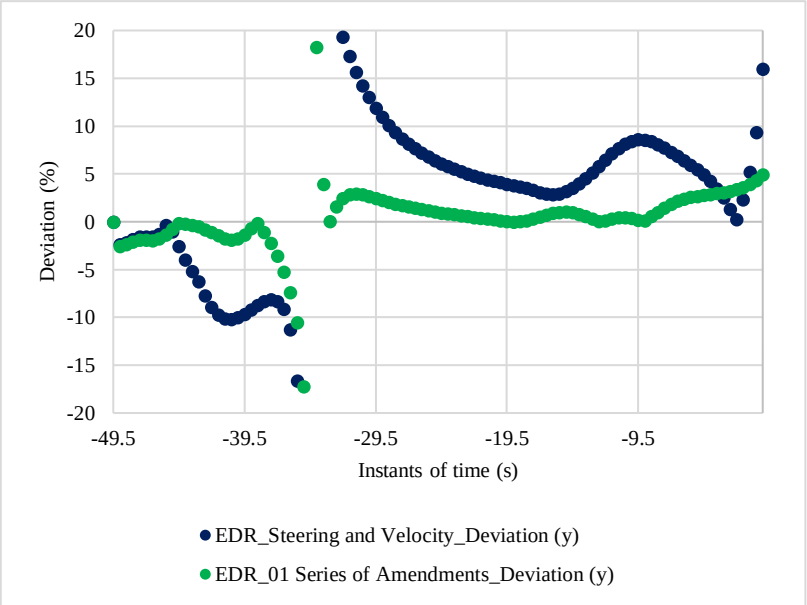

Figure 7.11 – Deviation of results analysis for *y* component concerning AVL trajectory "A" (99 data points).

Analysing Figure 7.11, it may be observed that for both trajectories, at the time instants -35.0 s and -34.0 s, the deviations increase sharply. The same conclusions can be drawn as for the *x*-position component: these time instants represent the phase where the *y*-position component transitions from negative to positive, causing the deviation for both trajectories to shift from negative to positive. After this phase, the results' deviations tend to stabilise. However, for the "EDR_Steering and Velocity" trajectory, the deviations oscillate more frequently, with greater amplitudes and a sharp peak near the time instant 0 s. In contrast, the results' deviation in the "EDR_01 Series of Amendments" trajectory remains more stable, with only a slight increase in the final time instants.

For the 99 data points, for trajectory "EDR_Steering and Velocity" the average deviation of results obtained for the *y*-position component was 4.26% and for "EDR_01 Series of Amendments" was 1.04%.

Regarding the total distance travelled by the vehicle in the *y*-position component, the deviation of results obtained for "EDR_Steering and Velocity" was -0.45% and for "EDR_01 Series of Amendments" was 1.08%.

Based on the results presented so far, it has been demonstrated that the trajectory defined by the dynamics model for newer EDRs, compliant with the latest EU 2022/545 regulation (referred to as "EDR_01 Series of Amendments"), produced the most accurate *x* and *y*

trajectory positions compared to the theoretical trajectory in AVL. Although a significant deviation was observed for both trajectories when their position components changed sign, conducting a simulation with another dynamics software would be worthwhile. This would help determine whether the deviation is an error inherent in the AVL simulation or if it represents a plausible deviation in the simulations carried out.

7.2.2. Validation of Vehicle Pre-impact Trajectory "B"

It shall now be introduced a new trajectory ("Trajectory B") that is more complex (with curves and counter curves) than trajectory "A" from the previous subchapter, in order to evaluate the consistency of the dynamics models' results. The trajectories will be based on the *Hockenheimring* racetrack (Germany), also available for simulations in AVL VSM™ software. The theoretical trajectory generated in AVL (AVL_Trajectory "B") is presented in Figure 7.12.

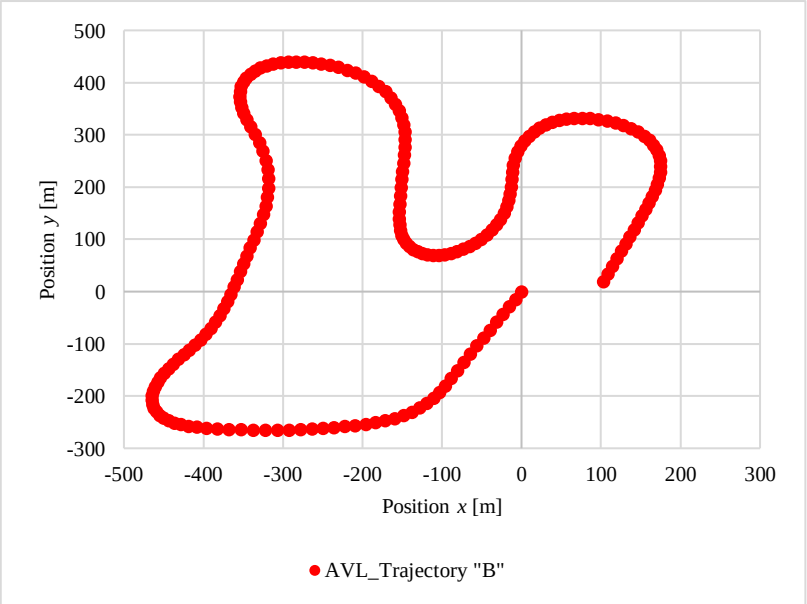

Figure 7.12 - Vehicle trajectory "B" generated in AVL.

This trajectory has a total distance of approximately 2570 meters and was performed in 103.5 seconds. The vehicle dynamics inputs during the trajectory are shown in Appendix C, Table C.3.

The vehicle characteristics to be applied to the pre-impact dynamics models developed are the same as those presented in Table 7.2, except for the average front and rear tyres'

cornering stiffnesses. For these parameters, the values are now 52830 N/rad for the front tyres and 40180 N/rad for the rear tyres.

Having imported both the data from Table C.3 and the vehicle characteristics for this trajectory into the simulator's Python code, it was possible to obtain two vehicle trajectories (Figure 7.13). The names of the simulated trajectories follow the same principle established in subchapter 7.2.1, and the trajectories' *x* and *y* positions, as a function of time, are shown in Table C.4. Additionally, the initial *x* and *y* positions of trajectory "B" are referenced at the origin of the Cartesian coordinate system (0,0), with an initial heading of approximately 241.7º.

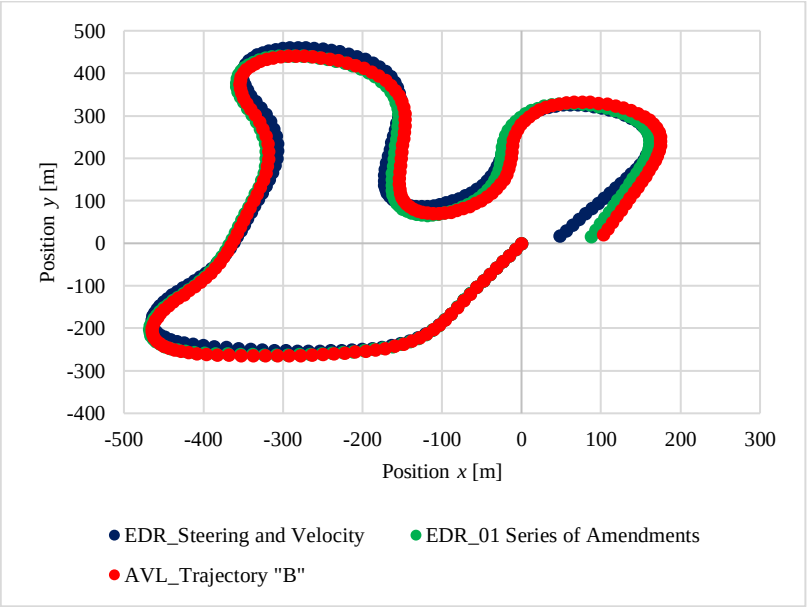

Figure 7.13 – Comparison of trajectories between AVL trajectory "B" and simulator-generated ones.

By observing Figure 7.13, the three trajectories allow to draw the same conclusions in terms of vehicle movements during its trajectory since they are similar in terms of shape (same conclusion as Trajectory "A").

Then, the same procedure was used for the results' deviation analysis as in subchapter 7.2.1 for trajectory "A", which will be simplified in this subchapter, just referring to the results in terms of values obtained.

Starting with the *x*-position component, one data point out of the total 208 was excluded for the same reasons outlined in subchapter 7.2.1. Both EDR trajectories show a point with

a pronounced deviation, which is not representative of the overall behaviour of the results' deviations over time. This point corresponds to instant -20.5 s at (*x*;*y*) position (-0.733; 279.2) [*m*] in the AVL trajectory. Although this instant coincides with that of Trajectory "A", it is purely coincidental. Excluding this point, the analysis was conducted on the remaining 207 data points.

Considering the 207 data points, for trajectory "EDR_Steering and Velocity" the average deviation of results obtained for the *x*-position component was 11.32% and for "EDR_01 Series of Amendments" was 12.41%.

Concerning the results' deviation obtained in terms of total distance travelled by the vehicle in the *x*-position component, for "EDR_Steering and Velocity" was 5.77% and for "EDR_01 Series of Amendments" was 0.12%.

Focusing now on the *y*-position component, also 207 data points were considered for the same reasons already mentioned. The point that was not considered for analysis, for both trajectories, corresponds to the instant of time -70.0 s which corresponds to (*x*;*y*) position (-365.8; -4.937) [m] of AVL trajectory.

For trajectory "EDR_Steering and Velocity" the average results' deviation obtained for the *y*-position component was 11.23% and for "EDR_01 Series of Amendments" was 1.91%.

Regarding the total distance travelled by the vehicle in the *y*-position component, for "EDR_Steering and Velocity" the results' deviation was 5.73% and for "EDR_01 Series of Amendments" was 0.13%.

In Table 7.4, the comparison of the deviation of results between trajectories "A" and "B", respectively to their theoretical trajectory in AVL is shown.

Table 7.4 – Results' deviation comparison between simulator-generated trajectories ("A", "B") and AVL-generated ones.

TRAJECTORY	*"A"*		*"B"*	
Component	*x*	*y*	*x*	*y*
Results' deviation between position component – "EDR_Steering and Velocity" [%]	2.12	4.26	11.3	11.2
Results' deviation between position component – "EDR_01 Series of Amendments" [%]	1.37	1.04	12.4	1.91
Results' deviation between total distance component – "EDR_Steering and Velocity" [%]	0.26	-0.45	5.77	5.73
Results' deviation between total distance component – "EDR_01 Series of Amendments" [%]	0.0028	1.08	0.12	0.132

From Table 7.4, by analysing each line, it is clear that the trajectories generated by the simulator for new regulation EDRs ("EDR_01 Series of Amendments") produced the best results in terms of comparison between AVL-generated trajectories. These results were expected since for new regulation EDRs there are more inputs concerning the vehicle dynamics during its trajectory, i.e., the dynamic model calculations become more refined and, therefore, results closer to the real trajectory can be obtained. However, looking at the results obtained, it is fair to say that with just two inputs of vehicle dynamics, the trajectories for older EDR regulation presented positive results.

Since a concrete reason for the increase in deviation during the signal transition of the position components could not be identified, the actual deviation may be lower than reported, which would enhance the credibility of the simulator's results.

7.2.3. Sensitivity of Results

This subchapter intends to study the sensitivity of the simulator's results when inputs with error deviations are introduced by the user. This necessity arises because, generally, the vehicle characteristics inputs introduced for the dynamics calculation contain errors, i.e., they are not exactly the same as the real characteristics of the vehicle, often approximations, and this will lead to deviations in the calculation of vehicles' pre-impact trajectories. For

example, concerning the tyres' cornering stiffness input, the values to be entered are average values, so an initial error is automatically introduced.

For this analysis, the "EDR_Steering and Velocity" and "EDR_01 Series of Amendments" trajectories "B" will be used. Error deviations will be presented by introducing a 10% error deviation in each vehicle characteristic input from its original value in the simulator's template for calculation (Figure 7.14). The reference values of the vehicle characteristics for trajectory "B" are the same as those presented in subchapter 7.2.2.

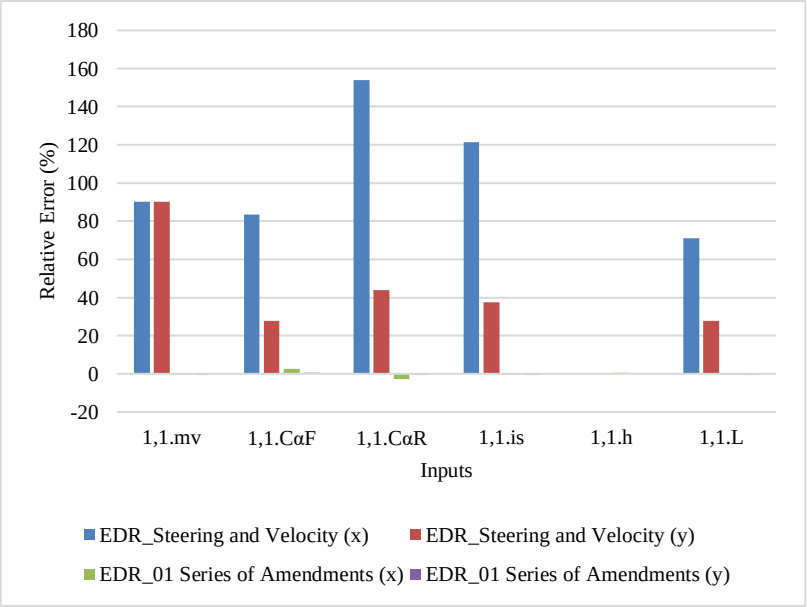

Figure 7.14 – Output relative error variation as a function of 10% deviation in the input for the simulator-generated trajectory "B".

Looking at Figure 7.14 it is clear that for the "EDR_Steering and Velocity" trajectory, a 10% deviation in any vehicle characteristic input will cause the relative error to increase significantly, which means that this dynamic model is quite sensitive to input error deviations. Also, by the analysis carried out, the relative error variation is higher for the rear tyre cornering stiffness and an error deviation for the COG's height input will not influence the trajectory results because that input is not considered in this model, as shown in subchapter 7.1.2.

Figure 7.14 does not allow to clearly understand the behaviour for the "EDR_01 Series of Amendments" trajectory relative error variation, since the difference in sensitivity between the two models is quite significant, so, a new chart was created just for this trajectory (Figure 7.15).

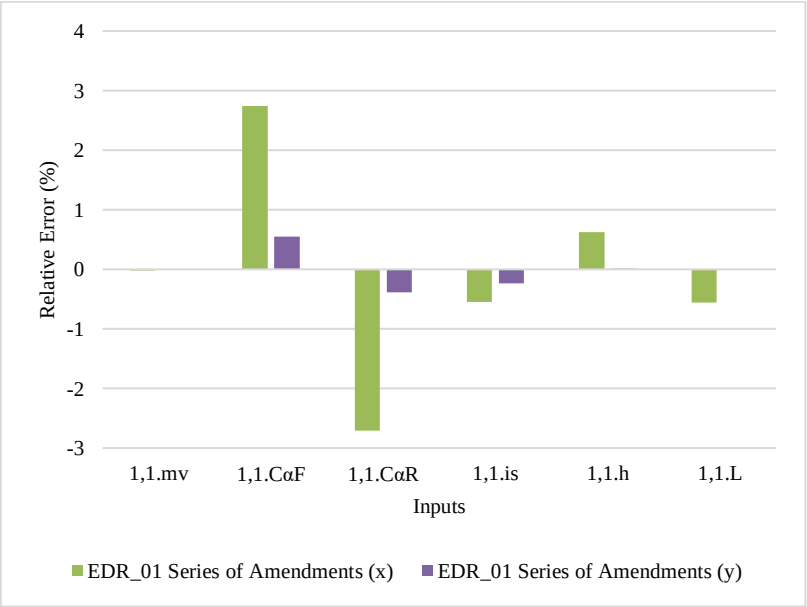

Figure 7.15 – Output relative error variation as a function of 10% deviation in the input for "EDR_01 Series of Amendments" trajectory.

Analysing the values from Figure 7.15 and comparing them with the values from Figure 7.14 for the "EDR_Steering and Velocity" model, it can be concluded that the "EDR_01 Series of Amendments" model is much less sensitive in terms of error deviations in the vehicle characteristics inputs. It would be necessary to introduce values with very gross errors into the model to create a significant distortion of values compared to a real trajectory. Curiously, for most input variables (except for the front tyres' cornering stiffness (C_{α_F}) and vehicle's COG (h)) the relative error variation contributed favourably to approximate the trajectory generated in the simulator to the real one, whereas an error deviation in the rear tyres' cornering stiffness (C_{α_R}) variable being the most favourable.

Overall, and based on the content already presented in subchapter 7.2, the dynamics model "EDR_01 Series of Amendments" produced the best results when comparing its simulated trajectory to a real/theoretical one.

Finally, the values presented in Figures 7.14 and 7.15 are also shown in Table 7.5.

Table 7.5 – Output relative error summary for both "EDR_Steering and Velocity" and "EDR_01 Series of Amendments" dynamic models.

	DYNAMICS MODEL	*EDR_STEERING AND VELOCITY OUTPUT RELATIVE ERROR [%]*		*EDR_01 SERIES OF AMENDMENTS OUTPUT RELATIVE ERROR [%]*	
	COMPONENT	*x*	*y*	*x*	*y*
Input variables	1,1.m_v	90.3	90.3	-0.02	-0.01
	1,1.$C\alpha_F$	83.6	27.8	2.74	0.55
	1,1.$C\alpha_R$	154.0	44.0	-2.71	-0.39
	1,1.i_s	121.4	37.5	-0.55	-0.24
	1,1.h	0	0	0.62	0.01
	1,1.l	71.2	27.8	-0.56	-0.01

7.3. Simulator Implementation in Real-World Case Studies

Finally, in this subchapter, the goal is to implement the pre-impact dynamics simulator developed into two real-world case studies. One case consists of a frontal crash, denominated as "Real Case A" and the second one consists of a rollover crash ("Real Case B").

For these two real cases, a forensic approach will be applied, allowing conclusions to be drawn based on the generated trajectory as well as the simulator's inputs and outputs.

7.3.1. Frontal Crash (Real Case "A")

Before proceeding with the analysis using the PIDS, let's first understand what is known in advance about this case. From the report at the accident's site made by the law enforcement authorities, it is known that the vehicle responsible for the accident ("A", the one equipped with an EDR and where the analysis will be based) performed an unsuccessful overtaking to vehicle "B". Consequently, it collided head-on with vehicle "C", which was entering the oncoming traffic lane, causing fatalities to the passengers of vehicle "C". The *croquis* elaborated by the law enforcement authorities concerning what happened is presented in Figure 7.16.

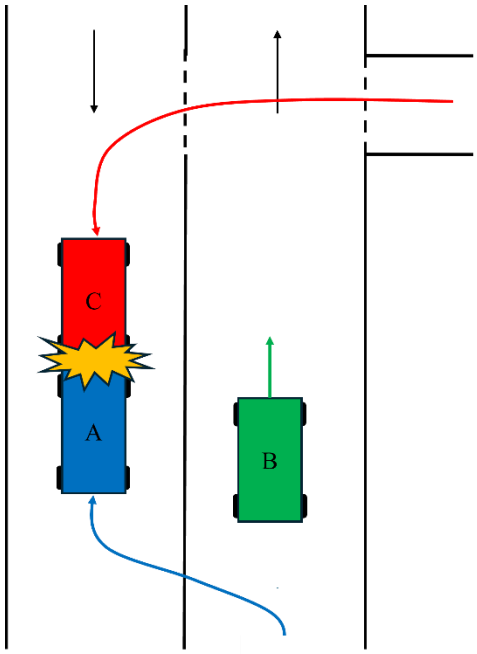

Figure 7.16 – *Croquis* Real Case "A".

Since fatalities have occurred, it is necessary to proceed with a judicial investigation to understand the behaviour of vehicle "A" up until the moment of collision (or impact). At this point, it can be introduced the use of the simulator developed to find more information about what happened.

First, an accredited and authorized professional retrieved the recorded data from the EDR, in this case using the BOSCH CDR tool (subchapter 5.5); a PDF file was generated containing all the information inherent to the recorded events. From the EDR report it was concluded that it only exists one event related to this accident, i.e., only 5 seconds of movement of vehicle "A" prior to the moment of impact is available. As an example, a print screen of the information from the BOSCH CDR tool's PDF report concerning the recorded pre-crash data for this event is shown in Figure 7.17.

Pre-Crash Data -5 to 0 sec (Record 1, Most Recent)

Time (sec)	Engine RPM (Combustion Engine) (RPM)	ABS Activity	Stability Control	Steering Input (deg)	Speed, Vehicle Indicated (MPH [km/h])	Accelerator Pedal (%)	Service Brake Activation
-5.0	4,672	No ABS Activity	No ESC Activity	2	83 [133]	100	Off
-4.5	4,800	No ABS Activity	No ESC Activity	6	86 [139]	100	Off
-4.0	4,992	No ABS Activity	No ESC Activity	0	89 [143]	100	Off
-3.5	5,184	No ABS Activity	No ESC Activity	-2	93 [149]	100	Off
-3.0	5,312	No ABS Activity	No ESC Activity	-8	95 [153]	100	Off
-2.5	5,440	No ABS Activity	No ESC Activity	-2	99 [159]	100	Off
-2.0	5,440	No ABS Activity	No ESC Activity	10	99 [159]	0	Off
-1.5	4,672	ABS Activity	No ESC Activity	8	89 [143]	0	On
-1.0	4,096	ABS Activity	No ESC Activity	16	83 [134]	0	On
-0.5	3,456	ABS Activity	No ESC Activity	4	71 [115]	0	On
0.0	3,136	ABS Activity	No ESC Activity	4	63 [101]	0	On

Figure 7.17 – Real Case "A" pre-crash data from BOSCH CDR tool's PDF report.

Once the simulator's template was filled in with the available and necessary information about the event recorded for this accident (Appendix D, Figure D.1), it was possible to simulate the pre-impact trajectory of the vehicle "A" according to subchapter 7.1.4 (Figure 7.18). In this case, by the available dynamic variables, the "EDR_Steering and Velocity" dynamics model (subchapter 7.1.2) was used. The last available point is (198.1; 3.05) [m] at $t_0 - 0.012$ s.

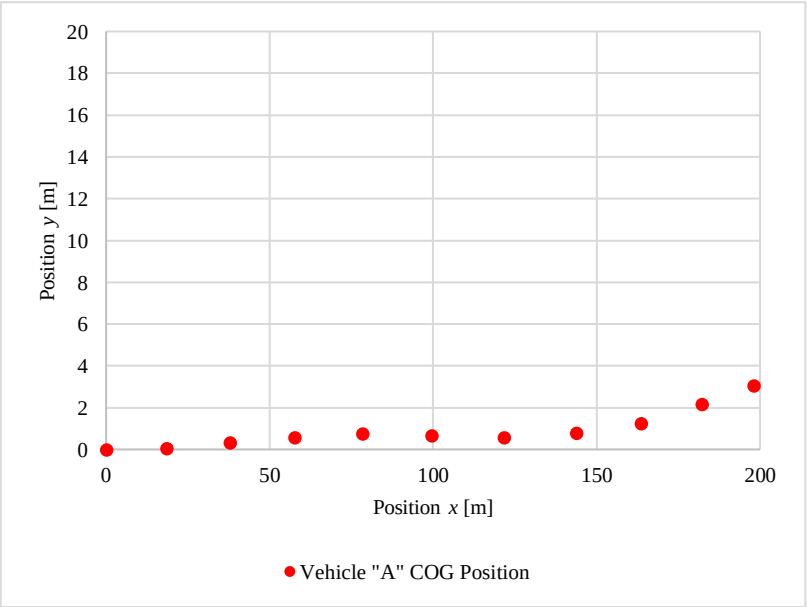

Figure 7.18 – Pre-impact trajectory of Vehicle "A".

In addition, Table 7.6. presents the chronological summary of vehicle "A"'s COG positions during the pre-impact trajectory.

Table 7.6 - Summary of Vehicle "A"'s COG positions during the pre-impact trajectory.

INSTANT OF TIME [s]	*COG'S x POSITION [m]*	*COG'S y POSITION [m]*
-5.012	0	0
-4.512	18.47	0.066
-4.012	37.78	0.330
-3.512	57.64	0.575
-3.012	78.33	0.763
-2.512	99.58	0.684
-2.012	121.7	0.563
-1.512	143.7	0.803
-1.012	163.6	1.26
-0.512	182.2	2.19
-0.012	198.1	3.050

In a first analysis of Figure 7.18 and Table 7.6., Vehicle "A"'s driver performed an overall straight trajectory during this 5 s period. From t = -5.012 s, he first performed a slight left turn with a maximum lateral deviation of 0.763 *m* (t = -3.012 s), then corrected the vehicle's positioning with a slight right turn until t = -2.012 s and, finally, from t = -1.512 s onwards, he performed a slight left turn until the collision.

Since there is a "Last Data Sample" of 0.012 s before t_0, Vehicle "A"'s pre-impact trajectory is only available until t = -0.012 s, i.e., until 0.012 s before collision (last known instant in which the EDR read the values of the variables to be recorded).

At this stage, let's introduce more simulator's output data (Table 7.7) to understand the evolution of certain dynamic components that will help to validate the trajectory obtained as well as to understand when the driver realized the imminent collision and his reaction manoeuvres.

Table 7.7 – Simulator's output data for vehicle "A" (Real Case "A").

INSTANT OF TIME [s]	*VEHICLE SPEED [km/h]*	*TPS (%)*	*STEERING INPUT (º)*	*SERVICE BRAKE ACTUATION [BOOLEAN]*	*ABS ACTIVITY [BOOLEAN]*	*ESP ACTIVITY [BOOLEAN]*	*VEHICLE HEADING ANGLE [º]*
-5.012	133	100	2	0	0	0	0
-4.512	139	100	6	0	0	0	0.180
-4.012	143	100	0	0	0	0	0.709
-3.512	149	100	-2	0	0	0	0.709
-3.012	153	100	-8	0	0	0	0.539
-2.512	159	100	-2	0	0	0	-0.129
-2.012	159	0	10	0	0	0	-0.293
-1.512	143	0	8	1	1	0	0.524
-1.012	134	0	16	1	1	0	1.22
-0.512	115	0	4	1	1	0	2.66
-0.012	101	0	4	1	1	0	3.04

Table 7.7 data was plotted into charts (Figures 7.19, 7.20) to facilitate the evaluation.

Comparing Figures 7.19 and 7.20, it can be seen that from t = -5.012 s until t = -2.512 s (during 2.50 s) the driver accelerated at full throttle (100%) from 133 km/h to 159 km/h. At t = -2.012 s, the vehicle's speed stayed at 159 km/h but the accelerator pedal was no longer actuated, which means that between t = -2.512 s and t = -2.012 s the driver realized the imminent collision with Vehicle "C" and removed his foot from the accelerator. Then, at t = -1.512 s it may be seen that the brake pedal was actuated in conjunction with the Antilock Braking System (ABS), which means that the wheels were slipping, therefore the most likely was an emergency braking being performed (full braking system's power request by the driver). The braking behaviour continued until the end of the pre-impact trajectory obtained without electronic stability assistance (ESP), allowing to conclude that there was no excessive rotation of the vehicle when escaping the collision. Although it cannot be specified the driver's reaction time in detail, given the EDR's low sampling rate, it can be stated with certainty, from the available data, that the driver's reaction time was between time intervals t = -2.512 s and t = -1.512 s, i.e., it was $\leq$ 1 s (the time where the driver stopped accelerating and started braking).

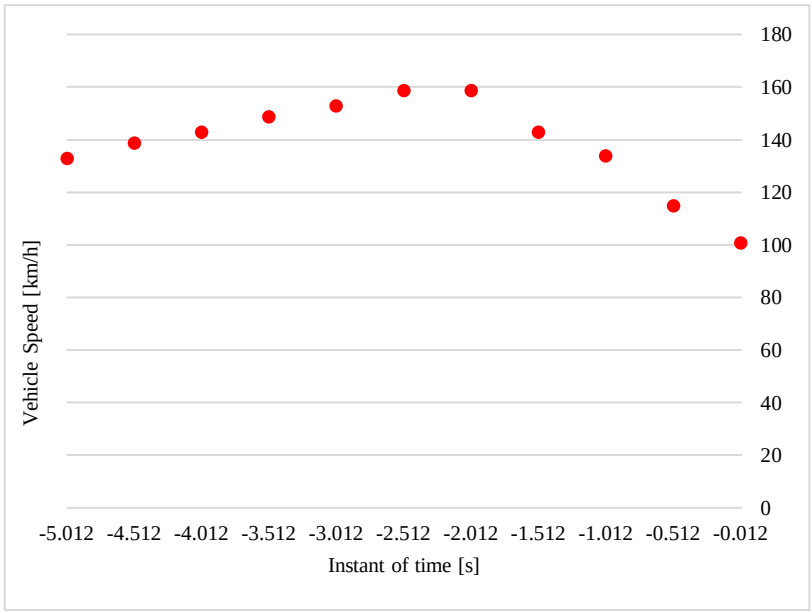

Figure 7.19 – Evolution of Vehicle "A"'s speed during pre-impact trajectory.

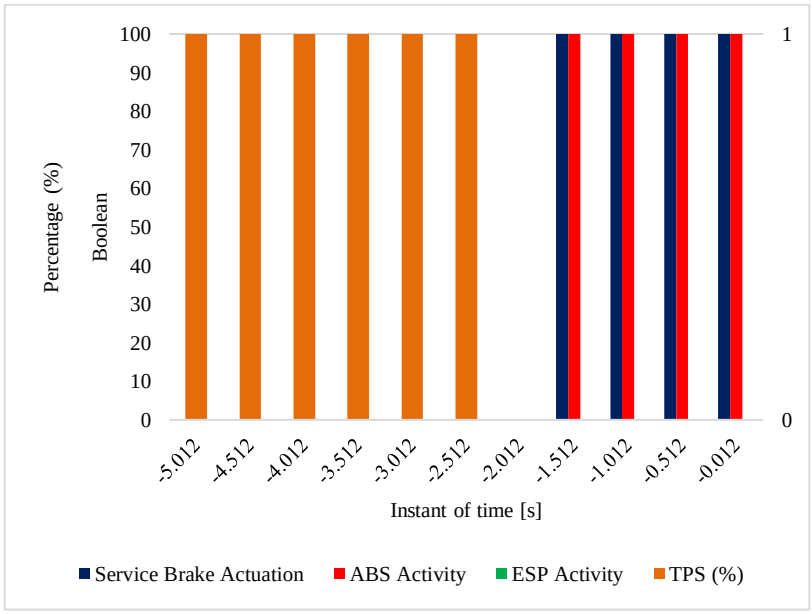

Figure 7.20 - Evolution of Vehicle "A"'s accelerator and active security systems actuation.

The previous analysis can be complemented with more data. In Figure 7.21, it can be observed that the vehicle heading angle series behaviour has the same shape as the pre-impact trajectory generated, since this is the angle that is the base for the trajectory's positioning coordinates. Analysing the steering wheel angle input, it can also be seen that from the time interval where the reaction time happened, the driver made left and right movements to avoid the collision. The vehicle's final heading angle before collision was 3.04º (referred to its start local reference position).

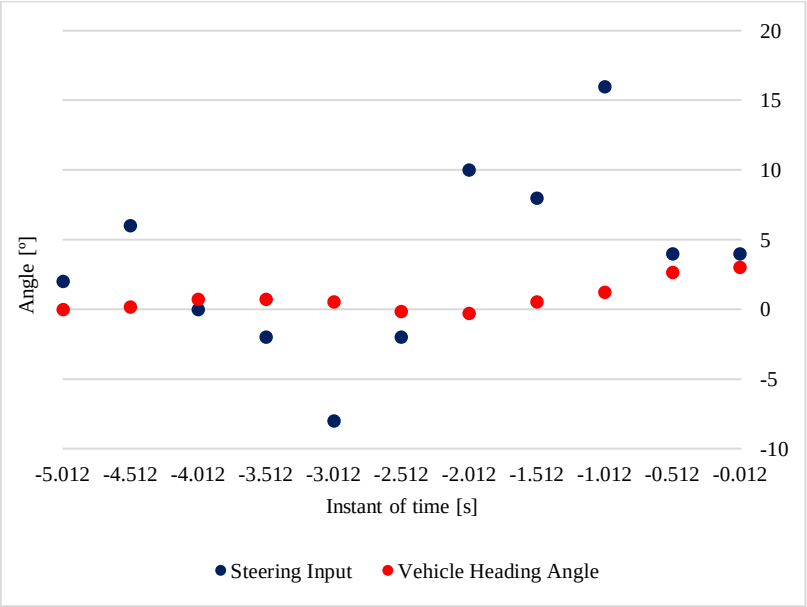

Figure 7.21 – Evolution of Vehicle "A"'s steering wheel and vehicle heading angles.

During the collision (Figure 7.22), the vehicle had the point of impact located in the fourth quadrant, with a PDOF angle of -0.22º. The vehicle "A"'s rotation angle (or departure angle, θ) calculated by the simulator was 0.22º (situated in the first quadrant). The vehicle's point of impact and rotation were validated through photographic records of Vehicle "A". The vehicle ended up with a final heading angle of 3.26º, after the collision.

Figure 7.22 represents a bird-eye view of the vehicle "A", depicted as a rectangle, during the collision. The blue rectangle represents vehicle "A"'s approach position and the "Change in Velocity" vector represents the direction and position of vehicle "C" during collision by a PDOF angle. Finally, the rectangle with a dotted line outline represents vehicle "A"'s departure position by a θ angle referenced to its approach position (counterclockwise rotation).

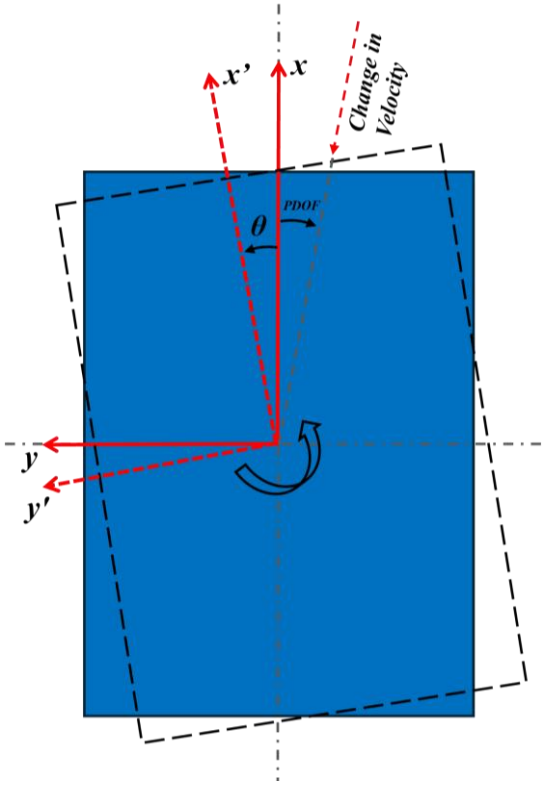

Figure 7.22 – Vehicle "A"'s schematic of the impact mechanism during the collision (not to scale).

With the study of vehicle "A"'s behaviour before and after the collision completed, it was demonstrated that with EDR data and using the PIDS, it was possible to closely replicate the pre-impact trajectory developed by Vehicle "A", understand its pre-impact behaviours, its driver reactions, as well as understand its behaviour after impact. From this analysis, it was scientifically possible to validate what happened in this accident and corroborate the accident's report from the law enforcement authorities.

7.3.2. Rollover Crash (Real Case "B")

In this Real Case "B", a rollover crash using the developed pre-impact dynamics simulator is going to be evaluated. From the law enforcement authorities report, the information that is known before proceeding with the analysis is that the vehicle was out of control, resulting in a rollover behaviour. The *croquis* elaborated by the law enforcement authorities concerning what happened is presented in Figure 7.23. There were no other vehicles involved in this accident and there were fatalities to regret in vehicle "A".

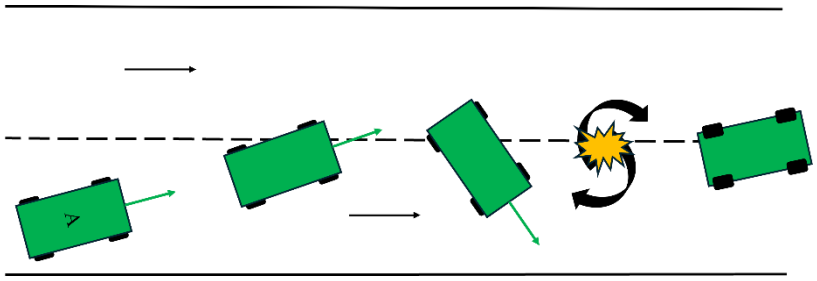

Figure 7.23 - *Croquis* Real Case "B".

Vehicle "A" is equipped with an EDR that allowed to make the pre-impact analysis using the most refined dynamics model developed: "EDR_01 Series of Amendments". The same technical evaluation procedure used in Real Case "A" will be adopted.

The data from EDR was retrieved and it was concluded that there are two events related to this accident (two multiple events with a time interval between them of 0.7 s). The template developed was filled in with the available and necessary information about the events (Appendix E, Figure E.1) and it was possible to simulate the pre-impact trajectory of vehicle "A" (Figure 7.24). In addition, Table 7.8. presents the chronological summary of Vehicle "A"'s COG positions during the pre-impact trajectory.

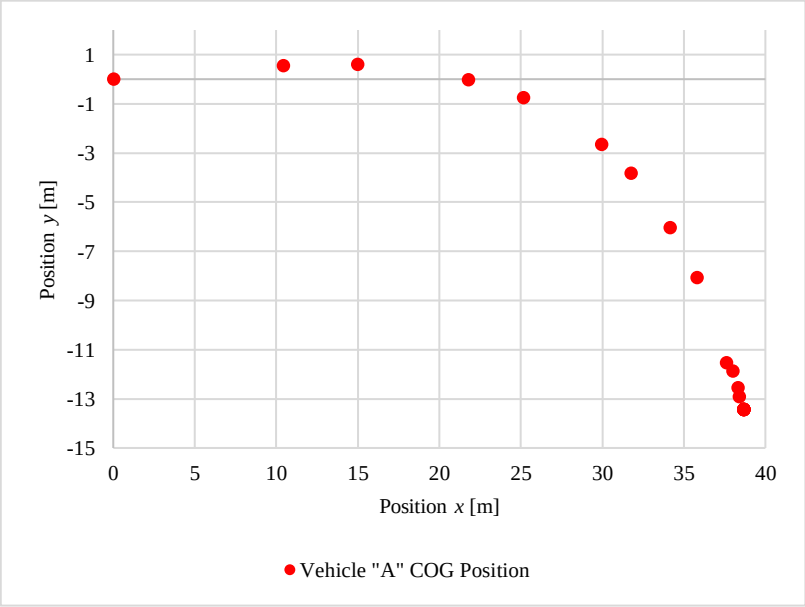

Figure 7.24 - Pre-impact trajectory of Vehicle "A" (Real Case "B").

Table 7.8 - Summary of Vehicle "A"'s COG positions during the pre-impact trajectory.

INSTANT OF TIME *[s]*	*COG'S x POSITION* *[m]*	*COG'S y POSITION* *[m]*
-5.7	0	0
-5.2	10.4	0.551
-5.0	15.0	0.608
-4.7	21.8	-0.0255
-4.5	25.1	-0.742
-4.2	29.9	-2.64
-4.0	31.7	-3.83
-3.7	34.1	-6.02
-3.5	35.8	-8.07
-3.2	37.6	-11.5
-3.0	38.0	-11.9
-2.7	38.3	-12.5
-2.5	38.4	-12.9
-2.2	38.7	-13.4
-2.0	38.7	-13.4
-1.7	38.7	-13.4
-1.5	38.7	-13.4
-1.2	38.7	-13.4
-1.0	38.7	-13.4
-0.7	38.7	-13.4
-0.5	38.7	-13.4
0.0	38.7	-13.4

Analysing Figure 7.24, it can be observed a pre-impact trajectory with cornering to the right side and, from table 7.8 it can be retrieved that there are 22 data points, although, graphically, there are only 14 data points. In Table 7.8, it can be seen that from t = -2.2 s to t = 0 s, those 9 data points are the same (are overlapping) as if vehicle "A" had stopped.

Now, with Figure 7.25, where the evolution of vehicle "A"'s speed is shown, it can be verified that from t = -2.2 s the vehicle "A"'s speed was zero (or close to zero). Since the dynamics model calculates the vehicle "A"'s positioning in the x and y position components through its speed, the reason for the 9 data points being overlapped is found.

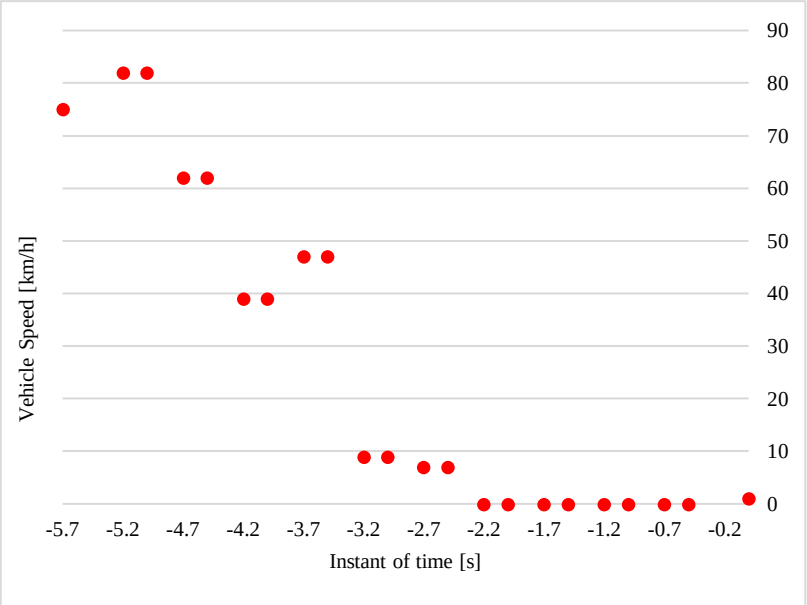

Figure 7.25 - Evolution of Vehicle "A"'s speed during pre-impact trajectory.

However, no conclusions about the movement of the vehicle in those instants can yet be drawn. Did the vehicle stop? Does that make sense? Let's introduce more information about vehicle "A"'s behaviour during its pre-impact trajectory, to answer the previous questions. The data summary is also presented in Appendix F, Table F.1.

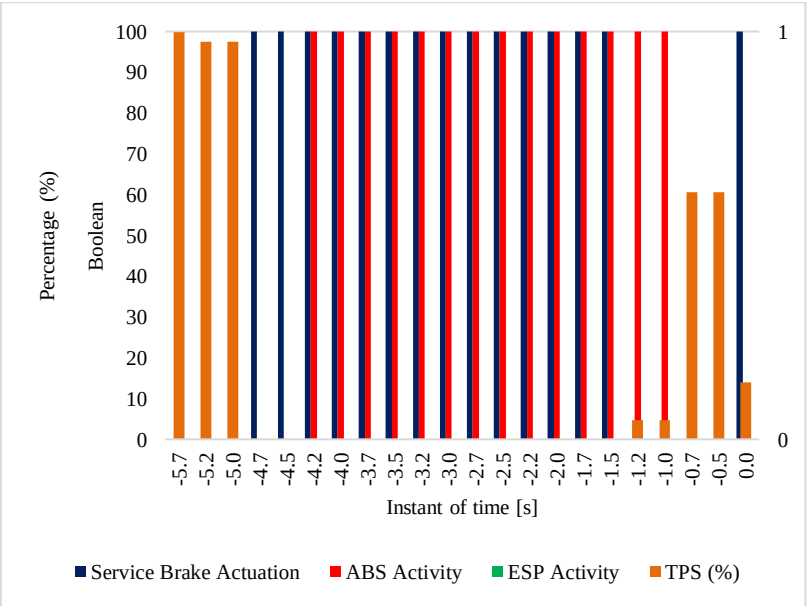

Figure 7.26 - Evolution of Vehicle "A"'s accelerator and active security systems actuation.

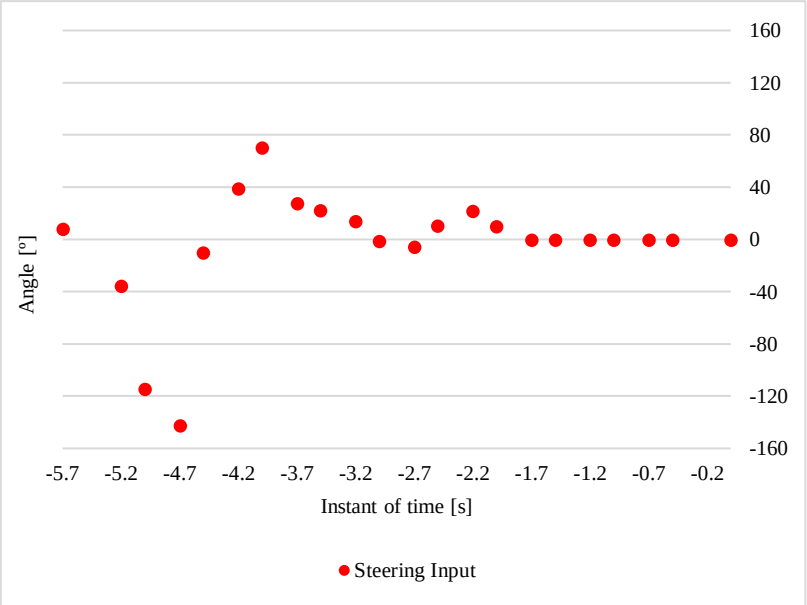

Figure 7.27 - Evolution of Vehicle "A"'s steering wheel input.

Starting with Figure 7.26, which represents the evolution of the accelerator and active security system's actuation during the pre-impact trajectory of the vehicle "A", and Figure 7.27, which represents the steering wheel angle input during the pre-impact trajectory, it can be observed that the accelerator pedal was at full throttle between t = -5.7 s and t = -5.0 s. Also, during that time interval of only 0.7 s, it may be seen that the steering wheel input angle increased considerably from 8.3º to -114.5º (a clockwise rotation of 106.2º). After only 0.3 s (at t = -4.7 s) it can only be seen a brake pedal actuation (lasts at the least until t = -4.5 s) and, during that time interval of 0.2 s, an abrupt variation of the steering wheel input angle from -142.5º to -10.1º (anticlockwise rotation of 132.4º) can also be observed. At this stage, by the type of manoeuvre performed and very short reaction times, it may be concluded that it was quite likely the driver was trying to perform a dangerous driving manoeuvre, in this case, a drift manoeuvre (full throttle + abrupt vehicle's rotation to the right followed by braking + abrupt vehicle's rotation to the left).

The rotation to the left continued to increase at least at t = -4.0 s, where it reached a peak value of 70.6º; it must be pointed out the fact that the ABS was already actuating, meaning that wheel slipping was occurring. Following that, from t = -3.5 s to t = -3.2 s (0.3 s) vehicle "A"'s speed dropped abruptly from 47 km/h to 9 km/h and at t = -2.2 s it was 0 km/h. Since the vehicle's speed for the EDR is measured by the ABS/ESP module (average of vehicle's wheels speed) and since there was still vehicle acceleration (Figure 7.28) even with a vehicle

speed measured by the ABS of zero, it may be concluded that the vehicle's wheels were locked, which means the rollover had already occurred and the vehicle's wheels were facing up in the air. The rollover is expected to have occurred between the abrupt change in vehicle's speed, i.e., between t = -3.5 s to t = -3.2 s. Figure 7.28 can corroborate that, due to the sudden increase in lateral acceleration in this time interval, which also indicates that the vehicle rolled sideways from left to right (negative lateral acceleration gain, points highlighted in green). Since this vehicle's EDR does not measure the roll angle, a deeper analysis of the rollover behaviour could not be made.

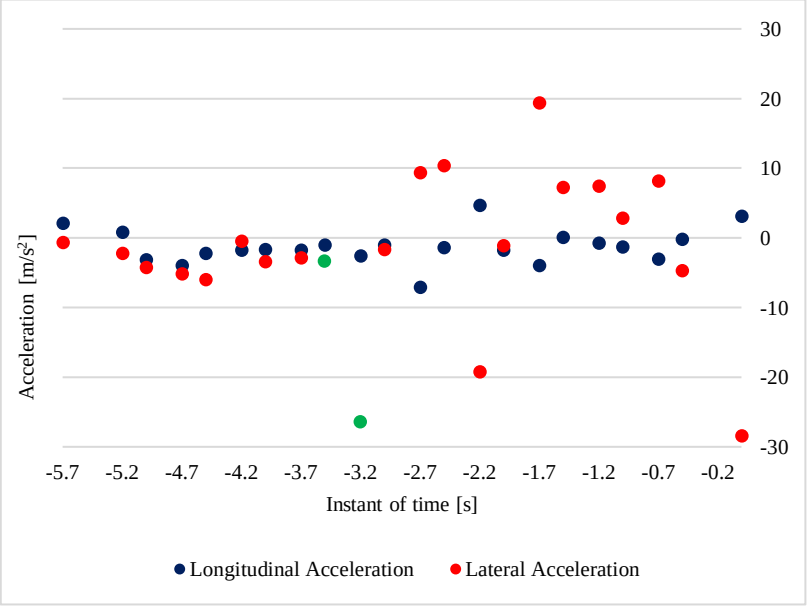

Figure 7.28 – Evolution of Vehicle "A"'s longitudinal and lateral accelerations.

Since the rollover is expected to have occurred from *t* = -3.5 s, it should only be considered the pre-impact trajectory as reliable up to that instant of time (Figure 7.29).

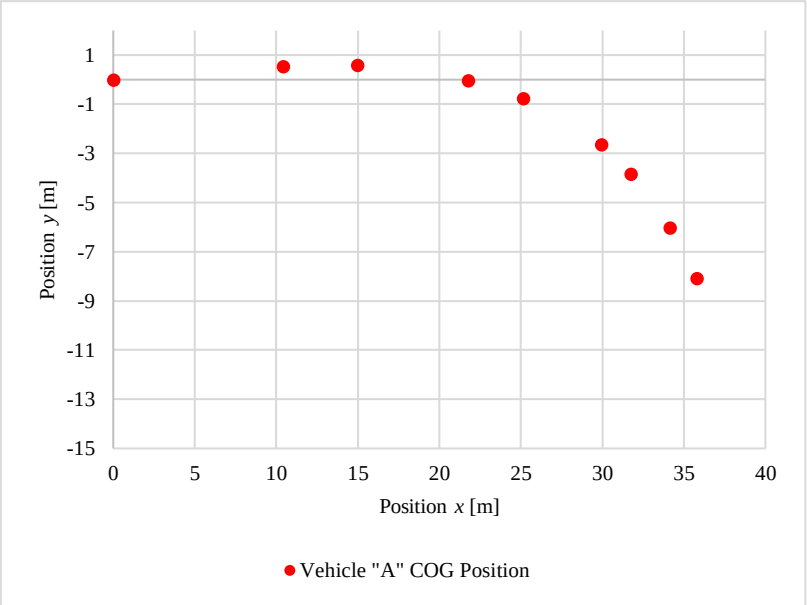

Figure 7.29 - Pre-impact trajectory of Vehicle "A" (Real Case "B") before rollover.

Now the previous questions can be answered "Did the vehicle stop? Does that make sense?". The answer is No! As previous stated, the vehicle did not stop, but since the vehicle speed variable was measured at the wheels by the ABS module and they were locked due to rollover behaviour (wheels facing up), although the vehicle's speed was not zero, for EDR measures it would be. This is a technical limitation when evaluating this type of road accident, which car manufacturers will still need to work around.

Finally, it may be studied the post-crash behaviour of vehicle "A". It must be emphasised that the start of the events was triggered after the rollover behaviour, so it may be difficult to relate the impacts suffered and may be already disturbed data. Since two multiple events are available with a time interval between them of 0.7 s, there will be two post-crash behaviours with a 0.7 s difference (instants t = -0.7 s and t = 0 s).

For instant of time t = -0.7 s (Figure 7.29), the impact point was situated in the third quadrant with a value of 262.02º (referred to the approach vector) and since the Δv_x and Δv_y were both positive, a clockwise rotation happened with a departure angle (θ) of -82.35º (situated in the fourth quadrant).

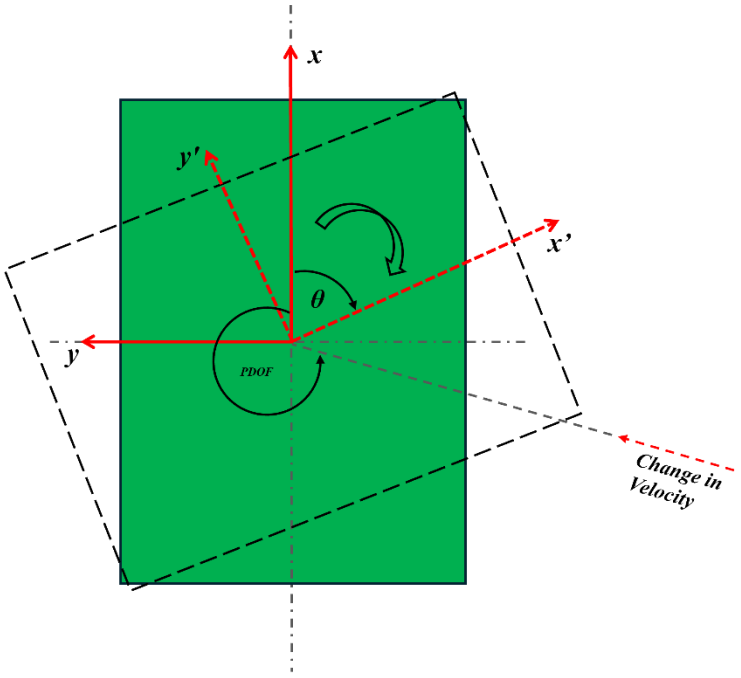

Figure 7.30 - Vehicle "A"'s schematic of the impact mechanism during the collision for EDR Event 2 (not to scale).

On the other hand, for instant of time t = 0 s (Figure 7.30), the impact point was situated in the second quadrant with a value of 115.77º (referred to the approach vector) and since its Δv_x and Δv_y had opposite signs, an anticlockwise rotation happened with a departure angle (θ) of 64.61º (situated in the first quadrant).

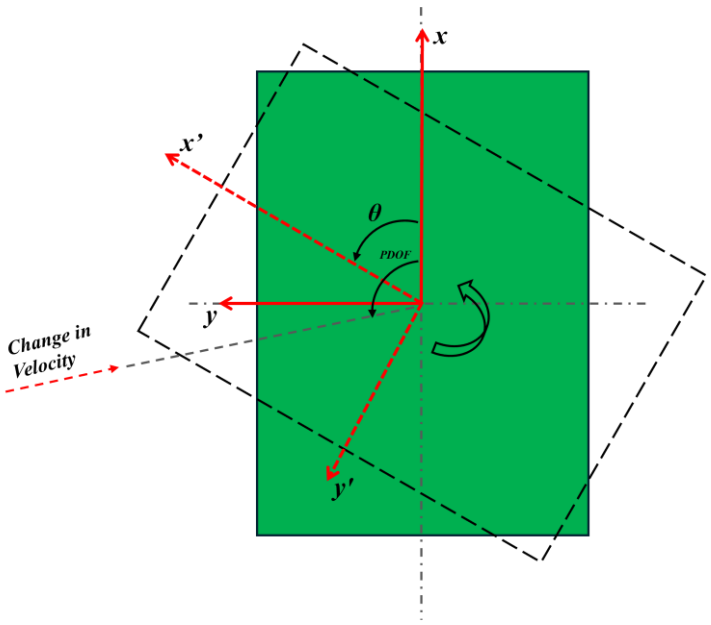

Figure 7.31 - Vehicle "A"'s schematic of the impact mechanism during the collision for EDR Event 1 (not to scale).

With the study of vehicle “A”’s behaviour before and after the collision completed, it was verified, once again, that with EDR data and using the PIDS developed, it was possible to closely replicate the pre-impact trajectory developed by Vehicle “A” and corroborate the accident’s report from the law enforcement authorities.

For the two real-world case studies presented in this report, the PIDS results were quite positive, that is, it achieved the project’s goals.

8. Conclusions and Future Work

8.1. Final Conclusions

The Development of a Pre-Impact Dynamics Simulator for a Vehicle Involved in a Road Accident, as detailed in this Master's thesis, successfully achieved its core goal: improving the reconstruction of vehicle trajectories before a collision by using Event Data Recorder (EDR) data. This technology, mandatory in European Union (EU) since 2022 and in the United States of America and Canada since 2013, was the key technology for attaining this project's goals. By integrating EDR outputs into a detailed vehicle dynamics model, this study highlights a significant enhancement in the accuracy and efficiency of road accident reconstruction.

Validation results confirmed that the developed simulator effectively replicates pre-impact vehicle movements, offering valuable insights for both Forensic Investigators and Engineers. The reliability of the simulator was further confirmed through validation using AVL VSM™ software, highlighting its practical applicability in real-world scenarios.

For the two trajectories employed to validate the simulator's dynamics calculations, the dynamics model used for newer EDRs (EDR_01 Series of Amendments) showed the most precise results, with an average deviation of 6.89% for the *x*-position component and 1.48% for the *y*-position component. Conversely, the dynamics model created for older EDR regulations (EDR_Steering and Velocity) also performed well, despite being based on only two vehicle dynamics data inputs: steering wheel angle and vehicle speed. This model exhibited an average deviation of 6.71% for the *x*-position component and 7.73% for the *y*-position component. When examining the total distance travelled in each position component, the model for newer EDRs achieved superior accuracy, with an average deviation of 0.06% for the *x*-position and 0.61% for the *y*-position. The older EDR model recorded average deviations of 3.02% and 2.64% for the *x* and *y* positions, respectively. The cause of deviation spikes during the transition phases of the position signals remains unclear, suggesting that the actual deviations might be smaller than reported, thereby enhancing the simulator's credibility.

Additionally, the analysis revealed that the dynamics model for older EDR regulations is highly sensitive to inaccuracies in vehicle characteristic inputs, which can substantially

affect the behaviour of simulated trajectories. This finding reinforces the critical importance of using accurate and original vehicle specifications to ensure reliable simulation results.

The investigation into drivers' behaviour and the role of on-board safety assistance technologies provided a deeper understanding of the factors contributing to road accidents. The integration of these findings with the developed simulator facilitated the analysis of two real-world case studies, leading to a clearer forensic interpretation of the causes of those accidents.

Overall, the domain of EDR-based accident reconstruction is relatively new, with limited research specifically focusing on pre-impact dynamics. This Master's thesis attempts to be one of the pioneering works in this field, establishing a framework for more advanced and precise simulations. It introduces a technical evaluation procedure that effectively integrates EDR data with vehicle dynamics models, creating a systematic approach to pre-impact analysis. This study hopes to contribute to the scientific literature by demonstrating how EDR data can be reused to analyse pre-impact scenarios, thus broadening its original field of application.

The pre-impact dynamics simulator developed in this project marks a substantial advancement in vehicle accident reconstruction. Its proven ability to accurately simulate pre-crash events, along with its potential for further enhancements, positions it as a critical tool for accident Investigators, Engineers and Researchers dedicated to improving road safety. With ongoing development and refinement, this simulator could play a key role in understanding and mitigating the causes of vehicle accidents, ultimately contributing to the development of safer vehicles and, consequently, enhancing road safety.

8.2. Areas of Future Improvements

From the results obtained in the simulator developed, the following improvements can be made to obtain even better results:

1. Pre-impact dynamics models: They are simplified dynamics models, limiting their accuracy in scenarios involving complex manoeuvres and interactions. To enhance precision, more sophisticated models should be developed that incorporate, for example, additional external forces, vehicle roll, and variations in road surface

conditions. This approach would enable better simulation of real-world vehicle pre-impact trajectories, leading to a more accurate reconstruction of pre-impact events.

2. Post-crash model: It assumes the EDR is aligned with the vehicle's longitudinal axis, an assumption that may not always be true. Future enhancements should incorporate mathematical models accounting for both longitudinal and lateral offsets of EDR's position. This refined approach would allow for a more precise calculation of vehicles' total delta-V in varied crash scenarios, improving accuracy in impact and departure angles.

3. Vehicle speed measurement: The current speed measurement relies on wheel sensors from the Antilock Braking System (ABS) control unit, which can compromise accuracy during, for example, rollover events where wheels may lock. In addition, in scenarios where the ABS is actuating, wheel slippage may also result in recorded speeds lower than the actual vehicle speed. To bypass this limitation, future improvements could integrate alternative data from speed-tracking systems to obtain more reliable pre-impact trajectories, even during high-slip events.

4. Type of pre-impact trajectory: Incorporating 3D trajectory generation into the simulator would enhance the clarity and detail of pre-impact vehicle trajectories, especially in complex crash scenarios. A 3D visualization would allow for better representation of elevation changes, vehicle roll, and yaw angles, providing more accurate insights into vehicle motion before impact. This upgrade would also improve the simulator's utility in training, analysis, and safety assessments by offering a more comprehensive view of pre-impact dynamics.

5. Testing simulation error using real simulated pre-impact scenarios: To improve the accuracy of the simulator, it is recommended to evaluate simulation errors by comparing outputs with known, simulated real-world pre-impact scenarios rather than solely relying on software theoretical dynamics models. This approach enables a direct measure of result veracity, highlighting discrepancies and suggesting necessary adjustments.

Bibliographic References

Autoridade Nacional Segurança Rodoviária [ANSR]. (n.d.). *Tempo de Reação na Condução*.

AVL LIST GMBH. (2023). *AVL VSM 2023 User's Guide*. AVL LIST GMBH.

Brach, R. M., & Brach, R. M. (2011). *Vehicle Accident Analysis and Reconstruction Methods*. SAE International.

Code of Federal Regulations. (2013). *49 CFR Part 563*. https://www.govinfo.gov/content/pkg/CFR-2011-title49-vol6/pdf/CFR-2011-title49-vol6-part563.pdf

EU Darts Group. (n.d.). *An overview of our activities: the introduction and regulation in Europe regarding EDR in (motor) vehicles.*

European Commission. (2022). COMMISSION DELEGATED REGULATION (EU) 2022/545. *Official Journal of the European Union*, 1–6.

European Parliament, & Council of the European Union. (2019). REGULATION (EU) 2019/2144. *Official Journal of the European Union*, 1–40.

FARO. (n.d.). *The Advantages of LiDAR in Accident Reconstruction*. Retrieved 1 August 2024, from https://www.faro.com/en/Resource-Library/Article/Accident-Reconstruction-LiDAR

Fernández, J. G. (2012). *A Vehicle Dynamics Model for Driving Simulators*. Chalmers University of Technology.

Francisco, A. G. (2022). *DEVELOPMENT OF NEW METHODOLOGIES FOR ROAD ACCIDENT RECONSTRUCTION WITH CDR TOOL*. Instituto Politécnico de Leiria.

Gillespie, T. D. (1992). *Fundamentals of Vehicle Dynamics*. Society of Automotive Engineers, Inc.

Gouribhatla, R., & Pulugurtha, S. S. (2022). Drivers' behavior when driving vehicles with or without advanced driver assistance systems: A driver simulator-based study.

Transportation Research Interdisciplinary Perspectives, *13*. https://doi.org/10.1016/j.trip.2022.100545

Green, M. (2000). 'How Long Does It Take to Stop?' Methodological Analysis of Driver Perception-Brake Times. In *TRANSPORTATION HUMAN FACTORS* (Vol. 2, Issue 3).

Guiggiani, M. (2014). The science of vehicle dynamics: Handling, braking, and ride of road and race cars. In *The Science of Vehicle Dynamics: Handling, Braking, and Ride of Road and Race Cars*. Springer Netherlands.

ISO 8855 Road vehicles-Vehicle dynamics and road-holding ability-Vocabulary. (2011). www.iso.org

Jazar, R. N. (2008). *Vehicle Dynamics: Theory and Application*. Springer.

Mahmoudzadeh, A., Razi-Ardakani, H., & Kermanshah, M. (2019). Studying crash avoidance maneuvers prior to an impact considering different types of driver's distractions. *Transportation Research Procedia*, *37*, 203–210. https://doi.org/10.1016/j.trpro.2018.12.184

Martins, J. (2020). *Acidentes e Conflitos em Veículos Automóveis e sua Avaliação*. Juribook.

Martins, R. F. G. (2018). *Implementação de metodologias de reconstrução científica de acidentes.*

National Highway Traffic Safety Administration. (2022). *AMENDING PART 563 EVENT DATA RECORDERS (EDRS)*.

Robert Bosch GmbH. (n.d.). *The Bosch CDR Tool Key Applications for Insurance and Law Enforcement Crash Investigators*.

Robert Bosch GmbH. (2018). *Automotive Handbook* (10th ed.). WILEY.

Ruth, R. (2019). *Using EDR Delta V in Traffic Crash Reconstruction* (pp. 1–118).

Shelby, S. G. (2011). DELTA-V AS A MEASURE OF TRAFFIC CONFLICT SEVERITY. *3rd International Conference on Road Safety and Simulation*, 1–20.

The Drone Centre. (2023, June 15). *Drones for Road Accident Reconstruction*. https://thedronecentre.ae/drones-for-road-accident-reconstruction/

United Nations Economic Commission for Europe. (2021a). UN Regulation No 160 – Uniform provisions concerning the approval of motor vehicles with regard to the Event Data Recorder. *Official Journal of the European Union*, 1–19.

United Nations Economic Commission for Europe. (2021b). UN Regulation No 160 – Uniform provisions concerning the approval of motor vehicles with regard to the Event Data Recorder [2021/1215]. *Official Journal of the European Union*, 1–23.

Utriainen, R., Koisaari, T., Kari, T., & Heikkilä, H. (2023). Which not-at-fault crashes are unavoidable by using current active safety technology? *IATSS Research*, *47*(1), 44–49. https://doi.org/10.1016/j.iatssr.2023.01.002

Wallentowitz, H. (2004). *Automotive Engineering II Vertical Vehicle Dynamics*. www.ika.rwth-aachen.de

Wrona, R., & Rybicka, I. (2021). Errors in controlling cars cause tragic accidents involving motorcyclists. *Open Engineering*, *11*(1), 1025–1033. https://doi.org/10.1515/eng-2021-0099

Appendix A – EDR Input Data Template File

GENERAL INFORMATIONS														
Number of Events														
Norme														
SYSTEM STATUS AT EVENT (SSAE)														
Event	Event Type	Ignition Cycle (Crash)	Ignition Cycle (Download)	Int. Time ΔV (lateral) sec	Int. Time ΔV (longitudinal) sec	MAX ΔV (lateral) km/h	MAX ΔV (longitudinal) km/h	MAX ΔV (Resultant) km/h	In. Event to Curr. Event. (sec)	Last Data Sample (sec)	Prev. Event to Curr. Event. (sec)	MAX ΔV. time (lateral) sec	MAX ΔV. time (longitudinal) sec	MAX ΔV. time (Resultant) sec
1 (MOST RECENT)														
PRE-CRASH DATA (PCD)														
Time (sec)	Vehicle Speed (km/h)	TPS(%)	Engine rpm	Steering input (°)	Service Brake Actuation	ABS Activity	ESP Activity	Longitudinal Acceleration (g)	Lateral Acceleration (g)	Angular velocity (°/s)	Event	Algorithm triggering		
-5														
-4.5														
-4														
-3.5														
-3														
-2.5														
-2														
-1.5														
-1														
-0.5														
0														
SIGN CONVENTION INPUTS (SCI)														
Lateral Convention	1	)-Right. 1-Left)												
YAW Convention	1	se. 1-Counter clockwise												
Steering Convention	1	se. 1-Counter clockwise												
BICYCLE MODEL INPUTS (BMI)														
Vehicle's mass		kg												
Tyre Cornering Stiffness Front		N/rad												
Tyre Cornering Stiffness Rear		N/rad												
FRONT axle weight		kg												
REAR axle weight		kg												
Steering ratio		-												
CG height		m												
Wheelbase		m												
POST-CRASH DATA (POCD)														
Event	ΔV (longitudinal) km/h	ΔV (lateral) km/h												
1 (MOST RECENT)														

Figure A.1 – Excel format template file for Event Data Recorder (EDR) input data.

Appendix B – Simulator Python Code

1. EDR_INPUT.py file Python code:

```
import numpy as np
# Array lists inputs:
csv_data = []
SSAE = []
PCD = []
PCD_short = []
SCI = []
BMI = []
POCD = []
# Read CSV file with EDR Input data:
import csv
with open("INPUTCSV","r") as csvfile:
crashdata = csv.reader(csvfile,delimiter=";")
for row in crashdata:
csv_data.append(row)
# General informations input for pyhton:
events = int(csv_data[1][1])
norme = csv_data[2][1]
# System status at event input for python:
for i in range(5,5+events):
SSAE.append(csv_data[i])
# Pre-crash data input for python:
ctrl = 5 + events + 2
for i in range(ctrl,ctrl+(events*11)):
PCD.append(csv_data[i])
# Sign convention, input for python:
```

```
ctrl = ctrl + (events*11) + 1
for i in range(ctrl,ctrl+3):#ctrl + 3):
SCI.append(csv_data[i][1])
# Bicycle model, input for python:
ctrl = ctrl + 4
for i in range(ctrl,ctrl + 8):
BMI.append(csv_data[i][1])
# Post-Crash data, input for python:
ctrl = ctrl + 10
for i in range(ctrl,ctrl+events):
POCD.append(csv_data[i])
# Organize pre-crash data chronologically:
ctrl1 = 0 # control variable for PCD
ctrl2 = 0 # control variable for SSAE
for i in range(0,events):
for k in range(0,11):
PCD[ctrl1][0] = float(PCD[ctrl1][0]) - float(SSAE[ctrl2][10]) + float(SSAE[ctrl2][9])
PCD[ctrl1][0] = round(PCD[ctrl1][0],3)
ctrl1 += 1
ctrl2 += 1
PCD = sorted(PCD, reverse = False) # values in ascending order by time.
for i in range(0,len(PCD)):
PCD[i][0] = PCD[i][0] - PCD[len(PCD)-1][0] - float(SSAE[0][10])
PCD[i][0] = round(PCD[i][0],3)
# Eliminate repeated values, if necessary.
for row in PCD:
if row not in PCD_short:
PCD_short.append(row)
# Export chronologically organized values to a CSV file, for subsequent data processing.
```

```
    f = open("OUTPUTCSV","w", newline='')
    w = csv.writer(f,delimiter=";")
    for line in PCD_short:
    w.writerow(line)
    f.close()
    print("EDR data was imported successfully!")
```

2. BICYCLE MODEL_EDR.py file Python code:

```
import numpy as np
import matplotlib.pyplot as plt
# Variables
v_x = []
Steer = []
r = []
δ = []
v_y = []
depart_angles = []
yaw = []
xx = []
yy = []
v = []
R = []
β = []
β_accumulated = []
# Import Array lists from EDR_INPUT file:
import EDR_INPUT
PCD = EDR_INPUT.PCD_short
SSAE = EDR_INPUT.SSAE
SCI = EDR_INPUT.SCI
```

```
BMI = EDR_INPUT.BMI
POCD = EDR_INPUT.POCD
# Referencial signals convertion: ---------------------------
#-> If y is positive Right side:
if int(SCI[0]) == 0:
for i in range(0,len(SSAE)):
SSAE[i][6] = float(SSAE[i][6])*(-1)
#-> If steering is positive clockwise:
if int(SCI[2]) == 0:
for i in range(0,len(PCD)):
PCD[i][4] = float(PCD[i][4])*(-1)
# Convert values to SI and assign lists: ------------------------------------
#-> speed (v) km/h to m/s:
for i in range(0,len(PCD)):
v.append(float(PCD[i][1])*(10/36))
# for i in range(0, len(SSAE)):
# SSAE[i][6] = float(SSAE[i][6])*(10/36)
# SSAE[i][7] = float(SSAE[i][7])*(10/36)
#-> Steering wheel angle input deg to rad:
for i in range(0,len(PCD)):
Steer.append(np.deg2rad(float(PCD[i][4])))
# Assign variables from BMI: ----------------------------------------------
m = float(BMI[0])
Cα_F = float(BMI[1])
Cα_R = float(BMI[2])
m_f = float(BMI[3])
m_r = float(BMI[4])
i_s = float(BMI[5])
h = float(BMI[6])
```

```
l = float(BMI[7])
# Calculate β, R, yaw, yaw rate, v_x and v_y for each instant time: ---------
#-> Obtain δ:
if i_s != 0:
for i in range(0,len(Steer)):
δ.append(Steer[i]/i_s)
else:
for i in range(0,len(Steer)):
δ.append(Steer[i])
#-> Calculate a1 and a2:
a_1 = (m_r*l)/m
a_2 = (m_f*l)/m
#-> Calculate simplified "Understeer Gradient", K:
K = (m/l)*((a_2/Cα_F)-(a_1/Cα_R))
#-> Calculate Radius of turn and β for each instant of time: ------
for i in range(0, len(PCD)):
if δ[i] != 0:
R.append((1/δ[i])*(l+K*v[i]**2))
β.append(l/R[i])
v_x.append(v[i]*np.cos(β[i]))
v_y.append(v[i]*np.sin(β[i]))
r.append(v[i]/R[i])
else:
R.append(0)
β.append(0)
v_x.append(v[i]*np.cos(β[i]))
v_y.append(v[i]*np.sin(β[i]))
r.append(0)
#-> Calculate impact angles, departure vector:
```

```
for i in range(0,len(PCD)):
ctrl = int(PCD[i][12])
if ctrl == 1:
event = int(PCD[i][11])
Δv_x = float(POCD[event-1][1])
Δv_y = float(POCD[event-1][2])
total_ΔV = np.sqrt(Δv_x**2+Δv_y**2)
PDOF = np.arctan(Δv_y/Δv_x)
V3 = np.sqrt(v[i]**2+total_ΔV**2-2*v[i]*total_ΔV*np.cos(PDOF))
depart_angle = np.abs(np.arcsin(np.sin(PDOF)*total_ΔV/V3))
if np.sign(Δv_x) == np.sign(Δv_y):
depart_angle = -depart_angle
depart_angles.append([event,depart_angle])
#-> Calculate vehicle's x and y positions, local referencial:
for i in range(0,len(PCD)):
if i == 0:
xx.append(0)
yy.append(0)
yaw.append(0)
else:
if int(PCD[i-1][12]) == 1:
event = int(PCD[i-1][11])
for k in range(0,len(depart_angles)):
if depart_angles[k][0] == event:
rotate_offset = depart_angles[k][1]
yaw.append(yaw[i-1]+r[i-1]*(np.abs(float(PCD[i][0])-float(PCD[i-1][0])))+rotate_offset)
else:
yaw.append(yaw[i-1]+r[i-1]*(np.abs(float(PCD[i][0])-float(PCD[i-1][0]))))
xx.append(xx[i-1]+(np.cos(yaw[i])*v_x[i-1]-np.sin(yaw[i])*v_y[i-
1])*(np.abs(float(PCD[i][0])-float(PCD[i-1][0]))))
```

```
yy.append(yy[i-1]+(np.sin(yaw[i])*v_x[i-1]+np.cos(yaw[i])*v_y[i-
1])*(np.abs(float(PCD[i][0])-float(PCD[i-1][0]))))

print("Dynamic calculation for old regulation EDRs was performed successfully!"+"\t")

# plotting points as a scatter plot

plt.scatter(xx, yy, label= "Vehicle's COG center", color= "red",

marker= "X")

# x-axis label

plt.xlabel('Position x [m]')

# frequency label

plt.ylabel('Position y [m]')

# plot title

plt.title("VEHICLE'S PRE-IMPACT TRAJECTORY")

# showing legend

plt.legend()

# function to show the plot

plt.show()

print("Pre-impact trajectory chart was successfully generated!"+"\n")

print("Developed by Luís Miguel Gomes"+"\n"+"Department of Automotive
Engineering"+"\n"\

"Polytechnic University of Leiria, 2024")
```

3. BICYCLE MODEL_EDR_SERIES01.py file Python code:

```
import numpy as np

import matplotlib.pyplot as plt

from sympy import symbols, Eq, solve, solveset

from scipy.optimize import fsolve

# Variables

v_x = []

Steer = []

a_x = []
```

```
a_y = []
r = []
δ = []
v_y = []
depart_angles = []
yaw = []
xx = []
yy = []
Fz_F = []
Fz_R = []
v = []
K = []
β = []
# Import Array lists from EDR_INPUT file:
import EDR_INPUT
PCD = EDR_INPUT.PCD_short
SSAE = EDR_INPUT.SSAE
SCI = EDR_INPUT.SCI
BMI = EDR_INPUT.BMI
POCD = EDR_INPUT.POCD
# Referencial signals convertion: ----------
#-> If y is positive Right side:
if int(SCI[0]) == 0:
for i in range(0,len(SSAE)):
SSAE[i][6] = float(SSAE[i][6])*(-1)
for i in range(0,len(PCD)):
PCD[i][9] = float(PCD[i][9])*(-1)
#-> If yaw is positive clockwise:
if int(SCI[1]) == 0:
```

```
for i in range(0,len(PCD)):
PCD[i][10] = float(PCD[i][10])*(-1)
#-> If steering is positive clockwise:
if int(SCI[2]) == 0:
for i in range(0,len(PCD)):
PCD[i][4] = float(PCD[i][4])*(-1)
# Convert values to SI and assign lists: ------------------------------------
#-> speed km/h to m/s:
for i in range(0,len(PCD)):
v.append(float(PCD[i][1])*(10/36))
# for i in range(0, len(SSAE)):
# SSAE[i][6] = float(SSAE[i][6])*(10/36)
# SSAE[i][7] = float(SSAE[i][7])*(10/36)
#-> Steering input deg to rad:
for i in range(0,len(PCD)):
Steer.append(np.deg2rad(float(PCD[i][4])))
#-> a_x g to m/s^2:
for i in range(0,len(PCD)):
a_x.append(float(PCD[i][8])*9.80665)
#-> a_y g to m/s^2:
for i in range(0,len(PCD)):
a_y.append(float(PCD[i][9])*9.80665)
#-> r deg/s to rad/s:
for i in range(0,len(PCD)):
r.append(float(PCD[i][10])*0.017453)
# Assign variables from BMI: ------------------------------------------------
m = float(BMI[0])
Cα_F = float(BMI[1])
Cα_R = float(BMI[2])
```

```
m_f = float(BMI[3])
m_r = float(BMI[4])
i_s = float(BMI[5])
h = float(BMI[6])
l = float(BMI[7])
g = 9.81
# Calculate vy for each instant time: ------------------------------
#-> Obtain δ:
if i_s != 0:
for i in range(0,len(Steer)):
δ.append(Steer[i]/i_s)
else:
for i in range(0,len(Steer)):
δ.append(Steer[i])
#-> Calculate a1 and a2:
a_1 = (m_r*l)/m
a_2 = (m_f*l)/m
#-> Calculate vertical reactions:
for i in range(0,len(a_x)):
if a_x[i] < 0:
Fz_F.append((m*9.81*a_2/l)+\
(m*np.abs(a_x[i])*h/l))
Fz_R.append((m*9.81*a_1/l)-\
(m*np.abs(a_x[i])*h/l))
else:
Fz_F.append((m*9.81*a_2/l)-\
(m*np.abs(a_x[i])*h/l))
Fz_R.append((m*9.81*a_1/l)+\
(m*np.abs(a_x[i])*h/l))
```

```
#-> Calculate "Understeer Gradient", K:
for i in range(0,len(a_x)):
K.append((Fz_F[i]/Cα_F)-(Fz_R[i]/Cα_R))
#-> Calculate Radius of turn and β for each instant of time: ------
for i in range(0, len(PCD)):
β.append(δ[i]-(K[i]*a_y[i]/g))
v_x.append(v[i]*np.cos(β[i]))
v_y.append(v[i]*np.sin(β[i]))
#-> Calculate impact angles, departure vector:
for i in range(0,len(PCD)):
ctrl = int(PCD[i][12])
if ctrl == 1:
event = int(PCD[i][11])
Δv_x = float(POCD[event-1][1])
Δv_y = float(POCD[event-1][2])
total_ΔV = np.sqrt(Δv_x**2+Δv_y**2)
PDOF = np.arctan(Δv_y/Δv_x)
V3 = np.sqrt(v[i]**2+total_ΔV**2-2*v[i]*total_ΔV*np.cos(PDOF))
depart_angle = np.abs(np.arcsin(np.sin(PDOF)*total_ΔV/V3))
if np.sign(Δv_x) == np.sign(Δv_y):
depart_angle = -depart_angle
depart_angles.append([event,depart_angle])
#-> Calculate vehicle's x and y positions, local referencial:
for i in range(0,len(PCD)):
if i == 0:
xx.append(0)
yy.append(0)
yaw.append(0)
else:
```

```
if int(PCD[i-1][12]) == 1:

event = int(PCD[i-1][11])

for k in range(0,len(depart_angles)):

if depart_angles[k][0] == event:

rotate_offset = depart_angles[k][1]

yaw.append(yaw[i-1]+r[i-1]*(np.abs(float(PCD[i][0])-float(PCD[i-1][0])))+rotate_offset)

else:

yaw.append(yaw[i-1]+r[i-1]*(np.abs(float(PCD[i][0])-float(PCD[i-1][0]))))

xx.append(xx[i-1]+(np.cos(yaw[i])*v_x[i-1]-np.sin(yaw[i])*v_y[i-
1])*(np.abs(float(PCD[i][0])-float(PCD[i-1][0]))))

yy.append(yy[i-1]+(np.sin(yaw[i])*v_x[i-1]+np.cos(yaw[i])*v_y[i-
1])*(np.abs(float(PCD[i][0])-float(PCD[i-1][0]))))

print("Dynamic calculation for new regulation EDRs was performed successfully!"+"\t")

# plotting points as a scatter plot

plt.scatter(xx, yy, label= "vehicle's center", color= "red",

marker= "X")

# x-axis label

plt.xlabel('xx')

# frequency label

plt.ylabel('yy')

# plot title

plt.title("Vehicle's position - In space")

# showing legend

plt.legend()

# function to show the plot

plt.show()

print("Pre-impact trajectory chart was successfully generated!"+"\n")

print("Developed by Luís Miguel Gomes"+"\n"+"Department of Automotive
Engineering"+"\n"\

"Polytechnic University of Leiria, 2024")
```

Appendix C – Tables (Simulator validation in AVL)

Table C.1 – Trajectory "A" AVL Dynamics Data.

INSTANT OF TIME [s]	*VEHICLE SPEED [km/h]*	*STEERING WHEEL ANGLE [º]*	*LONGITUDINAL ACCELERATION [m/s²]*	*LATERAL ACCELERATION [m/s²]*	*ANGULAR VELOCITY [º/s]*
-49.5	102.7	-4.16E-01	1.30E+00	-8.46E-02	-2.95E-03
-49.0	105.0	6.48E-02	1.29E+00	-9.94E-03	1.60E-06
-48.5	107.3	5.90E-01	1.21E+00	8.65E-02	3.21E-03
-48.0	109.2	4.35E-01	9.00E-01	8.63E-02	2.67E-03
-47.5	110.8	-4.70E-01	8.47E-01	-5.17E-02	-2.32E-03
-47.0	112.3	-8.47E-02	8.42E-01	-5.24E-02	-1.23E-03
-46.5	113.8	2.26E+00	8.37E-01	3.09E-01	1.15E-02
-46.0	115.3	5.94E+00	8.29E-01	9.16E-01	3.12E-02
-45.5	116.8	9.35E+00	8.19E-01	1.56E+00	5.06E-02
-45.0	118.2	1.06E+01	8.11E-01	1.87E+00	5.79E-02
-44.5	119.7	9.89E+00	8.07E-01	1.82E+00	5.42E-02
-44.0	121.1	8.03E+00	8.05E-01	1.53E+00	4.40E-02
-43.5	122.6	7.22E+00	8.01E-01	1.34E+00	3.94E-02
-43.0	122.8	7.04E+00	-3.99E+00	1.27E+00	4.06E-02
-42.5	112.7	4.84E+00	-6.03E+00	1.11E+00	3.20E-02
-42.0	101.7	-1.01E+00	-6.16E+00	1.38E-01	-3.35E-03
-41.5	90.69	-1.10E+01	-5.95E+00	-1.33E+00	-6.08E-02
-41.0	80.56	-2.24E+01	-5.24E+00	-2.72E+00	-1.29E-01
-40.5	71.81	-3.40E+01	-4.37E+00	-3.65E+00	-1.92E-01
-40.0	64.93	-4.63E+01	-3.28E+00	-4.24E+00	-2.49E-01
-39.5	60.26	-5.75E+01	-1.87E+00	-4.55E+00	-2.95E-01
-39.0	57.92	-6.53E+01	-1.06E+00	-4.74E+00	-3.32E-01
-38.5	56.49	-7.38E+01	-6.58E-01	-5.10E+00	-3.70E-01
-38.0	55.54	-8.16E+01	-6.02E-01	-5.51E+00	-4.11E-01
-37.5	54.71	-8.32E+01	-5.36E-01	-5.53E+00	-4.22E-01
-37.0	54.08	-8.46E+01	-4.68E-01	-5.50E+00	-4.26E-01
-36.5	53.44	-8.59E+01	-4.62E-01	-5.53E+00	-4.34E-01
-36.0	53.22	-8.29E+01	-3.65E-03	-5.29E+00	-4.19E-01
-35.5	53.76	-8.03E+01	2.97E-01	-5.17E+00	-4.08E-01
-35.0	54.69	-7.56E+01	5.55E-01	-5.04E+00	-3.91E-01
-34.5	56.25	-6.93E+01	9.44E-01	-4.83E+00	-3.62E-01
-34.0	58.26	-6.46E+01	1.09E+00	-4.76E+00	-3.42E-01
-33.5	60.41	-5.31E+01	1.18E+00	-4.27E+00	-2.94E-01
-33.0	62.65	-4.07E+01	1.24E+00	-3.49E+00	-2.29E-01
-32.5	64.95	-3.23E+01	1.27E+00	-2.94E+00	-1.85E-01
-32.0	67.30	-2.18E+01	1.31E+00	-2.10E+00	-1.27E-01
-31.5	69.70	-1.34E+01	1.34E+00	-1.35E+00	-7.77E-02
-31.0	72.11	-8.15E+00	1.35E+00	-8.62E-01	-4.74E-02
-30.5	74.54	-4.46E+00	1.35E+00	-4.90E-01	-2.56E-02

-30.0	76.97	-2.31E+00	1.35E+00	-2.58E-01	-1.27E-02
-29.5	79.40	-8.14E-01	1.35E+00	-1.05E-01	-4.85E-03
-29.0	81.83	-2.05E-01	1.35E+00	-2.72E-02	-1.16E-03
-28.5	84.26	-6.24E-01	1.35E+00	-6.29E-02	-2.77E-03
-28.0	86.68	-1.28E+00	1.35E+00	-1.53E-01	-6.51E-03
-27.5	89.10	-1.50E+00	1.34E+00	-1.96E-01	-8.03E-03
-27.0	91.52	-1.24E+00	1.34E+00	-1.77E-01	-6.95E-03
-26.5	93.93	-7.12E-01	1.34E+00	-1.12E-01	-4.17E-03
-26.0	96.33	-3.74E-01	1.33E+00	-5.93E-02	-2.14E-03
-25.5	98.71	-3.90E-01	1.32E+00	-5.50E-02	-2.06E-03
-25.0	101.1	-6.17E-01	1.31E+00	-8.97E-02	-3.34E-03
-24.5	103.4	-7.29E-01	1.30E+00	-1.15E-01	-4.07E-03
-24.0	105.7	-6.77E-01	1.29E+00	-1.14E-01	-3.87E-03
-23.5	108.0	-5.30E-01	1.14E+00	-9.26E-02	-3.02E-03
-23.0	109.7	-4.29E-01	8.52E-01	-7.30E-02	-2.35E-03
-22.5	111.2	-5.41E-01	8.46E-01	-8.47E-02	-2.85E-03
-22.0	112.8	-7.80E-01	8.41E-01	-1.28E-01	-4.24E-03
-21.5	114.3	-7.98E-01	8.36E-01	-1.41E-01	-4.44E-03
-21.0	115.8	-4.33E-01	8.30E-01	-9.17E-02	-2.57E-03
-20.5	117.3	9.67E-02	8.25E-01	1.04E-03	3.92E-04
-20.0	118.7	3.42E-01	8.20E-01	5.79E-02	1.89E-03
-19.5	120.2	1.98E-01	8.15E-01	4.57E-02	1.21E-03
-19.0	121.7	-1.05E-01	8.09E-01	-7.87E-03	-4.60E-04
-18.5	123.1	-4.05E-01	8.04E-01	-6.59E-02	-2.16E-03
-18.0	124.4	-8.20E-01	-1.15E+00	-1.32E-01	-4.11E-03
-17.5	114.7	-1.94E+00	-6.23E+00	-2.87E-01	-1.04E-02
-17.0	103.6	-4.40E+00	-6.15E+00	-6.28E-01	-2.46E-02
-16.5	92.64	-1.11E+01	-5.93E+00	-1.45E+00	-6.28E-02
-16.0	82.43	-1.97E+01	-5.36E+00	-2.50E+00	-1.16E-01
-15.5	73.24	-3.14E+01	-4.69E+00	-3.45E+00	-1.77E-01
-15.0	65.89	-4.34E+01	-3.49E+00	-4.16E+00	-2.36E-01
-14.5	60.62	-5.46E+01	-2.33E+00	-4.47E+00	-2.81E-01
-14.0	57.74	-6.45E+01	-1.13E+00	-4.76E+00	-3.25E-01
-13.5	56.27	-7.14E+01	-6.43E-01	-5.02E+00	-3.57E-01
-13.0	55.32	-7.92E+01	-5.88E-01	-5.40E+00	-3.94E-01
-12.5	54.48	-8.23E+01	-5.40E-01	-5.54E+00	-4.14E-01
-12.0	53.87	-8.29E+01	-3.84E-01	-5.47E+00	-4.15E-01
-11.5	53.40	-8.40E+01	-3.70E-01	-5.48E+00	-4.21E-01
-11.0	53.15	-8.22E+01	-9.22E-02	-5.34E+00	-4.12E-01
-10.5	53.51	-7.98E+01	2.13E-01	-5.21E+00	-4.02E-01
-10.0	54.26	-7.67E+01	4.08E-01	-5.13E+00	-3.90E-01
-9.5	55.55	-6.94E+01	8.76E-01	-4.86E+00	-3.60E-01
-9.0	57.57	-6.22E+01	1.12E+00	-4.59E+00	-3.27E-01
-8.5	59.74	-5.31E+01	1.18E+00	-4.22E+00	-2.87E-01
-8.0	61.97	-4.18E+01	1.23E+00	-3.58E+00	-2.33E-01
-7.5	64.27	-3.21E+01	1.27E+00	-2.92E+00	-1.83E-01

-7.0	66.62	-2.19E+01	1.31E+00	-2.09E+00	-1.26E-01
-6.5	69.01	-1.31E+01	1.33E+00	-1.33E+00	-7.67E-02
-6.0	71.42	-6.82E+00	1.35E+00	-6.85E-01	-4.01E-02
-5.5	73.85	-3.28E+00	1.35E+00	-3.57E-01	-1.86E-02
-5.0	76.28	-1.17E+00	1.35E+00	-1.35E-01	-6.65E-03
-4.5	78.71	-7.05E-01	1.35E+00	-8.22E-02	-3.66E-03
-4.0	81.14	-5.24E-01	1.35E+00	-6.51E-02	-2.76E-03
-3.5	83.57	-4.50E-01	1.35E+00	-5.37E-02	-2.33E-03
-3.0	86.00	-6.29E-01	1.35E+00	-7.36E-02	-3.14E-03
-2.5	88.42	-9.56E-01	1.34E+00	-1.18E-01	-4.92E-03
-2.0	90.84	-1.15E+00	1.34E+00	-1.53E-01	-6.15E-03
-1.5	93.25	-1.08E+00	1.34E+00	-1.54E-01	-5.94E-03
-1.0	95.65	-9.15E-01	1.33E+00	-1.36E-01	-5.11E-03
-0.5	98.04	-8.80E-01	1.32E+00	-1.29E-01	-4.81E-03
0.0	100.4	-9.48E-01	1.31E+00	-1.45E-01	-5.28E-03

Table C.2 – Trajectory "A" *x* and *y* positions comparison.

INSTANT OF TIME [s]	*TRAJECTORY "A" - AVL*		*TRAJECTORY "A" – EDR_STEERING AND VELOCITY*		*TRAJECTORY "A" – EDR_01 SERIES OF AMENDMENTS*	
	x	*y*	*x*	*y*	*x*	*y*
-49.5	0	0	0	0	0	0
-49.0	-14.30	-1.906	-14.14	-1.861	-14.14	-1.858
-48.5	-28.92	-3.855	-28.60	-3.771	-28.60	-3.765
-48.0	-43.83	-5.864	-43.37	-5.758	-43.37	-5.744
-47.5	-58.97	-7.922	-58.41	-7.800	-58.41	-7.776
-47.0	-74.32	-9.995	-73.66	-9.839	-73.66	-9.806
-46.5	-89.88	-12.10	-89.12	-11.91	-89.12	-11.86
-46.0	-105.6	-14.32	-104.8	-14.14	-104.8	-14.07
-45.5	-121.6	-16.82	-120.6	-16.76	-120.6	-16.60
-45.0	-137.6	-19.75	-136.5	-19.94	-136.5	-19.61
-44.5	-153.8	-23.17	-152.4	-23.76	-152.6	-23.14
-44.0	-170.0	-27.08	-168.5	-28.15	-168.7	-27.13
-43.5	-186.4	-31.40	-184.6	-33.02	-184.9	-31.51
-43.0	-202.8	-36.10	-200.7	-38.34	-201.3	-36.26
-42.5	-218.5	-40.90	-216.8	-44.05	-217.6	-41.23
-42.0	-232.7	-45.48	-231.5	-49.52	-232.5	-45.98
-41.5	-245.4	-49.56	-244.7	-54.36	-246.0	-50.27
-41.0	-256.8	-52.84	-256.7	-58.17	-258.1	-53.76
-40.5	-267.1	-55.10	-267.7	-60.70	-269.0	-56.14
-40.0	-276.5	-56.24	-277.6	-61.85	-278.9	-57.23
-39.5	-285.2	-56.21	-286.6	-61.61	-287.9	-56.97
-39.0	-293.3	-54.97	-294.8	-60.00	-296.1	-55.35
-38.5	-300.8	-52.49	-302.3	-57.06	-303.6	-52.43
-38.0	-307.6	-48.74	-308.9	-52.80	-310.3	-48.21

-37.5	-313.4	-43.76	-314.3	-47.31	-315.7	-42.78
-37.0	-318.0	-37.76	-318.3	-40.89	-319.9	-36.41
-36.5	-321.1	-31.00	-320.9	-33.84	-322.5	-29.39
-36.0	-322.7	-23.80	-321.9	-26.48	-323.6	-22.04
-35.5	-322.8	-16.39	-321.4	-19.11	-323.1	-14.67
-35.0	-321.3	-9.019	-319.4	-11.91	-321.1	-7.470
-34.5	-318.3	-1.920	-316.0	-5.106	-317.7	-0.6682
-34.0	-314.0	4.742	-311.4	1.191	-313.1	5.608
-33.5	-308.4	10.79	-305.6	6.831	-307.3	11.22
-33.0	-301.8	16.16	-298.8	11.83	-300.5	16.17
-32.5	-294.3	20.89	-291.4	16.28	-293.0	20.56
-32.0	-286.1	25.07	-283.2	20.22	-284.8	24.44
-31.5	-277.4	28.85	-274.6	23.85	-276.2	28.01
-31.0	-268.2	32.40	-265.6	27.33	-267.1	31.44
-30.5	-258.6	35.84	-256.2	30.73	-257.7	34.81
-30.0	-248.7	39.26	-246.4	34.15	-247.9	38.20
-29.5	-238.4	42.73	-236.3	37.63	-237.8	41.66
-29.0	-227.8	46.28	-225.9	41.20	-227.4	45.23
-28.5	-216.8	49.93	-215.1	44.88	-216.6	48.90
-28.0	-205.6	53.67	-204.0	48.64	-205.5	52.66
-27.5	-194.0	57.47	-192.6	52.46	-194.1	56.48
-27.0	-182.0	61.34	-180.9	56.33	-182.4	60.36
-26.5	-169.8	65.26	-168.8	60.25	-170.3	64.31
-26.0	-157.2	69.26	-156.3	64.26	-157.9	68.34
-25.5	-144.3	73.35	-143.6	68.35	-145.2	72.47
-25.0	-131.0	77.52	-130.6	72.53	-132.1	76.68
-24.5	-117.5	81.77	-117.2	76.78	-118.7	80.97
-24.0	-103.6	86.08	-103.5	81.09	-105.1	85.33
-23.5	-89.43	90.47	-89.45	85.47	-91.06	89.76
-23.0	-74.97	94.91	-75.13	89.91	-76.75	94.27
-22.5	-60.30	99.40	-60.57	94.41	-62.21	98.83
-22.0	-45.41	103.9	-45.80	98.95	-47.46	103.4
-21.5	-30.32	108.5	-30.82	103.5	-32.50	108.1
-21.0	-15.02	113.1	-15.62	108.1	-17.33	112.7
-20.5	0.4882	117.7	-0.2141	112.7	-1.956	117.4
-20.0	16.19	122.4	15.38	117.4	13.61	122.2
-19.5	32.09	127.2	31.17	122.1	29.38	127.1
-19.0	48.18	132.0	47.16	127.0	45.33	132.0
-18.5	64.46	136.9	63.34	131.8	61.48	137.0
-18.0	80.94	141.8	79.72	136.8	77.83	142.0
-17.5	96.93	146.6	96.28	141.7	94.36	147.0
-17.0	111.5	150.8	111.6	146.1	109.6	151.6
-16.5	124.6	154.4	125.5	149.9	123.5	155.6
-16.0	136.4	157.3	138.0	152.7	135.9	158.7
-15.5	147.0	159.2	149.3	154.5	147.2	160.9
-15.0	156.6	160.1	159.5	155.0	157.3	161.8

-14.5	165.4	159.9	168.6	154.2	166.4	161.4
-14.0	173.5	158.5	176.8	152.2	174.7	159.8
-13.5	180.9	156.0	184.1	148.8	182.2	156.9
-13.0	187.7	152.2	190.5	144.3	188.8	152.7
-12.5	193.5	147.3	195.7	138.7	194.3	147.4
-12.0	198.1	141.3	199.5	132.1	198.6	141.1
-11.5	201.3	134.7	201.8	125.0	201.4	134.2
-11.0	203.1	127.5	202.7	117.7	202.7	126.9
-10.5	203.3	120.1	201.9	110.3	202.4	119.5
-10.0	202.1	112.7	199.8	103.2	200.7	112.3
-9.5	199.4	105.6	196.3	96.53	197.6	105.4
-9.0	195.3	98.91	191.6	90.42	193.2	99.06
-8.5	190.0	92.73	185.8	84.92	187.8	93.25
-8.0	183.7	87.15	179.0	80.07	181.3	88.05
-7.5	176.5	82.18	171.6	75.80	174.1	83.38
-7.0	168.6	77.72	163.5	72.02	166.2	79.16
-6.5	160.1	73.62	154.9	68.55	157.8	75.23
-6.0	151.1	69.73	145.9	65.24	149.0	71.41
-5.5	141.8	65.89	136.6	61.95	139.9	67.59
-5.0	132.1	62.01	126.9	58.62	130.4	63.69
-4.5	122.1	58.05	116.8	55.19	120.6	59.67
-4.0	111.8	53.98	106.5	51.68	110.5	55.54
-3.5	101.1	49.81	95.80	48.07	100.0	51.29
-3.0	90.18	45.52	84.80	44.37	89.27	46.93
-2.5	78.89	41.13	73.47	40.59	78.19	42.46
-2.0	67.28	36.65	61.81	36.74	66.79	37.90
-1.5	55.34	32.08	49.81	32.83	55.06	33.25
-1.0	43.07	27.42	37.49	28.86	43.01	28.51
-0.5	30.48	22.69	24.83	24.82	30.63	23.67
0.0	17.58	17.86	11.85	20.72	17.94	18.75

Table C.3 - Trajectory "B" AVL Dynamics Data.

INSTANT OF TIME [s]	*VEHICLE SPEED [km/h]*	*STEERING WHEEL ANGLE [º]*	*LONGITUDINAL ACCELERATION [m/s²]*	*LATERAL ACCELERATION [m/s²]*	*ANGULAR VELOCITY [º/s]*
-103.5	115.9	-1.43E+00	8.30E-01	-2.17E-01	-7.13E-03
-103.0	117.4	-1.12E+00	8.25E-01	-2.12E-01	-6.16E-03
-102.5	118.9	-7.57E-01	8.19E-01	-1.48E-01	-4.28E-03
-102.0	120.4	-4.05E-01	8.14E-01	-8.67E-02	-2.36E-03
-101.5	121.8	-4.25E-02	8.09E-01	-2.12E-02	-3.63E-04
-101.0	123.3	4.01E-01	8.03E-01	5.62E-02	1.98E-03
-100.5	124.7	1.20E+00	7.96E-01	1.96E-01	6.38E-03
-100.0	126.2	2.34E+00	7.88E-01	4.12E-01	1.27E-02
-99.5	127.6	3.44E+00	7.80E-01	6.34E-01	1.88E-02
-99.0	129.0	3.36E+00	7.73E-01	6.94E-01	1.90E-02

-98.5	127.9	7.40E-01	-5.27E+00	2.41E-01	4.17E-03
-98.0	117.0	-4.95E+00	-6.20E+00	-6.06E-01	-2.54E-02
-97.5	106.3	-1.63E+01	-5.36E+00	-2.45E+00	-9.61E-02
-97.0	98.56	-2.88E+01	-2.97E+00	-4.35E+00	-1.65E-01
-96.5	95.09	-3.26E+01	-1.11E+00	-4.84E+00	-1.77E-01
-96.0	93.15	-3.40E+01	-9.84E-01	-4.72E+00	-1.82E-01
-95.5	91.53	-3.61E+01	-7.64E-01	-4.92E+00	-1.92E-01
-95.0	90.32	-3.97E+01	-5.46E-01	-5.39E+00	-2.21E-01
-94.5	89.76	-3.93E+01	1.10E-01	-5.30E+00	-2.09E-01
-94.0	90.10	-3.59E+01	4.92E-01	-5.00E+00	-1.95E-01
-93.5	91.31	-3.06E+01	8.11E-01	-4.38E+00	-1.68E-01
-93.0	92.75	-2.28E+01	8.47E-01	-3.42E+00	-1.27E-01
-92.5	94.28	-1.50E+01	8.69E-01	-2.32E+00	-8.48E-02
-92.0	95.85	-8.06E+00	8.80E-01	-1.29E+00	-4.56E-02
-91.5	97.43	-5.29E+00	8.80E-01	-7.83E-01	-2.81E-02
-91.0	99.01	-7.76E+00	8.73E-01	-1.05E+00	-4.02E-02
-90.5	100.6	-1.17E+01	8.63E-01	-1.68E+00	-6.27E-02
-90.0	102.1	-1.25E+01	8.57E-01	-1.93E+00	-6.85E-02
-89.5	103.6	-8.84E+00	8.60E-01	-1.50E+00	-4.98E-02
-89.0	105.2	-5.24E+00	8.61E-01	-8.78E-01	-2.88E-02
-88.5	106.7	-5.57E+00	8.57E-01	-8.44E-01	-2.92E-02
-88.0	108.3	-7.83E+00	8.50E-01	-1.22E+00	-4.22E-02
-87.5	109.8	-7.68E+00	8.45E-01	-1.29E+00	-4.23E-02
-87.0	111.3	-5.15E+00	8.43E-01	-9.46E-01	-2.90E-02
-86.5	112.3	-4.10E+00	-3.09E+00	-6.34E-01	-2.09E-02
-86.0	102.2	-8.29E+00	-6.06E+00	-1.24E+00	-4.81E-02
-85.5	91.74	-1.56E+01	-5.54E+00	-2.29E+00	-9.35E-02
-85.0	82.31	-2.30E+01	-4.87E+00	-3.11E+00	-1.35E-01
-84.5	73.98	-3.06E+01	-4.28E+00	-3.68E+00	-1.74E-01
-84.0	67.02	-3.92E+01	-3.45E+00	-4.10E+00	-2.12E-01
-83.5	61.48	-4.87E+01	-2.57E+00	-4.43E+00	-2.50E-01
-83.0	58.12	-5.74E+01	-1.26E+00	-4.67E+00	-2.82E-01
-82.5	56.56	-6.65E+01	-6.14E-01	-5.09E+00	-3.22E-01
-82.0	55.61	-7.18E+01	-5.32E-01	-5.44E+00	-3.51E-01
-81.5	54.93	-7.03E+01	-2.16E-01	-5.33E+00	-3.46E-01
-81.0	55.20	-6.61E+01	3.69E-01	-5.02E+00	-3.27E-01
-80.5	56.57	-5.88E+01	1.07E+00	-4.63E+00	-2.97E-01
-80.0	58.71	-5.08E+01	1.18E+00	-4.23E+00	-2.63E-01
-79.5	60.92	-4.45E+01	1.22E+00	-3.92E+00	-2.35E-01
-79.0	63.17	-3.75E+01	1.25E+00	-3.52E+00	-2.03E-01
-78.5	65.46	-3.06E+01	1.28E+00	-3.00E+00	-1.67E-01
-78.0	67.80	-2.60E+01	1.30E+00	-2.62E+00	-1.41E-01
-77.5	70.16	-2.40E+01	1.31E+00	-2.50E+00	-1.29E-01
-77.0	72.52	-2.29E+01	1.31E+00	-2.48E+00	-1.24E-01
-76.5	74.90	-2.05E+01	1.32E+00	-2.32E+00	-1.13E-01
-76.0	77.29	-1.48E+01	1.34E+00	-1.81E+00	-8.45E-02

-75.5	79.70	-6.60E+00	1.35E+00	-9.02E-01	-4.04E-02
-75.0	82.13	1.41E+00	1.35E+00	4.52E-02	2.23E-03
-74.5	84.56	8.42E+00	1.34E+00	9.48E-01	4.16E-02
-74.0	86.96	1.42E+01	1.33E+00	1.77E+00	7.54E-02
-73.5	89.34	1.72E+01	1.32E+00	2.28E+00	9.36E-02
-73.0	91.70	1.76E+01	1.31E+00	2.44E+00	9.66E-02
-72.5	94.04	1.79E+01	1.31E+00	2.53E+00	9.80E-02
-72.0	96.38	1.74E+01	1.30E+00	2.56E+00	9.60E-02
-71.5	98.70	1.51E+01	1.30E+00	2.32E+00	8.39E-02
-71.0	101.0	1.23E+01	1.30E+00	1.95E+00	6.87E-02
-70.5	103.3	1.01E+01	1.29E+00	1.65E+00	5.71E-02
-70.0	105.7	7.86E+00	1.28E+00	1.35E+00	4.50E-02
-69.5	107.9	4.98E+00	1.15E+00	9.16E-01	2.90E-02
-69.0	109.6	1.81E+00	8.54E-01	3.83E-01	1.07E-02
-68.5	111.2	-2.24E-01	8.46E-01	4.41E-03	-7.61E-04
-68.0	112.7	-6.48E-01	8.41E-01	-1.06E-01	-3.46E-03
-67.5	114.2	-7.91E-01	8.36E-01	-1.32E-01	-4.30E-03
-67.0	115.7	-9.58E-01	8.31E-01	-1.63E-01	-5.21E-03
-66.5	117.2	-1.99E-01	8.26E-01	-9.86E-02	-2.29E-03
-66.0	118.7	4.49E+00	8.18E-01	6.23E-01	2.28E-02
-65.5	120.1	1.23E+01	8.00E-01	1.96E+00	6.54E-02
-65.0	121.5	1.79E+01	7.79E-01	3.04E+00	9.57E-02
-64.5	122.9	1.99E+01	7.66E-01	3.50E+00	1.05E-01
-64.0	124.2	2.21E+01	7.52E-01	3.83E+00	1.15E-01
-63.5	125.4	2.44E+01	7.35E-01	4.24E+00	1.26E-01
-63.0	126.6	2.61E+01	7.21E-01	4.49E+00	1.31E-01
-62.5	127.8	2.76E+01	7.07E-01	4.72E+00	1.36E-01
-62.0	128.0	2.72E+01	-1.40E+00	4.74E+00	1.39E-01
-61.5	125.5	2.74E+01	-1.16E+00	4.82E+00	1.34E-01
-61.0	123.1	2.35E+01	-1.59E+00	4.33E+00	1.19E-01
-60.5	117.8	1.20E+01	-4.37E+00	2.92E+00	7.70E-02
-60.0	108.0	-2.73E+00	-6.09E+00	2.87E-01	-1.24E-02
-59.5	97.41	-1.64E+01	-5.38E+00	-2.34E+00	-9.86E-02
-59.0	88.78	-2.41E+01	-4.21E+00	-3.53E+00	-1.43E-01
-58.5	81.77	-2.83E+01	-3.61E+00	-3.83E+00	-1.63E-01
-58.0	75.43	-3.27E+01	-3.33E+00	-3.96E+00	-1.84E-01
-57.5	70.12	-3.92E+01	-2.50E+00	-4.24E+00	-2.11E-01
-57.0	66.63	-4.69E+01	-1.30E+00	-4.60E+00	-2.44E-01
-56.5	65.03	-5.31E+01	-5.89E-01	-4.95E+00	-2.74E-01
-56.0	64.07	-5.64E+01	-5.00E-01	-5.15E+00	-2.88E-01
-55.5	63.21	-6.00E+01	-4.66E-01	-5.38E+00	-3.06E-01
-55.0	62.55	-5.86E+01	-1.71E-01	-5.29E+00	-3.01E-01
-54.5	62.71	-5.83E+01	1.66E-01	-5.19E+00	-2.98E-01
-54.0	63.20	-5.51E+01	5.21E-01	-5.06E+00	-2.87E-01
-53.5	64.70	-5.18E+01	1.01E+00	-4.85E+00	-2.71E-01
-53.0	66.64	-4.92E+01	1.13E+00	-4.80E+00	-2.62E-01

-52.5	68.79	-4.37E+01	1.22E+00	-4.53E+00	-2.38E-01
-52.0	71.02	-3.74E+01	1.25E+00	-4.07E+00	-2.07E-01
-51.5	73.30	-3.13E+01	1.28E+00	-3.55E+00	-1.75E-01
-51.0	75.62	-2.68E+01	1.30E+00	-3.10E+00	-1.48E-01
-50.5	77.96	-2.62E+01	1.30E+00	-3.07E+00	-1.43E-01
-50.0	80.29	-2.84E+01	1.29E+00	-3.40E+00	-1.55E-01
-49.5	82.58	-2.97E+01	1.28E+00	-3.71E+00	-1.64E-01
-49.0	84.86	-2.89E+01	1.28E+00	-3.75E+00	-1.60E-01
-48.5	87.14	-2.88E+01	1.28E+00	-3.80E+00	-1.58E-01
-48.0	89.39	-3.22E+01	1.26E+00	-4.22E+00	-1.75E-01
-47.5	91.57	-3.77E+01	1.23E+00	-4.95E+00	-2.02E-01
-47.0	93.64	-4.12E+01	1.20E+00	-5.50E+00	-2.18E-01
-46.5	95.56	-4.13E+01	1.11E+00	-5.65E+00	-2.16E-01
-46.0	97.37	-4.14E+01	1.04E+00	-5.72E+00	-2.14E-01
-45.5	96.80	-3.85E+01	-6.19E-01	-5.60E+00	-2.11E-01
-45.0	96.26	-3.83E+01	2.68E-01	-5.51E+00	-1.98E-01
-44.5	96.89	-3.48E+01	7.10E-01	-5.09E+00	-1.85E-01
-44.0	98.60	-3.07E+01	1.20E+00	-4.63E+00	-1.66E-01
-43.5	100.7	-2.63E+01	1.25E+00	-4.12E+00	-1.44E-01
-43.0	102.9	-2.25E+01	1.26E+00	-3.61E+00	-1.24E-01
-42.5	105.2	-1.88E+01	1.26E+00	-3.13E+00	-1.05E-01
-42.0	107.4	-1.21E+01	1.20E+00	-2.24E+00	-7.03E-02
-41.5	109.2	-2.82E+00	8.83E-01	-7.08E-01	-1.75E-02
-41.0	110.8	1.67E+00	8.47E-01	2.26E-01	9.14E-03
-40.5	112.3	4.47E-02	8.42E-01	9.30E-02	1.29E-03
-40.0	113.8	-1.23E+00	8.37E-01	-2.01E-01	-6.89E-03
-39.5	115.3	2.25E-01	8.32E-01	-4.08E-02	-3.65E-05
-39.0	116.8	3.29E+00	8.26E-01	4.76E-01	1.69E-02
-38.5	109.8	7.01E+00	-5.95E+00	1.14E+00	4.28E-02
-38.0	99.31	1.13E+01	-5.62E+00	1.84E+00	6.86E-02
-37.5	89.46	1.53E+01	-5.31E+00	2.28E+00	9.07E-02
-37.0	80.18	2.07E+01	-4.97E+00	2.71E+00	1.19E-01
-36.5	71.57	2.81E+01	-4.47E+00	3.20E+00	1.56E-01
-36.0	64.20	3.74E+01	-3.75E+00	3.68E+00	1.99E-01
-35.5	58.14	4.86E+01	-2.88E+00	4.09E+00	2.43E-01
-35.0	54.35	5.96E+01	-1.37E+00	4.41E+00	2.83E-01
-34.5	52.74	6.84E+01	-5.99E-01	4.78E+00	3.22E-01
-34.0	51.70	7.51E+01	-7.69E-01	5.11E+00	3.55E-01
-33.5	50.47	7.70E+01	-5.77E-01	5.14E+00	3.62E-01
-33.0	50.01	7.64E+01	-1.74E-01	5.00E+00	3.59E-01
-32.5	50.18	7.36E+01	2.45E-01	4.85E+00	3.49E-01
-32.0	51.30	6.81E+01	8.62E-01	4.63E+00	3.28E-01
-31.5	53.43	6.20E+01	1.33E+00	4.46E+00	3.05E-01
-31.0	56.26	5.48E+01	1.69E+00	4.27E+00	2.79E-01
-30.5	59.47	4.61E+01	1.78E+00	3.94E+00	2.43E-01
-30.0	62.75	3.81E+01	1.82E+00	3.54E+00	2.07E-01

-29.5	66.08	3.24E+01	1.85E+00	3.19E+00	1.77E-01
-29.0	69.42	2.95E+01	1.86E+00	3.06E+00	1.61E-01
-28.5	72.77	2.94E+01	1.85E+00	3.19E+00	1.60E-01
-28.0	76.09	3.10E+01	1.83E+00	3.52E+00	1.69E-01
-27.5	79.37	3.26E+01	1.77E+00	3.88E+00	1.80E-01
-27.0	82.15	3.33E+01	1.33E+00	4.12E+00	1.84E-01
-26.5	84.41	3.20E+01	1.27E+00	4.14E+00	1.77E-01
-26.0	86.66	2.91E+01	1.28E+00	3.90E+00	1.62E-01
-25.5	88.94	2.71E+01	1.28E+00	3.68E+00	1.49E-01
-25.0	91.21	2.87E+01	1.27E+00	3.90E+00	1.57E-01
-24.5	93.45	2.68E+01	1.28E+00	3.90E+00	1.50E-01
-24.0	95.74	1.79E+01	1.30E+00	2.84E+00	1.01E-01
-23.5	98.08	8.37E+00	1.32E+00	1.46E+00	5.00E-02
-23.0	100.4	-2.72E+00	1.31E+00	-7.68E-02	-7.55E-03
-22.5	102.8	-1.91E+01	1.26E+00	-2.51E+00	-9.87E-02
-22.0	97.16	-2.58E+01	-3.26E+00	-3.98E+00	-1.54E-01
-21.5	91.93	-2.79E+01	-2.71E+00	-4.21E+00	-1.59E-01
-21.0	86.85	-2.99E+01	-2.77E+00	-4.18E+00	-1.70E-01
-20.5	82.11	-3.35E+01	-2.36E+00	-4.36E+00	-1.88E-01
-20.0	78.28	-3.61E+01	-1.87E+00	-4.44E+00	-2.00E-01
-19.5	75.16	-3.85E+01	-1.55E+00	-4.46E+00	-2.10E-01
-19.0	72.73	-4.32E+01	-1.13E+00	-4.70E+00	-2.31E-01
-18.5	71.14	-4.89E+01	-6.09E-01	-5.07E+00	-2.57E-01
-18.0	70.08	-5.31E+01	-5.27E-01	-5.40E+00	-2.78E-01
-17.5	69.10	-5.41E+01	-4.99E-01	-5.50E+00	-2.85E-01
-17.0	68.52	-5.24E+01	8.04E-03	-5.35E+00	-2.77E-01
-16.5	69.04	-4.69E+01	5.55E-01	-4.90E+00	-2.53E-01
-16.0	70.72	-4.01E+01	1.21E+00	-4.34E+00	-2.20E-01
-15.5	72.96	-3.54E+01	1.26E+00	-3.94E+00	-1.95E-01
-15.0	75.23	-3.40E+01	1.27E+00	-3.86E+00	-1.86E-01
-14.5	77.50	-3.43E+01	1.27E+00	-4.01E+00	-1.89E-01
-14.0	79.76	-3.36E+01	1.27E+00	-4.08E+00	-1.86E-01
-13.5	81.98	-3.36E+01	1.16E+00	-4.15E+00	-1.84E-01
-13.0	82.77	-3.47E+01	-1.52E+00	-4.25E+00	-1.99E-01
-12.5	79.78	-4.00E+01	-1.38E+00	-4.88E+00	-2.19E-01
-12.0	77.68	-4.46E+01	-8.21E-01	-5.18E+00	-2.39E-01
-11.5	76.41	-4.81E+01	-6.00E-01	-5.43E+00	-2.57E-01
-11.0	75.33	-5.04E+01	-5.12E-01	-5.61E+00	-2.68E-01
-10.5	74.42	-5.04E+01	-3.63E-01	-5.60E+00	-2.69E-01
-10.0	74.24	-4.85E+01	2.72E-01	-5.42E+00	-2.59E-01
-9.5	75.00	-4.48E+01	7.38E-01	-5.11E+00	-2.43E-01
-9.0	76.85	-3.86E+01	1.23E+00	-4.61E+00	-2.15E-01
-8.5	79.08	-3.14E+01	1.28E+00	-3.92E+00	-1.77E-01
-8.0	81.39	-2.59E+01	1.30E+00	-3.28E+00	-1.45E-01
-7.5	83.72	-2.36E+01	1.31E+00	-3.03E+00	-1.31E-01
-7.0	86.06	-2.23E+01	1.31E+00	-2.95E+00	-1.24E-01

-6.5	88.41	-1.81E+01	1.32E+00	-2.54E+00	-1.02E-01
-6.0	90.78	-1.07E+01	1.33E+00	-1.64E+00	-6.28E-02
-5.5	93.18	-3.83E+00	1.34E+00	-6.41E-01	-2.31E-02
-5.0	95.58	-1.04E+00	1.33E+00	-1.72E-01	-5.93E-03
-4.5	97.97	-1.90E+00	1.32E+00	-2.53E-01	-9.89E-03
-4.0	100.3	-3.11E+00	1.31E+00	-4.51E-01	-1.69E-02
-3.5	102.7	-3.45E+00	1.30E+00	-5.48E-01	-1.94E-02
-3.0	105.0	-2.27E+00	1.29E+00	-4.15E-01	-1.36E-02
-2.5	107.3	-2.07E-01	1.21E+00	-9.82E-02	-2.24E-03
-2.0	109.2	1.80E+00	9.00E-01	2.52E-01	9.46E-03
-1.5	110.8	2.39E+00	8.47E-01	4.02E-01	1.33E-02
-1.0	112.3	1.26E+00	8.42E-01	2.56E-01	7.40E-03
-0.5	113.8	-2.32E-01	8.37E-01	7.53E-03	-6.44E-04
0.0	115.3	-1.35E+00	8.32E-01	-2.13E-01	-7.29E-03

Table C.4 - Trajectory "A" *x* and *y* positions comparison.

INSTANT OF TIME [s]	*TRAJECTORY "B" - AVL*		*TRAJECTORY "B" – EDR_STEERING AND VELOCITY*		*TRAJECTORY "B" – EDR_01 SERIES OF AMENDMENTS*	
	x	*y*	*x*	*y*	*x*	*y*
-103.5	0	0	0	0	0	0
-103.0	-7.681	-14.27	-7.701	-14.14	-7.698	-14.14
-102.5	-15.50	-28.70	-15.55	-28.44	-15.53	-28.45
-102.0	-23.46	-43.29	-23.52	-42.90	-23.50	-42.91
-101.5	-31.52	-58.05	-31.60	-57.54	-31.57	-57.55
-101.0	-39.69	-72.98	-39.79	-72.35	-39.74	-72.37
-100.5	-47.93	-88.11	-48.05	-87.35	-47.99	-87.38
-100.0	-56.23	-103.4	-56.35	-102.6	-56.28	-102.6
-99.5	-64.51	-119.0	-64.63	-118.0	-64.55	-118.0
-99.0	-72.74	-134.8	-72.84	-133.7	-72.76	-133.7
-98.5	-80.90	-150.8	-80.99	-149.6	-80.91	-149.7
-98.0	-88.60	-166.0	-89.06	-165.5	-89.02	-165.5
-97.5	-95.81	-179.7	-96.68	-179.8	-96.58	-179.9
-97.0	-103.0	-191.9	-104.3	-192.5	-104.0	-192.6
-96.5	-110.7	-202.9	-112.4	-203.5	-111.9	-203.8
-96.0	-119.1	-212.8	-121.3	-213.3	-120.6	-213.7
-95.5	-128.2	-221.8	-130.8	-222.0	-130.0	-222.6
-95.0	-138.0	-229.8	-141.1	-229.5	-140.0	-230.4
-94.5	-148.5	-236.6	-152.0	-235.6	-150.8	-237.0
-94.0	-159.7	-242.2	-163.5	-240.5	-162.1	-242.3
-93.5	-171.4	-246.8	-175.5	-244.1	-173.8	-246.4

-93.0	-183.6	-250.4	-187.9	-246.8	-186.1	-249.7
-92.5	-196.3	-253.3	-200.6	-248.7	-198.7	-252.3
-92.0	-209.3	-255.7	-213.7	-250.1	-211.6	-254.4
-91.5	-222.5	-257.8	-226.9	-251.4	-224.8	-256.4
-91.0	-236.0	-259.8	-240.4	-252.4	-238.2	-258.2
-90.5	-249.8	-261.5	-254.1	-253.1	-251.9	-259.8
-90.0	-263.8	-262.8	-268.1	-253.4	-265.8	-260.9
-89.5	-278.1	-263.6	-282.3	-253.1	-280.0	-261.6
-89.0	-292.6	-264.1	-296.7	-252.4	-294.4	-261.9
-88.5	-307.3	-264.4	-311.2	-251.6	-309.0	-262.1
-88.0	-322.2	-264.5	-326.0	-250.5	-323.8	-262.0
-87.5	-337.3	-264.2	-341.0	-249.0	-338.8	-261.6
-87.0	-352.7	-263.6	-356.1	-247.2	-354.0	-260.9
-86.5	-368.2	-262.8	-371.4	-245.1	-369.5	-260.0
-86.0	-383.1	-261.9	-386.9	-242.9	-385.0	-258.9
-85.5	-396.5	-260.7	-400.9	-240.4	-399.2	-257.7
-85.0	-408.5	-259.1	-413.3	-237.6	-411.8	-256.0
-84.5	-419.1	-256.9	-424.2	-234.3	-423.0	-253.7
-84.0	-428.5	-254.1	-433.7	-230.4	-432.8	-250.8
-83.5	-436.7	-250.7	-441.9	-226.0	-441.4	-247.0
-83.0	-443.9	-246.6	-448.8	-220.9	-448.7	-242.6
-82.5	-450.1	-241.7	-454.5	-215.2	-454.8	-237.4
-82.0	-455.4	-236.0	-459.1	-208.8	-459.8	-231.3
-81.5	-459.6	-229.6	-462.3	-201.8	-463.6	-224.6
-81.0	-462.6	-222.6	-464.3	-194.4	-466.2	-217.4
-80.5	-464.4	-215.0	-465.2	-186.8	-467.5	-209.8
-80.0	-465.1	-207.1	-464.9	-179.0	-467.7	-202.0
-79.5	-464.8	-198.8	-463.7	-170.9	-467.0	-193.9
-79.0	-463.4	-190.3	-461.6	-162.7	-465.2	-185.6
-78.5	-461.1	-181.7	-458.6	-154.5	-462.6	-177.2
-78.0	-458.0	-172.9	-454.9	-146.2	-459.3	-168.8
-77.5	-454.1	-164.2	-450.5	-137.9	-455.3	-160.2
-77.0	-449.6	-155.4	-445.4	-129.6	-450.5	-151.7
-76.5	-444.3	-146.6	-439.6	-121.3	-445.1	-143.2
-76.0	-438.3	-137.9	-433.2	-113.1	-439.1	-134.8
-75.5	-431.8	-129.1	-426.2	-105.0	-432.5	-126.3
-75.0	-425.0	-120.2	-418.9	-96.61	-425.6	-117.6
-74.5	-417.9	-111.1	-411.5	-87.95	-418.6	-108.6
-74.0	-410.8	-101.5	-404.1	-78.81	-411.7	-99.13
-73.5	-403.9	-91.41	-397.0	-69.08	-404.9	-89.11

-73.0	-397.3	-80.72	-390.2	-58.72	-398.5	-78.49
-72.5	-391.0	-69.43	-383.7	-47.74	-392.5	-67.28
-72.0	-385.2	-57.57	-377.7	-36.15	-386.8	-55.50
-71.5	-379.8	-45.14	-372.1	-23.98	-381.7	-43.16
-71.0	-374.8	-32.20	-366.9	-11.28	-376.8	-30.32
-70.5	-370.2	-18.78	-362.1	1.891	-372.3	-17.03
-70.0	-365.8	-4.937	-357.5	15.50	-368.1	-3.313
-69.5	-361.7	9.308	-353.2	29.51	-364.1	10.79
-69.0	-357.7	23.88	-348.9	43.87	-360.1	25.24
-68.5	-353.7	38.69	-344.6	58.48	-356.1	39.94
-68.0	-349.7	53.71	-340.2	73.29	-352.1	54.84
-67.5	-345.6	68.92	-335.8	88.29	-347.9	69.93
-67.0	-341.4	84.32	-331.2	103.5	-343.7	85.21
-66.5	-337.1	99.92	-326.6	118.9	-339.3	100.7
-66.0	-332.8	115.7	-321.8	134.4	-334.9	116.4
-65.5	-328.6	131.7	-317.3	150.3	-330.7	132.3
-65.0	-324.8	148.1	-313.3	166.5	-327.1	148.6
-64.5	-321.8	164.8	-310.2	183.1	-324.2	165.2
-64.0	-319.7	181.8	-308.1	200.0	-322.3	182.2
-63.5	-318.5	199.1	-307.0	217.2	-321.3	199.4
-63.0	-318.5	216.6	-307.2	234.6	-321.4	216.8
-62.5	-319.5	234.3	-308.7	252.2	-322.8	234.3
-62.0	-321.8	251.9	-311.6	269.7	-325.3	251.9
-61.5	-325.3	269.2	-315.9	286.9	-328.8	269.3
-61.0	-329.8	285.8	-321.5	303.4	-333.5	286.1
-60.5	-335.1	301.7	-328.0	319.2	-338.9	302.3
-60.0	-340.7	316.5	-334.6	334.2	-344.5	317.7
-59.5	-345.6	329.8	-340.6	348.0	-349.6	331.8
-59.0	-349.5	342.1	-345.2	360.7	-353.7	344.7
-58.5	-352.2	353.6	-348.5	372.6	-356.6	356.7
-58.0	-353.9	364.4	-350.6	383.7	-358.3	367.9
-57.5	-354.6	374.5	-351.6	394.1	-358.8	378.4
-57.0	-354.1	383.9	-351.4	403.9	-358.2	388.1
-56.5	-352.6	392.9	-350.0	413.0	-356.4	397.2
-56.0	-350.0	401.5	-347.4	421.7	-353.3	405.7
-55.5	-346.2	409.4	-343.5	429.7	-349.1	413.5
-55.0	-341.3	416.6	-338.5	436.9	-343.8	420.5
-54.5	-335.3	423.0	-332.6	443.2	-337.6	426.6
-54.0	-328.5	428.4	-325.7	448.6	-330.5	431.6
-53.5	-320.9	432.9	-318.1	453.0	-322.7	435.7

-53.0	-312.4	436.4	-309.8	456.4	-314.2	438.7
-52.5	-303.4	438.8	-300.8	458.8	-305.2	440.6
-52.0	-293.8	440.2	-291.4	460.2	-295.7	441.6
-51.5	-283.8	440.6	-281.5	460.7	-285.8	441.6
-51.0	-273.4	440.2	-271.4	460.4	-275.7	440.8
-50.5	-262.8	438.9	-260.9	459.3	-265.3	439.2
-50.0	-252.1	436.7	-250.2	457.4	-254.7	436.8
-49.5	-241.2	433.7	-239.5	454.6	-244.1	433.5
-49.0	-230.3	429.7	-228.6	450.8	-233.4	429.2
-48.5	-219.4	424.7	-217.9	445.9	-222.9	424.0
-48.0	-208.7	418.7	-207.3	440.1	-212.5	417.7
-47.5	-198.4	411.6	-197.1	433.1	-202.5	410.4
-47.0	-188.6	403.3	-187.5	424.7	-193.1	401.8
-46.5	-179.5	393.7	-178.7	415.1	-184.5	392.1
-46.0	-171.4	383.1	-171.1	404.2	-176.8	381.2
-45.5	-164.3	371.6	-164.7	392.3	-170.3	369.4
-45.0	-158.6	359.5	-159.7	379.8	-164.8	357.1
-44.5	-154.1	346.8	-156.1	367.0	-160.7	344.4
-44.0	-150.8	333.7	-153.8	353.7	-157.8	331.3
-43.5	-148.5	320.1	-152.7	340.1	-155.9	317.7
-43.0	-147.1	306.0	-152.6	326.1	-155.0	303.7
-42.5	-146.7	291.5	-153.3	311.8	-154.9	289.4
-42.0	-147.0	276.8	-154.9	297.3	-155.4	274.8
-41.5	-147.8	261.8	-157.0	282.5	-156.5	260.0
-41.0	-148.7	246.5	-159.2	267.5	-157.5	244.8
-40.5	-149.7	231.0	-161.3	252.3	-158.5	229.5
-40.0	-150.6	215.4	-163.4	236.8	-159.5	213.9
-39.5	-151.6	199.5	-165.6	221.2	-160.6	198.1
-39.0	-152.6	183.4	-167.9	205.3	-161.6	182.2
-38.5	-153.4	167.5	-169.9	189.2	-162.5	166.0
-38.0	-153.9	153.0	-171.5	174.1	-163.2	150.7
-37.5	-153.9	139.9	-172.5	160.3	-163.3	136.9
-37.0	-153.3	128.2	-172.8	147.9	-162.8	124.5
-36.5	-152.2	117.7	-172.3	136.7	-161.7	113.5
-36.0	-150.5	108.5	-171.1	126.9	-159.9	103.7
-35.5	-148.1	100.3	-169.1	118.2	-157.3	95.14
-35.0	-145.0	93.19	-166.2	110.7	-154.0	87.79
-34.5	-141.2	86.86	-162.5	104.1	-149.8	81.50
-34.0	-136.4	81.35	-157.8	98.42	-144.8	76.18
-33.5	-131.0	76.86	-152.4	93.78	-139.0	71.95

-33.0	-124.9	73.49	-146.3	90.28	-132.7	68.93
-32.5	-118.3	71.27	-139.8	87.91	-126.0	67.12
-32.0	-111.4	70.21	-132.9	86.64	-119.0	66.50
-31.5	-104.1	70.29	-125.8	86.42	-111.9	67.01
-31.0	-96.60	71.54	-118.4	87.24	-104.7	68.64
-30.5	-88.94	73.94	-110.8	89.08	-97.34	71.36
-30.0	-81.21	77.43	-103.0	91.88	-89.97	75.08
-29.5	-73.48	81.94	-95.15	95.57	-82.60	79.73
-29.0	-65.81	87.39	-87.17	100.1	-75.27	85.26
-28.5	-58.25	93.74	-79.18	105.5	-68.04	91.64
-28.0	-50.90	101.0	-71.29	111.8	-61.02	98.91
-27.5	-43.88	109.2	-63.65	119.1	-54.36	107.1
-27.0	-37.38	118.4	-56.41	127.4	-48.22	116.3
-26.5	-31.58	128.4	-49.77	136.7	-42.74	126.3
-26.0	-26.54	139.1	-43.83	146.8	-38.02	137.0
-25.5	-22.28	150.5	-38.60	157.7	-34.06	148.4
-25.0	-18.81	162.5	-34.11	169.2	-30.85	160.3
-24.5	-16.22	175.1	-30.51	181.3	-28.54	172.8
-24.0	-14.51	188.1	-27.79	194.0	-27.12	185.7
-23.5	-13.44	201.5	-25.60	207.1	-26.23	198.9
-23.0	-12.68	215.3	-23.62	220.6	-25.54	212.5
-22.5	-11.83	229.4	-21.39	234.4	-24.66	226.5
-22.0	-10.33	243.2	-18.19	248.3	-22.85	240.6
-21.5	-7.951	256.1	-14.13	261.2	-20.34	253.9
-21.0	-4.728	268.1	-9.283	273.0	-16.94	266.2
-20.5	-0.7330	279.2	-3.736	283.7	-12.72	277.5
-20.0	4.020	289.2	2.481	293.2	-7.696	287.7
-19.5	9.504	298.3	9.323	301.7	-1.915	296.9
-19.0	15.69	306.5	16.74	309.0	4.567	305.1
-18.5	22.57	313.7	24.74	315.2	11.76	312.2
-18.0	30.19	319.9	33.32	320.1	19.67	318.1
-17.5	38.47	324.9	42.39	323.6	28.21	322.8
-17.0	47.26	328.6	51.75	325.8	37.20	326.1
-16.5	56.47	331.0	61.23	326.6	46.50	328.2
-16.0	66.07	332.3	70.81	326.2	56.05	329.0
-15.5	76.04	332.6	80.54	324.8	65.87	328.9
-15.0	86.30	331.8	90.39	322.4	75.94	327.8
-14.5	96.75	330.1	100.3	319.1	86.18	325.7
-14.0	107.3	327.2	110.1	314.6	96.47	322.5
-13.5	117.8	323.3	119.7	309.1	106.7	318.3

-13.0	128.2	318.4	129.0	302.6	116.8	313.1
-12.5	137.8	312.5	137.7	295.1	126.5	306.9
-12.0	146.5	305.9	145.2	286.9	135.1	299.9
-11.5	154.1	298.4	151.3	278.0	142.6	292.1
-11.0	160.6	290.1	156.2	268.6	148.9	283.6
-10.5	165.9	281.2	159.6	258.7	153.8	274.4
-10.0	169.9	271.7	161.5	248.5	157.5	264.7
-9.5	172.7	261.7	162.1	238.2	159.8	254.7
-9.0	174.3	251.3	161.4	227.8	160.9	244.3
-8.5	174.7	240.5	159.6	217.3	160.9	233.6
-8.0	174.2	229.4	156.9	206.7	160.1	222.7
-7.5	172.8	218.0	153.3	195.9	158.4	211.5
-7.0	170.7	206.4	148.9	185.2	156.0	200.1
-6.5	167.7	194.6	143.7	174.4	152.8	188.6
-6.0	164.1	182.7	137.9	163.6	148.9	177.0
-5.5	160.0	170.6	131.5	152.7	144.7	165.1
-5.0	155.6	158.3	125.0	141.6	140.3	152.9
-4.5	151.0	145.6	118.2	130.2	135.7	140.4
-4.0	146.3	132.7	111.2	118.5	131.0	127.7
-3.5	141.4	119.5	103.9	106.6	126.0	114.7
-3.0	136.2	106.0	96.35	94.51	120.8	101.4
-2.5	130.8	92.29	88.53	82.20	115.4	87.86
-2.0	125.3	78.29	80.54	69.61	109.8	74.01
-1.5	119.8	64.04	72.50	56.75	104.3	59.89
-1.0	114.3	49.57	64.43	43.65	98.77	45.53
-0.5	108.8	34.87	56.30	30.35	93.22	30.96
0.0	103.1	19.99	48.03	16.87	87.57	16.19

Appendix D – Simulator Input CSV Data File (Real Case “A”)

GENERAL INFORMATIONS															
Number of Events	1														
Norm	American														
SYSTEM STATUS AT EVENT (SSAE)															
Event	Event Type	Ignition Cycle (Crash)	Ignition Cycle (Download)	Int. Time ΔV (lateral) sec	Int. Time ΔV (longitudinal) sec	MAX ΔV (lateral) km/h	MAX ΔV (longitudinal) km/h	MAX ΔV (Resultant) km/h	In. Event to Curr. Event. (sec)	Last Data Sample (sec)	Prev. Event to Curr. Event. (sec)	MAX ΔV. time (lateral) sec	MAX ΔV. time (longitudinal) sec	MAX ΔV. time (Resultant) sec	
1 (MOST RECENT)	FRONTAL	8277	8279			-6	-49		0	0.012	0	0.08	0.17	0.2575	
PRE-CRASH DATA (PCD)															
Time (sec)	Vehicle Speed (km/h)	TPS(%)	Engine rpm	Steering input (°)	Service Brake Actuation	ABS Activity	ESP Activity	Longitudinal Acceleration (g)	Lateral Acceleration (g)	Angular velocity (°/s)	Event	Algorithm triggering			
-5	133	100	4672	2	0	0	0				1	0			
-4.5	139	100	4800	6	0	0	0				1	0			
-4	143	100	4992	0	0	0	0				1	0			
-3.5	149	100	5184	-2	0	0	0				1	0			
-3	153	100	5312	-8	0	0	0				1	0			
-2.5	159	100	544	-2	0	0	0				1	0			
-2	159	0	544	10	0	0	0				1	0			
-1.5	143	0	4672	8	1	1	0				1	0			
-1	134	0	4096	16	1	1	0				1	0			
-0.5	115	0	3456	4	1	1	0				1	0			
0	101	0	3136	4	1	1	0				1	1			
SIGN CONVENTION INPUTS (SCI)															
Lateral Convention	0	)-Right. 1-Left)													
YAW Convention	(0-Clockwise. 1-Counter clockwise														
Steering Convention	1	se. 1-Counter clockwise													
BICYCLE MODEL INPUTS (BMI)															
Vehicle's mass	1395	kg													
Tyre Cornering Stiffness Front	50000	N/rad													
Tyre Cornering Stiffness Rear	50000	N/rad													
FRONT axle weight	837	kg													
REAR axle weight	558	kg													
Steering ratio	20	-													
CG height	0.5	m													
Wheelbase	2.631	m													
POST-CRASH DATA (POCD)															
Event	ΔV (longitudinal) km/h	ΔV (lateral) km/h													
1 (MOST RECENT)	-1043	4													

Figure D.1 – Real Case “A”, vehicle “B” simulator’s input data file.

Appendix E – Simulator Input CSV Data File (Real Case “B”)

GENERAL INFORMATIONS														
Number of Events	2													
Norme	American													
SYSTEM STATUS AT EVENT (SSAE)														
Event	Event Type	Ignition Cycle (Crash)	Ignition Cycle (Download)	Int. Time ΔV (lateral) sec	Int. Time ΔV (longitudinal) sec	MAX ΔV (lateral) km/h	MAX ΔV (longitudinal) km/h	MAX ΔV (Resultant) km/h	In. Event to Curr. Event. (sec)	Last Data Sample (sec)	Prev. Event to Curr. Event. (sec)	MAX ΔV. time (lateral) sec	MAX ΔV. time (longitudinal) sec	MAX ΔV. time (Resultant) sec
1 (MOST RECENT)		11154					5.6		0.7	0	0.7		0.3	
2		11154					1.34		0	0	0		0.2995	
PRE-CRASH DATA (PCD)														
Time (sec)	Vehicle Speed (km/h)	TPS (%)	Engine rpm	Steering input (°)	Service Brake Actuation	ABS Activity	ESP Activity	Longitudinal Acceleration (g)	Lateral Acceleration (g)	Angular velocity (°/s)	Event	Algorithm triggering		
-5	82	97.5	2174	-114.5	0	0	0	-0.32	-0.43	-20.06	1	0		
-4.5	62	0	2238	-10.1	1	0	0	-0.22	-0.61	-50.71	1	0		
-4	39	0	1858	70.6	1	1	0	-0.17	-0.34	-43.98	1	0		
-3.5	47	0	1446	22.3	1	1	0	-0.1	-0.34	-34.95	1	0		
-3	9	0	1068	-1	1	1	0	-0.1	-0.17	2.81	1	0		
-2.5	7	0	850	10.7	1	1	0	-0.14	1.06	15.77	1	0		
-2	0	0	440	10.2	1	1	0	-0.18	-0.11	31.84	1	0		
-1.5	0	0	38	0	1	1	0	0.01	0.74	16.25	1	0		
-1	0	4.7	0	0	0	1	0	-0.13	0.29	21.06	1	0		
-0.5	0	60.6	0	0	0	0	0	-0.02	-0.48	-25.47	1	0		
0	1	13.9	0	0	1	0	0	0.32	-2.89	-46.23	1	1		
-5	75	99.9	1974	8.3	0	0	0	0.22	-0.06	5.13	2	0		
-4.5	82	97.5	2174	-35.6	0	0	0	0.09	-0.22	-3.88	2	0		
-4	62	0	2238	-142.5	1	0	0	-0.4	-0.52	-35.13	2	0		
-3.5	39	0	1858	39.2	1	1	0	-0.18	-0.04	-45.62	2	0		
-3	47	0	1446	28	1	1	0	-0.18	-0.29	-32.06	2	0		
-2.5	9	0	1068	14.1	1	1	0	-0.26	-2.69	-8.2	2	0		
-2	7	0	850	-5.8	1	1	0	-0.72	0.96	39.55	2	0		
-1.5	0	0	440	21.9	1	1	0	0.48	-1.96	-0.63	2	0		
-1	0	0	38	0	1	1	0	-0.4	1.98	36.52	2	0		
-0.5	0	4.7	0	0	0	1	0	-0.07	0.76	43.64	2	0		
0	0	60.6	0	0	0	0	0	-0.31	0.84	69.96	2	1		
SIGN CONVENTION INPUTS (SCI)														
Lateral Convention	1	(0-Right. 1-Left)												
YAW Convention	1	:kwise. 1-Counter clockwise												
Steering Convention	1	:kwise. 1-Counter clockwise												
BICYCLE MODEL INPUTS (BMI)														
Vehicle's mass	2177	kg												
Tyre Cornering Stiffness Front	50000	N/rad												
Tyre Cornering Stiffness Rear	50000	N/rad												
FRONT axle weight	1306.2	kg												
REAR axle weight	870.8	kg												
Steering ratio	20	-												
CG height	1.21	m												
Wheelbase	3.22	m												
POST-CRASH DATA (POCD)														
Event	ΔV (longitudinal) km/h	ΔV (lateral) km/h												
1 (MOST RECENT)	59.25	-122.72												
2	23.36	166.58												

Figure E.1 - Real Case “B”, vehicle “A” simulator’s input data file.

Appendix F – Real Case "B" Input/Output Data Summary

Table F.1 - Real case "B" input/output data summary.

INSTANT OF TIME [s]	*VEHICLE SPEED [km/h]*	*TPS (%)*	*STEERING INPUT (º)*	*SERVICE BRAKE ACTUATION [BOOLEAN]*	*ABS ACTIVITY [BOOLEAN]*	*ESP ACTIVITY [BOOLEAN]*	*VEHICLE HEADING ANGLE [º]*	*LONGITUDINAL ACCELERATION [m/s²]*	*LATERAL ACCELERATION [m/s²]*	*ANGULAR VELOCITY [º/s]*
-5.7	75	99.9	8.3	0	0	0	0	2.16	-0.588	5.13
-5.2	82	97.5	-35.6	0	0	0	2.56	0.883	-2.16	-3.88
-5.0	82	97.5	-114.5	0	0	0	1.79	-3.14	-4.22	-20.1
-4.7	62	0	-142.5	1	0	0	-4.23	-3.92	-5.10	-35.1
-4.5	62	0	-10.1	1	0	0	-11.3	-2.16	-5.98	-50.7
-4.2	39	0	39.2	1	1	0	-26.5	-1.77	-0.392	-45.6
-4.0	39	0	70.6	1	1	0	-35.6	-1.67	-3.33	-44.0
-3.7	47	0	28	1	1	0	-48.8	-1.77	-2.84	-32.1
-3.5	47	0	22.3	1	1	0	-55.2	-0.981	-3.33	-35.0
-3.2	9	0	14.1	1	1	0	-65.7	-2.55	-26.4	-8.20
-3.0	9	0	-1	1	1	0	-67.3	-0.981	-1.67	2.81
-2.7	7	0	-5.8	1	1	0	-66.5	-7.06	9.41	39.6
-2.5	7	0	10.7	1	1	0	-58.6	-1.37	10.4	15.8
-2.2	0	0	21.9	1	1	0	-53.8	4.71	-19.2	-0.630
-2.0	0	0	10.2	1	1	0	-54.0	-1.77	-1.08	31.8
-1.7	0	0	0	1	1	0	-44.4	-3.92	19.4	36.5
-1.5	0	0	0	1	1	0	-37.1	0.0981	7.26	16.3
-1.2	0	4.7	0	0	1	0	-32.2	-0.686	7.45	43.6
-1.0	0	4.7	0	0	1	0	-23.5	-1.27	2.84	21.1
-0.7	0	60.6	0	0	0	0	-17.2	-3.04	8.24	70.0
-0.5	0	60.6	0	0	0	0	-85.2	-0.196	-4.71	-25.5

0.0	1	13.9	0	1	0	0	-97.9	3.14	-28.3	-46.2